ETL-0270

LEVEL II

Scattering from a vegetation layer with an irregular vegetation soil boundary

AD A109138

Richard A. Hevenor

OCTOBER 1981

U.S. ARMY CORPS OF ENGINEERS
ENGINEER TOPOGRAPHIC LABORATORIES
FORT BELVOIR, VIRGINIA 22060

81 12 31 009

E T L

UNCLASSIFIED

SECURITY CLASSIFICATION OF THIS PAGE (When Data Entered)

REPORT DOCUMENTATION PAGE

READ INSTRUCTIONS BEFORE COMPLETING FORM

1. REPORT NUMBER ETL – 0270	2. GOVT ACCESSION NO. AD-A109 238	3. RECIPIENT'S CATALOG NUMBER
4. TITLE (and Subtitle) SCATTERING FROM A VEGETATION LAYER WITH AN IRREGULAR VEGETATION SOIL BOUNDARY		5. TYPE OF REPORT & PERIOD COVERED Technical Report June 1979 – June 1980
		6. PERFORMING ORG. REPORT NUMBER
7. AUTHOR(s) Richard A. Hevenor		8. CONTRACT OR GRANT NUMBER(s)
9. PERFORMING ORGANIZATION NAME AND ADDRESS U.S. Army Engineer Topographic Laboratories Fort Belvoir, Virginia 22060		10. PROGRAM ELEMENT, PROJECT, TASK AREA & WORK UNIT NUMBERS 4A161102B52C
11. CONTROLLING OFFICE NAME AND ADDRESS U.S. Army Engineer Topographic Laboratories Fort Belvoir, Virginia 22060		12. REPORT DATE October 1981
		13. NUMBER OF PAGES 113
14. MONITORING AGENCY NAME & ADDRESS(if different from Controlling Office)		15. SECURITY CLASS. (of this report) Unclassified
		15a. DECLASSIFICATION/DOWNGRADING SCHEDULE

16. DISTRIBUTION STATEMENT (of this Report)

Approved for Public Release; Distribution Unlimited.

17. DISTRIBUTION STATEMENT (of the abstract entered in Block 20, if different from Report)

18. SUPPLEMENTARY NOTES

19. KEY WORDS (Continue on reverse side if necessary and identify by block number)

Electromagnetic Waves
Vegetation Scattering

20. ABSTRACT (Continue on reverse side if necessary and identify by block number)

A theoretical model is computed for the backscattering of electromagnetic waves from a layer of vegetation by using a first-order renormalization technique to determine volume scattering. The vegetation soil interface is assumed rough according to the tangent plane approximation and the scattering from this boundary is added incoherently to the volume scattering result. The mean wave in the vegetation is obtained using a bilocal approximation of the Dyson's equation. A free space dyadic Green's function is used, along with a correlation function of the dielectric fluctuationsthat are exponential in form and that also possess different correlation lengths (ℓ_x, ℓ_y) and

DD FORM 1 JAN 73 1473 EDITION OF 1 NOV 65 IS OBSOLETE

UNCLASSIFIED (ℓ sub x, ℓ sub y)

SECURITY CLASSIFICATION OF THIS PAGE (When Data Entered)

4Ø5 192

20. Continued

in the x, y, and z, directions. Effective propagation constants are obtained for both horizontal and vertical polarization. The scattered wave is solved for by using a two-dimensional Fourier transform technique, and the boundary conditions at either end of the vegetation layer are matched. The far field backscatter coefficients are computed for both horizontal and vertical polarizations. The mean and variance of the dielectric fluctuations are calcuiated with the aid of Peake's model for the dielectric constant of vegetation. The theory is matched to experimental data taken from a corn field. The resulting values for the correlation parameters are then used to monitor the growth pattern of the corn field over a period of time. Comparisons between the theoretical and experimental results over this time period are shown. The theory is also matched to experimental data from spring and fall deciduous trees.

PREFACE

The authority for performing the work described in this report is contained in Project 4A161102B52C, "Research in Geodetic, Cartographic, and Geographic Sciences."

The theory described is the result of in-house work and represents an application of the renormalization technique for studying scattering from certain types of vegetation. A solution for the mean wave is obtained by using the bilocal approximation of the Dyson's equation. A Fourier transform of the dyadic Green's function is used to compute a solution utilizing an anisotropic correlation function for the random dielectric fluctuations. The scattered waves are computed from the mean wave and finally the radar backscatter coefficient is calculated. The influence of a rough surface under the vegetation is considered by using a noncoherent technique.

This task was performed under the supervision of Dr. Frederick Rohde, Team Leader, Center for Theoretical and Applied Physical Sciences; Mr. Melvin Crowell, Jr., Director, Research Institute.

COL Daniel L. Lycan, CE and COL Edward K. Wintz, CE were Commanders and Directors and Mr. Robert P. Macchia was Technical Director of the Engineer Topographic Laboratories during the study period.

CONTENTS

ILLUSTRACTIONS

SCATTERING FROM A VEGETATION LAYER WITH AN IRREGULAR VEGETATION SOIL BOUNDARY

INTRODUCTION

PURPOSE This research report presents a theory for analyzing the nature of radar wave scattering from certain types of vegetation. The vegetation is simulated by a continuous random medium, and use is made of a first-order renormalization technique to calculate the radar backscatter coefficient. The influence of an irregular vegetation soil interface has also been considered, using a noncoherent approach.

BACKGROUND In a previous report,[1] a derivation was presented of the radar backscatter coefficient from a half space of random medium using a first-order renormalization solution for the scattered wave and an isotropic correlation function for the random dielectric fluctuations. Recently, Fung solved the problem of scattering from a vegetation layer by using a scalar first-order renormalization approach.[2] In his solution, however, he did not consider the existance of a rough vegetation soil boundary. He did consider an anisotropic correlation function in which the horizontal variation is different from the vertical.

Tsang and Kong solved the problem of volume scattering from a half space random medium that contains lateral and vertical fluctuations.[3] A radiative transfer approach was used to calculate the backscattering cross sections up to second order in approximation. This enabled the cross polarized terms to be obtained.

There are two important practical applications for developing and analyzing various radar scattering theories. The first application is radar image simulation of terrain features. In this problem, the radar system parameters and terrain parameters are known and used to calculate a radar response in the form of a gray tone or density.

---

[1] R.A. Hevenor, *Backscattering of Radar Waves By Vegetated Terrain*, U.S. Army Engineer Topographic Laboratories, Fort Belvoir, VA. ETL-0105, June 1977, AD-A047 669.

[2] A.K. Fung, "Scattering From a Vegetation Layer," *IEEE Transactions on Geoscience Electronics*, Vol. GE-17, No. 1, January 1979.

[3] L. Tsang and J.A. Kong, "Radiative Transfer Theory for Active Remote Sensing of Half Space Random Media," *Radio Science*, Vol. 13, No. 5, September-October 1978.

The scattering theories can be used to compute the radar backscatter coefficient, which in turn is used to calculate gray tone. Using scattering theories in this type of application is straightforward, even though a solution for any one particular scattering problem may be extremely complicated.

The second application is in the field of remote sensing of terrain in which the sensor responses must be used to determine various terrain parameters. Using scattering theories for this application is not straightforward.

However, there are two important uses of scattering theories that bear directly on remote sensing. The first use is a parameter sensitivity study. The theory can be used to analyze the influence of various vegetation, terrain, and radar parameters upon the sensor response. Such parameters as surface roughness, soil moisture, vegetation height, and density could be varied one at a time to determine the influence on the sensor response. This type of analysis should lead to determining what radar parameters are most sensitive to certain terrain parameter changes. This type of analysis assumes the existance of scattering theories that have been developed and compared with existing experimental data.

The second use is to analyze the radar response for two different types of terrain features to see if the two features could be distinguished from each other on an image. Once again, this would assume the existance of scattering theories that have been developed and tested against experimental data. These applications provide the incentive for developing, analyzing, and testing various scattering theories.

In this report, the geometry of the scattering problem to be solved and the basic technique used for the solution will be discussed. In the analysis section, the derivation of the necessary equations will be provided. In the results section, the resulting theory will be compared with existing experimental data, and a study on the sensitivity of the input parameters will be provided.

In this report, the rationalized MKS system of units is used. A line under a symbol will be used to represent a vector quantity. A double line under a symbol will be used to represent a dyadic. A list of the most important symbols is provided at the end of this report.

In figure 1, the scattering geometry of the vegetation problem is shown. A plane wave with a time harmonic of exp ($j\omega t$) is incident from free space at an angle θ_i onto a layer of vegetation. The mean thickness of the vegetation is L. The vegetation soil boundary is considered to be randomly rough according to the tangent plane approximation. The vegetation is simulated by a continuous random medium in which $\epsilon(\underline{r})$ and $\sigma(\underline{r})$ represent the three-dimensional random dielectric and conductivity fluctuations, respectively. These fluctuations consist of the sum of an average and a fluctuating component. The standard deviations of the fluctuations are represented by η_1 and η_2. The angle of refraction of the mean wave in the random medium is θ_e.

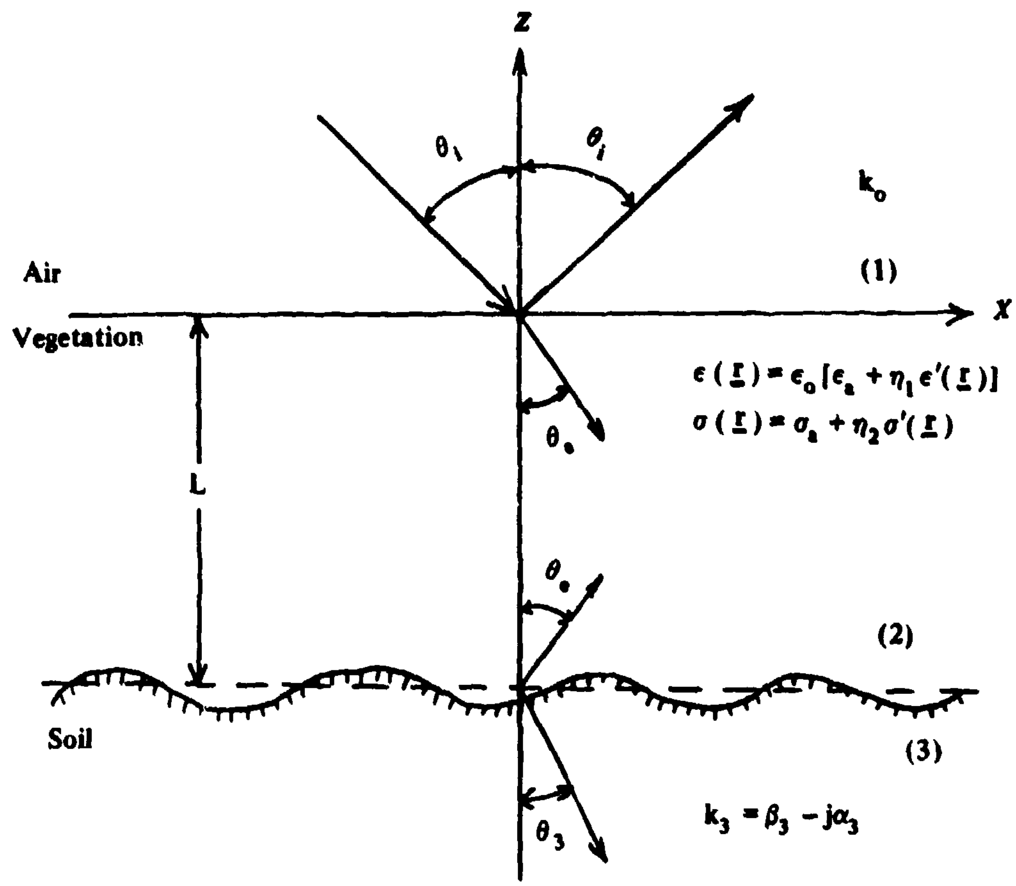

FIGURE 1. Scattering Geometry.

The soil below the vegetation represented by medium 3 is assumed homogeneous with a complex propagation constant k_3. The magnetic permeability for all three media is assumed to be that of free space. The electric field ($\underline{E}_i$) incident onto the vegetation layer can be written as follows:

$$\underline{E}_i = \left\{a_1 \underline{a}_x + a_2 \underline{a}_y + a_3 \underline{a}_z\right\} e^{-jk_o(x\sin\theta_i - z\cos\theta_i)}$$

where $\underline{a}_x$, $\underline{a}_y$, and $\underline{a}_z$ are unit vectors in the x, y, and z directions, respectively. The constants a_1, a_2, and a_3 are arbitrary, allowing for the consideration of both horizontal and vertical polarizations. A first-order renormalization method will be used to calculate the mean and scattered waves in the random medium. A solution will be developed first for the case where the vegetation soil boundary is a plane interface. The irregular boundary will be considered in a noncoherent manner afterwards. The dielectric and conductivity fluctuation terms ($\epsilon'(\underline{r})$ and $\sigma'(\underline{r})$ are considered as being generated by statistically homogeneous random processes. The means and correlation functions of the random processes are defined as follows:

$$<\epsilon'(\underline{r})> = <\sigma'(\underline{r})> = 0$$

$$<\epsilon'(\underline{r})\epsilon'(\underline{r}')> = <\sigma'(\underline{r})\sigma'(\underline{r}')> = e^{-|x-x'|/\ell_x} e^{-|y-y'|/\ell_y} e^{-|z-z'|/\ell_z}$$

where ℓ_x, ℓ_y, and ℓ_z are the correlation distances in the x, y, and z directions, respectively. The correlation functions have been chosen to be anisotropic. This representation, with unequal correlation distances, is believed to be closer to reality than an isotropic correlation function. This is because the size of vegetation scatterers in a horizontal plane is not the same as the size of the scatterers in a vertical plane. The mean wave in the random medium is determined from the bilocal approximation of the Dyson's equation:

$$[\nabla x \nabla x - k_s^2] <\underline{E}(\underline{r})> - \int_{V'} <\xi(\underline{r})\xi(\underline{r}')> <\underline{E}(\underline{r}')> \cdot \underline{\Gamma}(\underline{r},\underline{r}')\underline{dr}' = 0$$

where $<\underline{E}(\underline{r})>$ is the mean wave in the random medium.

$$\xi(\underline{r}) = -j\omega\mu_o\eta_2\sigma'(\underline{r}) + \omega^2\mu_o\epsilon_o\eta_1\epsilon'(\underline{r}).$$

$$k_a^2 \quad = -j\omega\mu_o\sigma_a + \omega^2\mu_o\epsilon_o\epsilon_a.$$

$\underline{\underline{\Gamma}}(\underline{r}, \underline{r}')$ is the dyadic Green's function.

V' is the volume of the random medium.

In the next section, plane wave solutions will be sought to the Dyson equation using an infinite space dyadic Green's function. It should be noted that the mean wave is located in the integrand, making any solution very difficult. Once the mean wave has been calculated and the appropriate boundary conditions have been matched for the mean waves in all three media, then the scattered wave in the vegetation layer can be calculated from the following equation:

$$[\nabla \mathrm{x}\, \nabla \mathrm{x} - k_a^2]\, \underline{E}_s(\underline{r}) = \xi(\underline{r}) <\underline{E}(\underline{r})>$$

where $E_s(r)$ is the scattered wave.

The mean wave acts as a source term for the scattered wave, which will be computed using a Fourier transform technique. This in turn will enable the scattered waves in air to be determined. The necessary boundary conditions will be matched, and the backscatter coefficient will be calculated for horizontal and vertical polarizations. The influence of the rough boundary between the vegetation and the soil will be considered apart from the volume scattering solution, using the tangent plane method. The backscatter coefficient for rough surface scattering will be modified by the attenuation through the vegetation. This result will then be added to the volume scattering solution to obtain a final answer for the backscatter coefficient. An elementary permittivity model will be developed that will relate certain parameters of the random media to the parameters of actual vegetation. A discussion of results section will follow in which the theoretical results are compared with actual experimental data. Also, a parameter sensitivity study will be conducted on the theory to determine the influence of various parameter changes upon the final result.

ANALYSIS

In this section, the necessary mathematical derivations will be provided to enable a scattering model for vegetation to be obtained. First, a solution for the mean wave will be presented and then the scattered wave will be calculated.

MEAN WAVE SOLUTION

The first step in obtaining a solution to the Dyson equation is to write the dyadic Green's function:

$$\underline{\underline{\Gamma}}(\underline{r},\underline{r}') = \left[\frac{\nabla\nabla'}{k_a^2} - \underline{\underline{I}}\right] G_o(\underline{r},\underline{r}') \tag{1}$$

where $\underline{\underline{I}}$ is the unit dyadic, and $G_o(\underline{r},\underline{r}')$ is the scalar Green's function that satisfies the following equation:

$$(\nabla^2 + k_a^2)\, G_o(\underline{r},\underline{r}') = \delta(\underline{r}-\underline{r}') \tag{2}$$

The solution for equation (2) is usually expressed in terms of $R = |\underline{r} - \underline{r}'|$. However, this particular form is not useful when working with an anisotropic correlation function that is expressed in rectangular coordinates. We shall therefore seek a solution to (2) that uses rectangular coordinates. Let $G_o(\underline{r},\underline{r}')$ take the following form:

$$G_o(\underline{r},\underline{r}') = \frac{1}{(2\pi)^3} \int \underline{dk}\, \widetilde{G}_o(\underline{k})\, e^{i\underline{k}\cdot(\underline{r}-\underline{r}')} \tag{3}$$

where

$$\underline{k} = k_x \underline{a}_x + k_y \underline{a}_y + k_z \underline{a}_z$$

Substituting (3) into (2) results in a solution for $\widetilde{G}_o(\underline{k})$.

$$\widetilde{G}_o(\underline{k}) = \frac{1}{k_a^2 - k_x^2 - k_y^2 - k_z^2} \tag{4}$$

When (4) is placed in (3) and integration is performed in the complex k_z plane, $G_o(\underline{r}, \underline{r}')$ becomes

$$G_o(\underline{r}, \underline{r}') = \frac{j}{8\pi^2} \int_{-\infty}^{\infty} dk_x \int_{-\infty}^{\infty} dk_y$$

$$\cdot \frac{\exp[j\{k_x(x-x') + k_y(y-y') - k_z' \,|z-z'|\}]}{k_z'} \tag{5}$$

$$k_z' = \sqrt{k_a^2 - k_x^2 - k_y^2}$$

Transforming (5) into polar form results in

$$G_o(\underline{r}, \underline{r}') = \frac{j}{8\pi^2} \int_{o}^{\infty} dk \int_{o}^{2\pi} d\theta$$

$$\cdot\, k \frac{\exp[j\{k(x-x')\cos\theta + k(y-y')\sin\theta - \sqrt{k_a^2 - k^2}\,|z-z'|\}]}{\sqrt{k_a^2 - k^2}} \tag{6}$$

$$k = \sqrt{k_x^2 + k_y^2} \qquad k_x = k\cos\theta \qquad k_y = k\sin\theta$$

When (6) is used in (1), the dyadic Green's function becomes

$$\underline{\underline{\Gamma}}(\underline{r}, \underline{r}') = \frac{j}{8\pi^2} \int_{o}^{\infty} dk \int_{o}^{2\pi} d\theta \frac{k}{\sqrt{k_a^2 - k^2}} \{\underline{C}(k, \theta)\underline{B}(k, \theta) / k_a^2 - \underline{\underline{I}}\} \tag{7}$$

$$\cdot \exp[j\{k(x-x')\cos\theta + k(y-y')\sin\theta - \sqrt{k_a^2 - k^2}\,|z-z'|\}]$$

where

$$\underline{C}(k, \theta) = \underline{a}_x (jk\cos\theta) + \underline{a}_y (jk\sin\theta) + \underline{a}_z f_2(k)$$

$$\underline{B}(k, \theta) = \underline{a}_x(-jk\cos\theta) + \underline{a}_y(-jk\sin\theta) + \underline{a}_z f_1(k)$$

$$f_1(k) = \begin{cases} j\sqrt{k_a^2 - k^2} & \text{when } z > z' \\ -j\sqrt{k_a^2 - k^2} & \text{when } z < z' \end{cases}$$

and

$$f_2(k) = \begin{cases} -j\sqrt{k_a^2 - k^2} & \text{when } z > z' \\ j\sqrt{k_a^2 - k^2} & \text{when } z < z' \end{cases}$$

Plane wave solutions to the Dyson equation take the following form:

$$<\underline{E}(\underline{r})> = \underline{A}e^{-j\underline{k}_e \cdot \underline{r}}$$

The vector $\underline{A}$ can be obtained by matching boundary conditions. The mean wave is seen to propagate with an effective propagation constant $\underline{k}_e$, which must be determined. When the above equation is placed in the Dyson equation along with the dyadic Green's function given by (7), the following equation is obtain when the cross correlation terms between the dielectric and conductivity are ignored:

$$[\nabla x \nabla x - k_o^2 \underline{\underline{\hat{\epsilon}}}] \underline{A}e^{-j\underline{k}_e \cdot \underline{r}} = 0 \tag{8}$$

$$\underline{\underline{\hat{\epsilon}}} = \frac{k_a^2}{k_o^2} \underline{\underline{I}} - \frac{1}{(2\pi)^3} \underline{\underline{M}} \tag{9}$$

$$\underline{\underline{M}} = j\pi(\eta^2\eta_2^2 - k_o^2\eta_1^2) \int d\underline{r}' \int_o^\infty dk \int_o^\pi d\theta$$

$$\cdot\, d(k)e^{-|x - x'|/\ell_x}e^{-|y - y'|/\ell_y}e^{-|z - z'|/\ell_z}$$

$$\cdot\, e^{+j\underline{k}_e \cdot (\underline{r} - \underline{r}')} [\underline{C}(k,\theta)\underline{B}(k,\theta)/k_a^2 - \underline{\underline{I}}] \exp[j\{k(x - x')\cos\theta$$

$$+ k(y - y')\sin\theta - \sqrt{k_a^2 - k^2}\,|z - z'|\}] \tag{10}$$

$$d(k) = k / \sqrt{k_a^2 - k^2}$$

$$\eta = \sqrt{\mu_o / \epsilon_o}$$

The integral in $\underline{r}'$ is allowed to be over all space. For the case where ℓ_z is very small this should be a good approximation except for the points extremely close to either boundary. By carrying out the integration in $\underline{r}'$, one obtains a result for M_{ij} that represents the $ij^{\underline{th}}$ element of the dyadic $\underline{\underline{M}}$.

$$\begin{aligned} M_{ij} = {} & 4K\ell_x \ell_y \ell_z \int_0^{\infty} dk \int_0^{2\pi} d\theta d(k) \Big\{ g(k) \\ & \cdot [F_{1i}(k,\theta)F_{1j}(k,\theta) + k_a^2 \delta_{ij}] + h(k)[F_{2i}(k,\theta)F_{2j}(k,\theta) \\ & + k_a^2 \delta_{ij}] \Big\} / \Big\{ [1 + \ell_x^2(k_{ex} + k\cos\theta)^2] \\ & \cdot [1 + \ell_y^2(k_{ey} + k\sin\theta)^2] \Big\} \end{aligned} \tag{11}$$

where

$$g(k) = \frac{-1}{1 + j\ell_z(k_{ez} + \sqrt{k_a^2 - k^2})} \qquad h(k) = \frac{1}{j\ell_z(k_{ez} - \sqrt{k_a^2 - k^2}) - 1}$$

$$F_{11}(k,\theta) = jk\cos\theta \qquad F_{12}(k,\theta) = jk\sin\theta \qquad F_{13}(k,\theta) = j\sqrt{k_a^2 - k^2}$$

$$F_{21}(k,\theta) = jk\cos\theta \qquad F_{22}(k,\theta) = jk\sin\theta \qquad F_{23}(k,\theta) = -j\sqrt{k_a^2 - k^2}$$

$$\delta_{ij} = 1 \text{ when } i = j$$

$$\delta_{ij} = 0 \text{ when } i \neq j$$

$$K = j\pi(\eta^2 \eta_2^2 - k_o^2 \eta_1^2) / k_a^2$$

The form of the incident wave dictates that $k_{ey} = 0$ and $k_{ex} = k_o \sin\theta_i$. This result makes the following elements of the $\hat{\underline{\underline{\epsilon}}}$ dielectric tensor become equal to zero:

$$\hat{\epsilon}_{12} = \hat{\epsilon}_{21} = \hat{\epsilon}_{23} = \hat{\epsilon}_{32} = 0$$

The above result is easily shown by considering a transformation of (11) back to rectangular coordinates and recognizing that the integrand is even in k_y. Carrying out the indicated differentiation in equation (8) and writing the result in matrix form produces

$$\begin{bmatrix} k_{ez}^2 - k_o^2\hat{\epsilon}_{11} & 0 & -k_{ez}k_o\sin\theta_i - k_o^2\hat{\epsilon}_{13} \\ 0 & k_{ez}^2 + k_o^2\sin\theta_i - k_o^2\hat{\epsilon}_{22} & 0 \\ k_{ez}k_o\sin\theta_i - k_o^2\hat{\epsilon}_{13} & 0 & k_o^2\sin^2\theta_i - k_o^2\hat{\epsilon}_{33} \end{bmatrix} \begin{bmatrix} A_x e^{-j\mathbf{k}_e \cdot \mathbf{r}} \\ A_y e^{-j\mathbf{k}_e \cdot \mathbf{r}} \\ A_z e^{-j\mathbf{k}_e \cdot \mathbf{r}} \end{bmatrix} = 0 \tag{12}$$

In forming the above matrix, use has been made of the fact that $k_{ey} = 0$ and $k_{ex} = k_o \sin\theta_i$. Now, only solutions for k_{ez} are needed. Two solutions can be developed for k_{ez}, one for a horizontally polarized wave and one for a vertically polarized wave. For a horizontally polarized wave, one has $A_x = A_z = 0$ and $A_y \neq 0$. The following equation can be used to determine k_{ez} for this case:

$$\left\{k_{ez}^2 + k_o^2\sin^2\theta_i - k_o^2\hat{\epsilon}_{22}\right\} A_y e^{-j\mathbf{k}_e \cdot \mathbf{r}} = 0 \tag{13}$$

Since the term outside the brackets is not zero, this means that the quantity inside the brackets must be zero.

$$k_{ez} = \pm k_o \sqrt{\sin^2\theta_i - \hat{\epsilon}_{22}} \tag{14}$$

The above result is not an explicit solution for k_{ez} since this quantity also appears in the integral of M_{22}. A first approximation for k_{ez} can be obtained by letting $\eta_1 = \eta_2 = 0$. This represents the case where there are no random fluctuations at all.

$$k_{ez}^{(0)} = -\sqrt{k_s^2 - k_o^2\sin^2\theta_i}$$

The above value can be used to compute M_{22}, which in turn can be used to calculate a new value of k_{ez} that will be called k_h. The minus sign on the square root is chosen over the plus sign to consider waves propagating in the minus z direction.

$$k_h = -k_o \sqrt{\sin^2\theta_i - \hat{\epsilon}_{22}} \tag{15}$$

When computing k_h in (15), the expression for $k_{ez}^{(o)}$ is used to calculate M_{22}. It is interesting to see that even when k_a is real, k_h still comes out complex so that the mean wave decays as it propagates into the medium. This decay has been explained as resulting from multiple scattering. It is not clear, however, how much multiple scattering is being considered. For a vertical polarized wave, $A_x \neq 0$, $A_y = 0$, and $A_z \neq 0$. This leads to the following determinant:

$$\begin{vmatrix} k_{ez}^2 - k_o^2\hat{\epsilon}_{11} & -k_{ez}k_o\sin\theta_i - k_o^2\hat{\epsilon}_{13} \\ -k_ok_{ez}\sin\theta_i - k_o^2\hat{\epsilon}_{13} & k_o^2(\sin^2\theta_i - \hat{\epsilon}_{33}) \end{vmatrix} = 0$$

The above determinant provides another solution for k_{ez}.

$$k_{ez} = k_o \left\{ \frac{-\hat{\epsilon}_{13}\sin\theta_i \pm \sqrt{\hat{\epsilon}_{13}^2\sin^2\theta_i - \hat{\epsilon}_{33}(\hat{\epsilon}_{11}\sin^2\theta_i - \hat{\epsilon}_{11}\hat{\epsilon}_{33} + \hat{\epsilon}_{13}^2)}}{\epsilon_{33}} \right\} \tag{16}$$

Once again a first approximation for k_{ez} can be obtained for the case where the random dielectric and conductivity fluctuations disappear ($\eta_1 = \eta_2 = 0$).

$$k_{ez}^{(0)} = -\sqrt{k_a^2 - k_o^2\sin^2\theta_i}$$

This value for k_{ez} can be used to calculate the elements of the dielectric tensor. These elements are used in (16) to compute a new value for k_{ez}, which will be called k_v.

$$k_v = -k_o \left\{ \frac{\hat{\epsilon}_{13}\sin\theta_i + \sqrt{\hat{\epsilon}_{13}^2\sin^2\theta_i - \hat{\epsilon}_{33}(\hat{\epsilon}_{11}\sin^2\theta_i - \hat{\epsilon}_{11}\hat{\epsilon}_{33} + \hat{\epsilon}_{13}^2)}}{\hat{\epsilon}_{33}} \right\}$$

The sign associated with the square root has been chosen as minus in order to consider waves propagating in the minus z direction. The effective propagation constant for the mean wave has been determined, and now the amplitude must be calculated by matching appropriate boundary conditions. The total mean electric field in air can be written as:

$$\underline{E}_1(r) = \Big\{ [a_1\underline{a}_x + a_2\underline{a}_y + a_3\underline{a}_z]\, e^{jk_o z\cos\theta_i} + [R_1\underline{a}_x + R_2\underline{a}_y + R_3\underline{a}_z]\, e^{-jk_o z\cos\theta_i} \Big\}\, e^{-jk_o x\sin\theta_i} \qquad z > 0 \tag{17}$$

The first bracketed term in (17) is the incident wave, and the second bracketed term is the reflected wave. The unknowns in (17) are represented by R_1, R_2, and R_3. However, it will not be necessary to obtain an explicit solution for them since they are not needed in determining the scattered waves. The total mean electric field in the vegetation $(E_2(r))$ can be written in the following form, using previous results:

$$\underline{E}_2(r) = \Big\{ T_2\underline{a}_y e^{p_1 z} e^{jq_1 z} + (T_1\underline{a}_x + T_3\underline{a}_z) e^{p_2 z} e^{jq_2 z} + V_2\underline{a}_y e^{-p_2 z} e^{-jq_2 z} + (V_1\underline{a}_x + V_3\underline{a}_x) e^{-p_2 z} e^{-jq_2 z} \Big\}\, e^{-jk_o x\sin\theta_i} \qquad -L < z < 0 \tag{18}$$

where

$$p_1 + jq_1 = -jk_h$$

$$p_1 = \mathrm{Im}(k_h) \qquad q_1 = -\mathrm{Re}(k_h)$$

also

$$p_2 + jq_2 = -jk_v$$

$$p_2 = \mathrm{Im}(k_v) \qquad q_2 = -\mathrm{Re}(k_v)$$

In (18), both upward and downward waves have been considered. The unknowns are represented by the amplitudes T_1, T_2, T_3, V_1, V_2, and V_3. An explicit solution for each of these is required in terms of propagation constants, medium characteristics, and layer thickness. The explicit solution is needed to compute the scattered waves. An expression for the mean wave in the homogeneous soil medium can be written as

$$\underline{E}_3(\underline{r}) = [W_1\underline{a}_x + W_2\underline{a}_y + W_3\underline{a}_z]e^{-jk_o x\sin\theta_i}e^{jk_3 z\cos\theta_3} \qquad z < -L \qquad (19)$$

In the soil, the mean wave propagates in the minus z direction and the constants W_1, W_2, and W_3 are the unknown amplitudes. Once again, no explicit solution will be required for these amplitudes since they are not needed to compute the scattered waves. To compute the six amplitudes of the mean wave in the vegetation, the following boundary conditions are used:

$$E_{1x} = E_{2x} \text{ at } z = 0$$

$$E_{1y} = E_{2y} \text{ at } z = 0$$

$$\frac{\partial E_{1z}}{\partial y} - \frac{\partial E_{1y}}{\partial z} = \frac{\partial E_{2z}}{\partial y} - \frac{\partial E_{2y}}{\partial z} \text{ at } z = 0$$

$$\frac{\partial E_{1x}}{\partial z} - \frac{\partial E_{1z}}{\partial x} = \frac{\partial E_{2x}}{\partial z} - \frac{\partial E_{2z}}{\partial x} \text{ at } z = 0$$

$$E_{2x} = E_{3x} \text{ at } z = -L$$

$$E_{2y} = E_{3y} \text{ at } z = -L$$

$$\frac{\partial E_{2z}}{\partial y} - \frac{\partial E_{2y}}{\partial z} = \frac{\partial E_{3z}}{\partial y} - \frac{\partial E_{3y}}{\partial z} \text{ at } z = -L$$

$$\frac{\partial E_{2x}}{\partial z} - \frac{\partial E_{2z}}{\partial x} = \frac{\partial E_{3x}}{\partial z} - \frac{\partial E_{3z}}{\partial x} \text{ at } z = -L$$

$$D_{1z} = D_{2z} \text{ at } z = 0$$

$$D_{2z} = D_{3z} \text{ at } z = -L$$

$$\underline{D}_1 = \epsilon_o \underline{E}_1$$

$$\underline{D}_2 = \epsilon_v E_{2x} \underline{a}_x + \epsilon_h E_{2y} \underline{a}_y + \epsilon_v E_{2z} \underline{a}_z$$

where

$$\epsilon_h = \frac{q_1^2 - p_1^2}{\omega^2 \mu_o} \text{ evaluated at } \theta_i = 0°$$

$$\epsilon_v = \frac{q_2^2 - p_2^2}{\omega^2 \mu_o} \text{ evaluated at } \theta_i = 0°$$

$$\underline{D}_3 = \epsilon_3 \underline{E}_3$$

where ϵ_3 is the dielectric constant of the soil. Two divergence conditions will also be used, along with the above boundary conditions.

$$\nabla \cdot \underline{E}_1 = 0 \quad \text{and} \quad \nabla \cdot \underline{E}_3 = 0$$

When the equations for the mean fields given by (17) through (19) are placed in the boundary conditions, the result is 12 equations and 12 unknowns. Explicit solutions are only required for the six amplitudes associated with the mean wave in the random medium. Solving for these six values yields the following results:

$$T_2 = \frac{2jk_o a_{12} a_2 \cos\theta_i}{a_{21} a_{12} - a_{11} a_{22}} \tag{20}$$

$$V_2 = \frac{-2jk_o a_2 a_{11} \cos\theta_i}{a_{21}a_{12} - a_{11}a_{22}} \tag{21}$$

$$T_1 = \frac{jk_o b_{12} \left\{ 2a_1 \cos\theta_i + \sin\theta_i (1 - \epsilon_o/\epsilon_v)[a_3 + a_1 \tan\theta_i] \right\}}{b_{21}b_{12} - b_{11}b_{22}} \tag{22}$$

$$V_1 = \frac{-jk_o b_{11} \left\{ 2a_1 \cos\theta_i + \sin\theta_i (1 - \epsilon_o/\epsilon_v)[a_3 + a_1 \tan\theta_i] \right\}}{b_{21}b_{12} - b_{11}b_{22}} \tag{23}$$

$$T_3 = \frac{1}{\epsilon_v \, [e^{-p_2L} e^{-jq_2L} - e^{p_2L} e^{jq_2L}]} \left\{ \frac{\epsilon_3 k_o \sin\theta_i}{k_3 \cos\theta_3} \cdot [T_1 e^{-p_2L} e^{-jq_2L} + V_1 e^{p_2L} e^{jq_2L}] - \epsilon_o e^{p_2L} e^{jq_2L} \cdot [a_3 - \tan\theta_i (T_1 + V_1 - a_1)] \right\} \tag{24}$$

$$V_3 = \epsilon_o/\epsilon_v \, [a_3 - \tan\theta_i (T_1 + V_1 - a_1)] - T_3 \tag{25}$$

The parameters used in the above equations are defined below:

$$a_{11} = (jk_3 \cos\theta_3 - p_1 - jq_1) e^{-p_1L} e^{-jq_1L}$$

$$a_{12} = (jk_3 \cos\theta_3 + p_1 + jq_1) e^{p_1L} e^{jq_1L}$$

$$a_{21} = jk_o \cos\theta_i + p_1 + jq_1$$

$$a_{22} = jk_o \cos\theta_i - p_1 - jq_1$$

$$b_{11} = e^{-p_2L} e^{-jq_2L} (p_2 + jq_2 - \alpha)$$

$$b_{12} = -e^{p_2L} e^{jq_2L} (p_2 + jq_2 + \alpha)$$

$$b_{21} = p_2 + jq_2 + jk_o\,[\cos\theta_i + \sin\theta_i \tan\theta_i (1 - \epsilon_o/\epsilon_v)]$$

$$b_{22} = -\left\{p_2 + j\dot{q}_2 - jk_o\,[\cos\theta_i + \sin\theta_i \tan\theta_i (1 - \epsilon_o/\epsilon_v)]\right\}$$

where

$$\alpha = j\left\{k_3 \cos\theta_3 + k_o^2 \sin^2\theta_i (1 - \epsilon_3/\epsilon_v) / (k_3 \cos\theta_3)\right\}$$

Now that the mean waves have been fully determined, the scattered waves can be calculated. The scattered waves in the upper medium (air) will then be used to compute the backscatter coeffieient.

SCATTERED WAVE SOLUTION

In the random medium, the scattered or incoherent field is calculated from the following equation:

$$[\nabla \mathrm{x}\, \nabla \mathrm{x} - k_s^2]\, \underline{E}_s^{(2)}(\underline{r}) = \xi(\underline{r}) < \underline{E}(\underline{r}) > \tag{26}$$

For our problem, the mean wave $< \underline{E}(\underline{r}) >$ is given by $\underline{E}_2(\underline{r})$ as shown in (18). A superscript 2 is used with $\underline{E}_s^{(2)}(\underline{r})$ to indicate clearly the scattered field in the random medium. A solution for this scattered field can be obtained by using a two-dimensional Fourier transform.

$$\underline{E}_s^{(2)}(\underline{r}) = \frac{1}{(2\pi)^2} \int \underline{dk}_t\, \underline{G}_s(\underline{k}_t, z) e^{j\underline{k}_t \cdot \underline{r}_t} \tag{27}$$

where

$$\underline{k}_t = k_x \hat{a}_x + k_y \hat{a}_y \qquad \underline{r}_t = x\hat{a}_x + y\hat{a}_y$$

$$\underline{G}_s(\underline{k}_t, z) = G_{sx}(\underline{k}_t, z)\hat{a}_x + G_{sy}(\underline{k}_t, z)\hat{a}_y + G_{sz}(\underline{k}_t, z)\hat{a}_z$$

When the complete expression for the mean wave in the random medium as given by (18) is placed in (26), a term of the form $\xi(r)\exp(-jk_o x \sin\theta_i)$ on the right side results. This term will be written as a two-dimensional Fourier transform.

$$S(\underline{k}_t, z) = \int \underline{dr}_t \xi(\underline{r}) e^{-jk_o x \sin\theta_i} e^{-j\underline{k}_t \cdot \underline{r}_t}$$

$$\xi(\underline{r}) e^{-jk_o x \sin\theta_i} = \frac{1}{(2\pi)^2} \int \underline{dk}_t S(\underline{k}_t, z) e^{j\underline{k}_t \cdot \underline{r}_t} \tag{28}$$

When (27) and (28) are placed in (26) and the result is put in matrix form,

$$\begin{bmatrix} (k_y^2 - k_s^2 - D_z^2) & -k_x k_y & jk_x D_z \\ -k_x k_y & (k_x^2 - k_s^2 - D_z^2) & jk_y D_z \\ jk_x D_z & jk_y D_z & (k_x^2 + k_y^2 - k_s^2) \end{bmatrix} \begin{bmatrix} G_{sx} \\ G_{sy} \\ G_{sz} \end{bmatrix} = \begin{bmatrix} f_x(z) \\ f_y(z) \\ f_z(z) \end{bmatrix} \tag{29}$$

where D_z represents the differential operator d/dz. The quantities on the right side of (29) are defined below:

$$f_x(z) = S(\underline{k}_t, z)[T_1 e^{p_2 z} e^{jq_2 z} + V_1 e^{-p_2 z} e^{-jq_2 z}]$$

$$f_y(z) = S(\underline{k}_t, z)[T_2 e^{p_1 z} e^{jq_1 z} + V_2 e^{-p_1 z} e^{-jp_1 z}]$$

$$f_z(z) = S(\underline{k}_t, z)[T_3 e^{p_2 z} e^{jq_2 z} + V_3 e^{-p_2 z} e^{-jq_2 z}]$$

Solutions for the quantities G_{sx}, G_{sy}, and G_{sz} can be obtained by solving the three differential equations in (29) using the method of variation of parameters.

$$G_{sx}(\underline{k}_t, z) = A_1 e^{-jk_z' z} + A_2 e^{jk_z' z} + \frac{1}{2jk_z' k_s^2} \left[\int_{-L}^{z} f(z) e^{jk_z' z} dz \right]$$

$$\cdot e^{-jk_z' z} - \frac{1}{2jk_z' k_s^2} \left[\int_{L}^{z} f(z) e^{-jk_z' z} dz \right] e^{jk_z' z} \tag{30}$$

$$G_{sy}(\underline{k}_t, z) = B_1 e^{-jk'_z z} + B_2 e^{jk'_z z} - \frac{1}{2jk_z k_a^2}\left[\int_{-L}^{z} h(z) e^{jk'_z z} dz\right]$$

$$\cdot e^{-jk'_z z} + \frac{1}{2jk_z k_a^2}\left[\int_{-L}^{z} h(z) e^{-jk'_z z} dz\right] e^{jk'_z z} \tag{31}$$

$$G_{sz}(\underline{k}_t, z) = \frac{(k_x A_1 + k_y B_1)}{k'_z} e^{-jk'_z z} - \frac{(k_x A_2 + k_y B_2)}{k'_z}$$

$$\cdot e^{jk'_z z} + \frac{e^{-jk'_z z}}{2jk_z'^2 k_a^2} \int_{-L}^{z} \left[k_x f(z) - k_y h(z)\right] e^{jk'_z z} dz$$

$$+ \frac{e^{jk'_z z}}{2jk_z'^2 k_a^2} \int_{-L}^{z} \left[k_x f(z) - k_y h(z)\right] e^{-jk'_z z} dz - \frac{f_z(z)}{k_z'^2} \tag{32}$$

$$k'_z = \sqrt{k_a^2 - k_x^2 - k_y^2}$$

$$f(z) = f_x(z)[k_a^2 - k_x^2] - k_y k_x f_y(z) + jk_x D_z f_z(z)$$

$$h(z) = \frac{k_y(k_a^2 - k_y^2)}{k_x} f_x(z) - (k_a^2 - k_y^2) f_y(z) - jk_y D_z f_z(z)$$

$$+ \frac{k_y}{k_x}(k_x^2 + k_y^2 - k_a^2) f_x(z)$$

The quantities A_1, A_2, B_1, and B_2 are not functions of z and at present, are unknown. Although the solutions for G_{sx}, G_{sy}, and G_{sz} are rather formidable in appearance, it will be found after some mathematical manipulations that a solution will emerge. The three components of the scattered electric field in the upper medium $(z > 0)$ can be written in the following form:

$$E^{(1)}_{sx}(r) = \frac{1}{(2\pi)^2} \int \underline{dk}_t A_x(\underline{k}_t) e^{j(k_x x + k_y y - k_{1z} z)} \tag{33}$$

$$E^{(1)}_{sy}(\underline{r}) = \frac{1}{(2\pi)^2} \int \underline{dk}_t A_y(\underline{k}_t) e^{j(k_x x + k_y y - k_{1z} z)} \tag{34}$$

$$E^{(1)}_{sz}(\underline{r}) = \frac{1}{(2\pi)^2} \int \underline{dk}_t A_z(\underline{k}_t) e^{j(k_x x + k_y y - k_{1z} z)} \tag{35}$$

where

$$k_{1z} = \sqrt{k_o^2 - k_x^2 - k_y^2}$$

The parameter k_{1z} w[illegible] obtained by taking any one of the field components given above and putting it i[illegible] the free space scalar wave equation. The superscript 1 is used to refer to the fiel[illegible] the upper medium, which is air. Therefore, $E^{(1)}_{sx}(\underline{r})$ would indicate the x component of the scattered electric field in air. The components of the scattered electric field in the soil $(z < -L)$ can be written as follows:

$$E^{(3)}_{sx}(\underline{r}) = \frac{1}{(2\pi)^2} \int \underline{dk}_t C_x(\underline{k}_t) e^{j(k_x x + k_y y + k_{3z} z)} \tag{36}$$

$$E^{(3)}_{sy}(\underline{r}) = \frac{1}{(2\pi)^2} \int \underline{dk}_t C_y(\underline{k}_t) e^{j(k_x x + k_y y + k_{3z} z)} \tag{37}$$

$$E^{(3)}_{sz}(\underline{r}) = \frac{1}{(2\pi)^2} \int \underline{dk}_t C_z(\underline{k}_t) e^{j(k_x x + k_y y + k_{3z} z)} \tag{38}$$

where

$$k_{3z} = \sqrt{k_3^2 - k_x^2 - k_y^2}$$

The superscript 3 refers to the computation of the scattered fields in the soil. The expression for k_{3z} is obtained by putting any one of the field components into the scalar wave equation, which has a propagation constant k_3. The unknowns associated with the scattered waves are represented by A_x, A_y, A_z, A_1, A_2, B_1, B_2, C_x, C_y, and C_z. The only unknowns for which an explicit solution is needed are A_x, A_y, and A_z. Since the only interest is in computing the backscattered far field in air, complete solutions for the scattered fields in the other mediums are not needed. The boundary conditions that the scattered waves must satisfy are provided below:

$$E^{(1)}_{sx} = E^{(2)}_{sx} \quad \text{at } z = 0$$

$$E^{(1)}_{sy} = E^{(2)}_{sy} \quad \text{at } z = 0$$

$$\frac{\partial E^{(1)}_{sz}}{\partial y} - \frac{\partial E^{(1)}_{sy}}{\partial z} = \frac{\partial E^{(2)}_{sz}}{\partial y} - \frac{\partial E^{(2)}_{sy}}{\partial z} \quad \text{at } z = 0$$

$$\frac{\partial E^{(1)}_{sx}}{\partial z} - \frac{\partial E^{(1)}_{sz}}{\partial x} = \frac{\partial E^{(2)}_{sx}}{\partial z} - \frac{\partial E^{(2)}_{sz}}{\partial x} \quad \text{at } z = 0$$

$$E^{(2)}_{sx} = E^{(3)}_{sx} \quad \text{at } z = -L$$

$$E^{(2)}_{sy} = E^{(3)}_{sy} \quad \text{at } z = -L$$

$$\frac{\partial E^{(2)}_{sz}}{\partial y} - \frac{\partial E^{(2)}_{sy}}{\partial z} = \frac{\partial E^{(3)}_{sz}}{\partial y} - \frac{\partial E^{(3)}_{sy}}{\partial z} \quad \text{at } z = -L$$

$$\frac{\partial E^{(2)}_{sx}}{\partial z} - \frac{\partial E^{(2)}_{sz}}{\partial x} = \frac{\partial E^{(3)}_{sx}}{\partial z} - \frac{\partial E^{(3)}_{sz}}{\partial x} \quad \text{at } z = -L$$

The boundary conditions given above, along with the divergence equations in the two homogeneous media allow ten independent equations to be formulated.

$$k_x A_x + k_y A_y = k_{1z} A_z \tag{39}$$

$$k_x C_x + k_y C_y = -k_{3z} C_z \tag{40}$$

$$A_x = A_1 + A_2 + \frac{1}{2jk_z' k_s^2} \int_{-L}^{o} f(z)[e^{jk_z' z} - e^{-jk_z' z}]\,dz \tag{41}$$

$$A_y = B_1 + B_2 + \frac{1}{2jk_z' k_s^2} \int_{-L}^{o} h(z)[e^{-jk_z' z} - e^{jk_z' z}]\,dz \tag{42}$$

$$C_x = e^{jk_{3z}L} \{A_1 e^{jk_z' L} + A_2 e^{-jk_z' L}\} \tag{43}$$

$$C_y = e^{jk_{3z}L} \{B_1 e^{jk_z' L} + B_2 e^{-jk_z' L}\} \tag{44}$$

$$jk_y A_z + jk_{1z} A_y = jk_y G_{sz}(k_t, o) - \left.\frac{\partial G_{sy}}{\partial z}\right|_{z = 0} \tag{45}$$

$$k_{1z} A_x + k_x A_z = j \left.\frac{\partial G_{sx}}{\partial z}\right|_{z = 0} + k_x G_{sz}(k_t, o) \tag{46}$$

$$jk_y G_{sz}(k_t, -L) - \left.\frac{\partial G_{sy}}{\partial z}\right|_{z = -L} = jk_y C_z e^{-jk_{3z}L} - jk_{3z} C_y e^{jk_{3z}L} \tag{47}$$

$$\left.\frac{\partial G_x}{\partial z}\right|_{z = -L} - jk_x G_{sx}(k_t, -L) = jk_{3z} C_x e^{-jk_{3z}L} - jk_x C_z e^{-jk_{3z}L} \tag{48}$$

A solution for A_x, A_y, and A_z using the above equations would be quite difficult for arbitrary values of k_x and k_y. However, since we are only interested in the backscattered far field in air, a basic expression for the far field can be obtained by using the Stratton-Chu integral as modified by Silver.[4] When equations (33) through (35) are evaluated on the surface $(z = 0)$ and placed into the Stratton-Chu integral, the following equation for the scattered far field ($\underline{E}_{sf}$) will result:

---

[4]S. Silver, *Microwave Antenna Theory and Design*, McGraw Hill, New York, 1947.

$$\underline{E}_{sf} = \frac{2\cos\theta_i\,(jk_o)e^{-jk_oR}}{4\pi R} \quad \underline{a}_x A_x(k_o\sin\theta_i, 0) + \underline{a}_y A_y(k_o\sin\theta_i, 0)$$

$$+ \underline{a}_z A_z(k_o\sin\theta_i, 0) \tag{49}$$

Where R is the distance from the origin of the coordinate system to the field point where $\underline{E}_{sf}$ is required. It can now be seen that solutions for A_x, A_y, and A_z are only needed for values of $k_x = k_o\sin\theta_i$ and $k_y = 0$. When the appropriate expressions for the derivatives are substituted into equations (45) through (48) and we let $k_y = 0$, the 10 equations (39) through (48) become.

$$k_x A_x = k_{1z} A_z \tag{50}$$

$$k_x C_x = k_{3z} C_z \tag{51}$$

$$A_x = A_1 + A_2 + \frac{I_1}{2jk_z' k_a^2} \tag{52}$$

$$A_y = B_1 + B_2 + \frac{I_2}{2jk_z' k_a^2} \tag{53}$$

$$C_x = e^{jk_{3z}L}\left[A_1 e^{jk_z'L} + A_2 e^{-jk_z'L}\right] \tag{54}$$

$$C_y = e^{jk_{3z}L}\left[B_1 e^{jk_z'L} + B_2 e^{-jk_z'L}\right] \tag{55}$$

$$jk_{1z}A_y = jk_z' B_1 - jk_z' B_2 - \frac{I_3}{2k_a^2} \tag{56}$$

$$k_{1z}A_x + k_x A_z = k_z' A_1 - k_z' A_2 + \frac{1}{2jk_a^2}(1 + k_x^2/k_z'^2)I_4$$

$$+ \frac{k_x^2}{k_z'}(A_1 - A_2) - \frac{k_x f_z(0)}{k_z'^2} \tag{57}$$

$$-k_z' B_1 e^{jk_z' L} + k_z' B_2 e^{-jk_z' L} = k_{3z} C_y e^{-jk_{3z} L} \tag{58}$$

$$A_2 (k_z'^3 + k_x^2 k_z') e^{-jk_z' L} - A_1 (k_z'^3 + k_x^2 k_z') e^{jk_z' L} + k_x f_z(-L)$$

$$= k_z'^2 e^{-jk_{3z} L} (k_{3z} C_x - k_x C_z) \tag{59}$$

The quantities I_1, I_2, I_3, and I_4 used in the above equations are integrals in z and are defined below:

$$I_1 = \int_{-L}^{o} f(z) \left[e^{jk_z' z} - e^{-jk_z' z} \right] dz$$

$$I_2 = \int_{-L}^{o} h(z) \left[e^{-jk_z' z} - e^{jk_z' z} \right] dz$$

$$I_3 = \int_{-L}^{o} h(z) \left[e^{jk_z' z} + e^{-jk_z' z} \right] dz$$

$$I_4 = \int_{-L}^{o} f(z) \left[e^{jk_z' z} + e^{-jk_z' z} \right] dz$$

The functions $f(z)$, $h(z)$ and k_z' can be evaluated at $k_y = 0$, before integration takes place. When all the above equations are used to solve for A_x, A_y, and A_z, the following results are derived:

$$A_x(k_x, o) = b_1 f_z(-L) + b_2 f_z(o) + \int_{-L}^{o} f(z) \left\{ b_5 e^{jk_z' z} \right.$$

$$\left. + \, b_6 e^{-jk_z' z} \right\} dz \tag{60}$$

$$A_y(k_x, o) = \frac{-1}{jk_a^2 \; k_{1z}(1+\tilde{a}_1) + k_z'(1-\tilde{a}_1)} \int_{-L}^{o} h(z)$$

$$\cdot \left\{ \tilde{a}_1 e^{-jk_z' z} + e^{jk_z' z} \right\} dz \qquad (61)$$

$$A_z(k_x, o) = k_x \left\{ b_1 f_z(-L) + b_2 f_z(o) + \int_{-L}^{o} f(z) \right.$$

$$\left. \cdot \left[b_5 e^{jk_z' z} + b_6 e^{-jk_z' z} \right] dz \right\} / k_{1z} \qquad (62)$$

In the above three equations, k_x is to be evaluated at $k_o \sin\theta_i$. The new quantities introduced into the above equations are defined below:

$$\tilde{a}_1 = (k_z' - k_{3z}) e^{-2jk_z' L} / (k_z' + k_{3z})$$

$$\tilde{a}_2 = \frac{\left[k_{3z}(k_z'^3 + k_x^2 k_z') - k_z'^2 (k_{3z}^2 + k_x^2) \right] e^{-2jk_z' L}}{\left[k_{3z}(k_z'^3 + k_x^2 k_z') + k_z'^2 (k_{3z}^2 + k_x^2) \right]}$$

$$\tilde{a}_3 = \frac{k_{3z} k_x e^{-jk_z' L}}{\left[k_{3z}(k_z'^3 + k_x^2 k_z') + k_z'^2 (k_{3z}^2 + k_x^2) \right]}$$

$$\tilde{a}_4 = k_z'^2 (k_{1z}^2 + k_x^2)$$

$$\tilde{a}_5 = k_{1z}(k_z'^3 + k_z' k_x^2)(1 - \tilde{a}_2)$$

$$\tilde{a}_6 = k_{1z}(k_z'^3 + k_z' k_x^2) \tilde{a}_3$$

$$\tilde{a}_7 = k_{1z}(k_z'^2 + k_x^2) / (2jk_a^2)$$

$$\tilde{a}_8 = \tilde{a}_5 + \tilde{a}_4 (\tilde{a}_2 + 1)$$

$$b_1 = 2k_{1z}(k_z{}^3 + k_z' k_x^2)\tilde{a}_3 \,/\, \tilde{a}_8$$

$$b_2 = -k_{1z}k_x(1 + \tilde{a}_2) \,/\, \tilde{a}_8$$

$$b_3 = \tilde{a}_7(1 + \tilde{a}_2) \,/\, \tilde{a}_8$$

$$b_4 = \tilde{a}_5 \,/\, (2j\tilde{a}_8 \; k_z' k_a^2)$$

$$b_5 = b_3 + b_4$$

$$b_6 = b_3 - b_4$$

If the receiver in the far field is sensitive to a unit polarization vector $\underline{e}_r$, then the received field (E_R) will be

$$E_R = \underline{e}_r \cdot \underline{E}_{sf}$$

where $\underline{e}_r$ in general has three components ($\underline{e}_r = \underline{a}_x e_{rx} + \underline{a}_y e_{ry} + \underline{a}_z e_{rz}$). The next step in calculating the backscatter coefficient is to determine the statistical average of $E_R E_R^*$, using (49).

$$\begin{aligned} \langle E_R E_R^* \rangle = \frac{4k_o^2 \cos^2\theta_i}{16\pi^2 R^2} \Big\{ & e_{rx} e_{rx}^* \langle A_x A_x^* \rangle + 2\mathrm{Re}[e_{rx} e_{ry} \\ & \cdot \langle A_x A_y^* \rangle] + 2\mathrm{Re}[e_{rx} e_{rz}^* \langle A_x A_z^* \rangle] + e_{ry}^2 \\ & \cdot \langle A_y A_y^* \rangle + 2\mathrm{Re}[e_{ry} e_{rz}^* \langle A_y A_z^* \rangle] + e_{rz} e_{rz}^* \\ & \cdot \langle A_z A_z^* \rangle \Big\} \end{aligned} \tag{63}$$

The brackets $< - - - - >$ around $E_R E_R^*$ are used to indicate the calculation of the statistical average. The possibility of e_{rx} and e_{rz} being complex is anticipated, with e_{ry} always being real. What is required now is the computation of each of the six terms inside the brackets of (63). The determination of $< A_y A_y^* >$ will be considered first:

$$< A_y A_y^* > = k_a^2 k_a^{*2} M_o M_o^* \int_{-L}^{o} dz \int_{-L}^{o} dz \int_{-\infty}^{\infty} dx \cdot \int_{-\infty}^{\infty} dx' \int_{-\infty}^{\infty} dy \int_{-\infty}^{\infty} dy' < \xi(\underline{r}) \xi^*(\underline{r}') > \cdot \hat{f}(z, z') \exp[-2jk_o(x - x')\sin\theta_i] \quad (64)$$

where

$$< \xi(\underline{r}) \xi^*(\underline{r}') > = (\omega^2 \mu_o^2 \eta_2^2 + k_o^4 \eta_1^2) e^{-|x - x'|/\ell x} e^{-|y - y'|/\ell y} e^{-|z - z'|/\ell z}$$

$$\begin{aligned}
\hat{f}(z, z') = {} & \tilde{a}_1 \tilde{a}_1^* T_2 T_2^* e^{D_1 z} e^{D_1^* z'} + \tilde{a}_1 T_2 a_1^* V_2^* e^{D_1 z} e^{D_2^* z'} \\
& + \tilde{a}_1 T_2 T_2^* e^{D_1 z} e^{-D_2^* z'} + \tilde{a}_1 T_2 V_2^* e^{D_1 z} e^{-D_1^* z'} \\
& + \tilde{a}_1 V_2 \tilde{a}_1^* T_2^* e^{D_2 z} e^{D_1^* z'} + \tilde{a}_1 \tilde{a}_1^* V_2 V_2^* e^{D_2 z} e^{D_2^* z'} \\
& + \tilde{a}_1 V_2 T_2^* e^{D_2 z} e^{-D_2^* z'} + \tilde{a}_1 V_2 V_2^* e^{D_2 z} e^{-D_1^* z'} \\
& + \tilde{a}_1^* T_2 T_2^* e^{-D_2 z} e^{D_1^* z'} + \tilde{a}_1^* T_2 V_2^* e^{-D_2 z} e^{D_2^* z'} \\
& + T_2 T_2^* e^{-D_2 z} e^{-D_2^* z'} + T_2 V_2^* e^{-D_2 z} e^{-D_1^* z'} \\
& + V_2 \tilde{a}_1^* T_2^* e^{-D_1 z} e^{D_1^* z'} + \tilde{a}_1^* V_2 V_2^* e^{-D_1 z} e^{D_2^* z'} \\
& + V_2 T_2^* e^{-D_1 z} e^{-D_2^* z'} + V_2 V_2^* e^{-D_1 z} e^{-D_1^* z'}
\end{aligned}$$

where

$$D_1 = p_1 + j(q_1 - k'_z) \quad \text{and} \quad D_2 = -(p_1 + jq_1 + jk'_z)$$

$$M_o = \frac{-1}{jk_a^2 \; k_{1z}(1 + a_1) + k'_z(1 - a_1)}$$

The form of $\hat{f}(z, z')$ given above appears to be very complicated. However, each of the 16 terms in $\hat{f}(z, z')$ consist of simple exponentials in z and z′ and therefore can be integrated easily. It should be remember when computing D_1 and D_2 that p_1 and q_1 are real, but k'_z will be complex. Making the substitution that $u = x - x'$ and $v = y - y'$ and transforming the x and y integrals into integrals in u and v produces

$$< A_y A_y^* > = (\omega^2 \mu_o^2 \eta_2^2 + k_o^4 \eta_1^2) k_a^2 k_a^{*2} M_o M_o^* \int_{-L}^{o} dz \int_{-L}^{o} dz' \int_{-\infty}^{\infty} du \int_{-\infty}^{\infty} dv \int_{-\infty}^{\infty} dx' \int_{-\infty}^{\infty} dy' \; f(z, z') \, e^{-2jk_o u \sin\theta_i} \, e^{-|u|/\ell_x} e^{-|v|/\ell_y} e^{-|z - z'|/\ell_z} \tag{65}$$

The integrals in x′ and y′ appear somewhat meaningless. These integrals actually represent the illuminated area in the xy plane, since it is physically unrealistic to have backscattered energy from a portion of the surface that is not illuminated. Considering the integrals in x′ and y′ to form the illuminated area (A_I) and carrying out the integrations in u and v will yield the following result:

$$< A_y A_y^* > = \frac{4\ell_x \ell_y A_I (\omega^2 \mu_o^2 \eta_2^2 + k_o^4 \eta_1^2) k_a^2 k_a^{*2} M_o M_o^*}{(1 + 4k_o^2 \ell_x^2 \sin^2\theta_i)} \int_{-L}^{o} dz \int_{-L}^{o} dz' \; \hat{f}(z, z') e^{-|z - z'|/\ell_z} \tag{66}$$

Consider now a typical term of $\hat{f}(z, z')$ which is of the form $Ae^{az}e^{bz'}$ where A,a, and b are not functions of z or z', and make a transformation of variables from z and z' to $n_z = z - z'$ and $z'' = z'$. Then, the results of carrying out the integration for this one term becomes

$$\int_{-L}^{0} dz \int_{-L}^{0} dz' \, Ae^{az} e^{bz'} e^{-|z - z'|/\ell_z} =$$

$$\frac{A\ell_z}{(a+b)} \left\{ \frac{1 - \ell_z b + \ell_z(a+b)e^{-L(a + 1/\ell_z)} - (1 + \ell_z a)e^{-L(a + b)}}{(1 + \ell_z a)\,(1 - \ell_z b)} \right.$$

$$\left. + \frac{1 - \ell_z a + \ell_z(a+b)e^{-L(1/\ell_z + b)} - e^{-L(a + b)}(1 + b\ell_z)}{(1 + \ell_z b)\,(1 - \ell_z a)} \right\}$$

When the answer for the integration in z and z' given above is used for each of the 16 terms in $\hat{f}(z, z')$, then the final result for $< A_y A_y^* >$ can be written.

$$< A_y A_y^* > = \frac{4\ell_x \ell_y \ell_z A_I(\omega^2 \mu_o^2 \eta_2^2 + k_o^4 \eta_1^2) k_a^2 k_a^{*2} M_o M_o^*}{(1 + 4k_o^2 \ell_x^2 \sin^2\theta_i)}$$

$$\cdot \sum_{n=1}^{16} \frac{A_n}{(c_n + d_n)} \left\{ \frac{1 - \ell_z d_n + \ell_z(c_n + d_n)e^{-L(c_n + 1/\ell_z)} - (1 + \ell_z c_n)e^{-L(c_n + d_n)}}{(1 + \ell_z c_n)\,(1 - \ell_z d_n)} \right. \tag{67}$$

$$\left. + \frac{1 - \ell_z c_n + \ell_z(c_n + d_n)e^{-L(d_n + 1/\ell_z)} - e^{-L(c_n + d_n)}(1 + d_n \ell_z)}{(1 + \ell_z d_n)\,(1 - \ell_z c_n)} \right\}$$

The values for the A_n's, the c_n's, and d_n's are provided in appendix A and simply come from the expression for $\hat{f}(z, z')$. Using the methodology for computing $< A_y A_y^* >$, one can caluclate all the remaining terms in (63). All of these other terms are given in appendix A. An expression for the radar backscatter coefficient (σ_v^o) can be written in terms of $< E_R E_R^* >$

$$\sigma_v^\circ = \frac{4\pi R^2}{A_I} \frac{< E_R E_R^* >}{\underline{E}_i \cdot \underline{E}_i^*} \tag{68}$$

The subscript v on σ_v° is used to indicate a volume scattering result from a plane layer of random media. No consideration for rough surface scattering is given in σ_v°. Using (63) and the expression for the incident wave given previously, one can write a final result for σ_v°:

$$\sigma_v^\circ = \frac{k_o^2 \cos^2\theta_i}{\pi(a_1 a_1^* + a_2 a_2^* + a_3 a_3^*)}$$

$$\cdot \Big\{ e_{rx} e_{rx}^* \alpha_{xx} + 2\mathrm{Re}\,[e_{rx} e_{ry} \alpha_{xy}]$$

$$+ 2\mathrm{Re}\,[e_{rx} e_{rz}^* \alpha_{xz}] + e_{ry}^2 \alpha_{yy} + 2k_o \sin\theta_i$$

$$\cdot \mathrm{Re}\,[e_{ry} e_{rz} \alpha_{xy} / k_{1z}] + e_{rz} e_{rz}^* \alpha_{zz} \Big\} \tag{69}$$

where

$$\alpha_{xx} = < A_x A_x^* > / A_I$$

$$\alpha_{xy} = < A_x A_y^* > / A_I$$

$$\alpha_{xz} = < A_x A_z^* > / A_I$$

$$\alpha_{yy} = < A_y A_y^* > / A_I$$

$$\alpha_{zz} = < A_z A_z^* > / A_I$$

Consider now the form of σ_v° for horizontal and vertical polarizations. The following parameters are used to describe a wave that is transmitted with horizontal polarization and horizontal polarization is received.

$$a_1 = 0 \qquad e_{rx} = 0$$

$$a_2 = 1 \qquad e_{ry} = 1$$

$$a_3 = 0 \qquad e_{rz} = 0$$

For these parameters, the backscatter coefficient can be given the additional subscripts of HH to indicate horizontal polarization transmit, and horizontal polarization receive.

$$\sigma^{\circ}_{HHv} = k_o^2 \, \alpha_{yy} \cos^2\theta_i / \pi \tag{(70)}$$

The case of vertical polarization transmit, vertical polarization receive can be characterized as follows:

$$a_1 = \cos\theta_i \qquad e_{rx} = \cos\theta_i$$

$$a_2 = 0 \qquad e_{ry} = 0$$

$$a_3 = \sin\theta_i \qquad e_{rz} = \sin\theta_i$$

The backscatter coefficient associated with these parameters can be given the additional subscripts VV.

$$\sigma^{\circ}_{VVv} = \frac{k_o^2 \cos^2\theta_i}{\pi} \left\{ \alpha_{xx} \cos^2\theta_i + 2\mathrm{Re}\left[\alpha_{xz} \cos\theta_i \sin\theta_i\right] + \alpha_{zz} \sin^2\theta_i \right\} \tag{71}$$

If a result is computed for the cross-polarized backscatter coefficient (HV or VH), the term will disappear. The reason for this is that the particular elements of the dyadic M, which would yield cross-polarized terms in the mean wave, are all zero. Next, let's consider the influence of an irregular vegetation-soil boundary.

MODIFYING THE VOLUME SCATTERING RESULTS TO INCORPORATE THE INFLUENCE OF AN IRREGULAR VEGETATION – SOIL BOUNDARY

In this section, we will consider what must be done to equations (70) and (71) to include the influence of a rough ground surface. It is expected that the influence of the rough surface would be greater when the angle of incidence is small. Also, as the vegetation height or density gets larger, less scattering is expected from the ground surface below. In what follows, the horizontal and vertical polarizations will be considered separately.

Consider a horizontally polarized wave incident from free space onto a layer of vegetation that has an average thickness L. The interface between the vegetation and soil will be considered as randomly rough in such a way that the tangent plane approximation is applicable. The radar backscatter coefficient (σ°_{HH}) will be considered as the sum of a term resulting from surface scattering and a term resulting from volume scattering.

$$\sigma^{\circ}_{HH} = \sigma^{\circ}_{HHS} \exp\left[-4\alpha_{e1} L \sec\psi_{e1}\right] + \sigma^{\circ}_{HHv} \tag{72}$$

In equation (72), σ°_{HHS} represents the backscatter coefficient for a randomly rough surface with a guassian distribution of surface heights. The subscript s indicates surface scattering. The quantity σ°_{HHS} is multiplied by a decaying exponential in which α_{e1} is the imaginary part of the effective propagation constant and ψ_{e1} is the true angle of refraction for the mean wave in the vegetation. The second subscript 1 on α_{e1} and ψ_{e1} is used to indicate horizontal polarization since these parameters will have different values for vertical polarization. The effective propagation constant (k_{e1}) can be obtained from k_h.

$$k_{e1}^2 = k_{ez}^2 + k_{ex}^2 = k_h^2 + k_o^2 \sin^2\theta_i$$

If we now let $k_{e1} = \beta_{e1} - j\alpha_{e1}$ and in place of k_h we put $jp_1 - q_1$, then we can solve for β_{e1} and α_{e1}.

$$\beta_{e1} = \rho_{e1}^{1/2} \cos(\phi_{e1}/2)$$

$$\alpha_{e1} = \rho_{e1}^{1/2} \sin(\phi_{e1}/2)$$

Where ρ_{e1} and ϕ_{e1} are defined below:

$$\rho_{e1} = \left\{ 4p_1^2 q_1^2 + (q_1^2 + k_o^2 \sin^2\theta_i - p_1^2)^2 \right\}^{1/4}$$

$$\phi_{e1} = \tan^{-1} \left\{ \frac{2p_1 q_1}{q_1^2 + k_o^2 \sin^2\theta_i - p_1^2} \right\}$$

The planes of constant phase for the mean wave in the random medium are used to calculate an expression for $\sec\psi_{e1}$.

$$\sec\psi_{e1} = \frac{\sqrt{k_o^2 \sin^2\theta_i + \rho_1^2(\beta_{e1}\cos\gamma_1 - \alpha_{e1}\sin\gamma_1)}}{\rho_1\,(\beta_{e1}\cos\gamma_1 - \alpha_{e1}\sin\gamma_1)}$$

Where ρ_1 and γ_1 are given below:

$$\rho_1 = \left\{ 4a_1^2 b_1^2 \sin^4\theta_i + [1 - (a_1^2 - b_1^2)\sin^2\theta_i]^2 \right\}^{1/4}$$

$$\gamma_1 = \tfrac{1}{2}\tan^{-1}\left[\frac{2a_1 b_1 \sin^2\theta_i}{1 - (a_1^2 - b_1^2)\sin^2\theta_i} \right]$$

$$a_1 = \frac{k_o\,\beta_{e1}}{\beta_{e1}^2 + \alpha_{e1}^2} \qquad b_1 = \frac{k_o\,\alpha_{e1}}{\beta_{e1}^2 + \alpha_{e1}^2}$$

Many derived expressions are available for the backscatter coefficient from a randomly rough surface using the tangent plane method. The following equation will be used:[5]

$$\sigma^{\circ}_{HHS} = \frac{R_o^2}{4m_s^2\cos^4\psi_{e1}} \Big\{ 1 - \sin^2\psi_{e1}\,[2(1 - g_o\cos^2\psi_{e1}) - \sin^2\psi_{e1}(1 + g_o^2)] \Big\} \exp[-\tan^2\psi_{e1}/(4m_s^2)] \qquad (73)$$

---

[5] R. A. Hevenor, *Backscattering of Electromagnetic Waves From a Surface Composed of Two Types of Surface Roughness*, U.S. Army Engineer Topographic Laboratories, Fort Belvoir, Virginia, FTL-TR-71-4, October 1971, AD-737 675.

The quantity R_o in (73) represents the Fresnel reflection coefficient and can be computed as follows:

$$R_o = \frac{\beta_{e1} \cos \psi_{e1} - \sqrt{\beta_3^2 - \beta_{e1}^2 \sin^2 \psi_{e1}}}{\beta_{e1} \cos \psi_{e1} + \sqrt{\beta_3^2 - \beta_{e1}^2 \sin^2 \psi_{e1}}}$$

In calculating R_o, we have neglected the effect of the imaginary parts of the propagation constants. The term m_s represents the ratio of the standard deviation of the surface fluctuations to the correlation distance. The quantity g_o is defined by the following expression:

$$g_o = 1 - \frac{2\beta_{e1} \cos \psi_{e1}}{\sqrt{\beta_3^2 - \beta_{e1}^2 \sin^2 \psi_{e1}}}$$

A final equation can now be written for σ^o_{HH} that considers both the volume-scattering and surface-scattering effects.

$$\sigma^o_{HH} = \frac{R_o^2}{4m_s^2 \cos^4 \psi_{e1}} \Big\{ 1 - \sin^2 \psi_{e1} \, [2(1 - g_o \cos^2 \psi_{e1})$$

$$- \sin^2 \psi_{e1} (1 + g_o^2)] \Big\} \exp [-\tan^2 \psi_{e1}/(4m_s^2)]$$

$$\cdot \exp[-4\alpha_{e1} L \sec \psi_{e1}] + k_o^2 \alpha_{yy} \cos^2\theta_i/\pi \qquad (74)$$

In the same manner, a complete solution for vertical polarization can be obtained:

$$\sigma^o_{VV} = \frac{r_o^2}{4m_s^2 \cos^4 \psi_{e2}} \Big\{ 1 + \frac{r_o' \sin^2 \psi_{e2} \cos \psi_{e2}}{\gamma_o^2} [2r_o \sin\psi_{e2}$$

$$+ r_o' \cos \psi_{e2}] + \frac{2r_o'}{r_o} \sin \psi_{e2} \cos^3 \psi_{e2} \Big\}$$

$$\cdot \exp\left[-\tan^2 \psi_{e2}/(4m_s^2)\right] \exp\left[-4\,\alpha_{e2}\, L \sec \psi_{e2}\right]$$

$$+ \frac{k_o^2 \cos^2\theta_i}{\pi} \left\{ \alpha_{xx} \cos^2\theta_i + 2\mathrm{Re}\left[\cos\theta_i \sin\theta_i\, \alpha_{xz}\right] + \alpha_{zz} \sin^2\theta_i \right\} \tag{75}$$

The new quantities introduced into the above equation are defined below:

$$\beta_{e2} = \rho_{e2}^{1/2} \cos(\phi_{e2}/2)$$

$$\alpha_{e2} = \rho_{e2}^{1/2} \sin(\phi_{e2}/2)$$

The quantities ρ_{e2} and ϕ_{e2} are given as follows:

$$\rho_{e2} = \left\{ 4p_2^2 q_2^2 + (q_2^2 + k_o^2 \sin^2\theta_i - p_2^2)^2 \right\}^{1/2}$$

$$\phi_{e2} = \tan^{-1} \left\{ \frac{2p_2 q_2}{q_2^2 + k_o^2 \sin^2\theta_i - p_2^2} \right\}$$

$$\sec \psi_{e2} = \frac{\sqrt{k_o^2 \sin^2\theta_i + \rho_2^2 (\beta_{e2}^2 \cos\gamma_2 - \alpha_{e2} \sin \gamma_2)^2}}{\rho_2 (\beta_{e2} \cos \gamma_2 - \alpha_{e2} \sin \gamma_2)}$$

$$\rho_2 = \left\{ 4a_2^2 b_2^2 \sin^4\theta_i + [1 - (a_2^2 - b_2^2) \sin^2\theta_i]^2 \right\}^{1/4}$$

$$\gamma_2 = \tfrac{1}{2} \tan^{-1} \left[\frac{2a_2 b_2 \sin^2\theta_i}{1 - (a_2^2 - b_2^2) \sin^2\theta_i} \right]$$

where a_2 and b_2 are

$$a_2 = \frac{k_o \beta_{e2}}{\beta_{e2}^2 + \alpha_{e2}^2} \qquad b_2 = \frac{k_o \alpha_{e2}}{\beta_{e2}^2 + \alpha_{e2}^2}$$

$$r_2 = \frac{\beta_3^2 \cos\psi_{e2} - \beta_{e2}\sqrt{\beta_3^2 - \beta_{e2}^2 \sin^2\psi_{e2}}}{\beta_3^2 \cos\psi_{e2} + \beta_{e2}\sqrt{\beta_3^2 - \beta_{e2}^2 \sin^2\psi_{e2}}}$$

$$r_o' = \frac{2\beta_3^2 \beta_{e2} \sin\psi_{e2} (\beta_3^2 - \beta_{e2}^2)}{\sqrt{\beta_3^2 - \beta_{e2}^2 \sin^2\psi_{e2}}\left\{\beta_e^2 \cos\psi_{e2} + \beta_{e2}\sqrt{\beta_3^2 - \beta_{e2}^2 \sin^2\psi_{e2}}\right\}}$$

Equations (74) and (75) are the final results for the radar backscatter coeffieient for horizontal and vertical polarizations. Before the results of computing equations (74) and (75) are shown, an elementary vegetation permittivity model must be developed that relates some of the model input parameters to the complex dielectric constants of vegetation and water.

DEVELOPMENT OF A VEGETATION PERMITTIVITY MODEL

To determine the influence of various vegetation parameters (such as moisture content) upon the calculation of the backscatter coefficient, one must relate some of the permittivity parameters in the scattering model to the physical parameters of the vegetation. Peake and Oliver's model[6] will be used to calculate the relative complex dielectric constant of vegetation ($\hat{\epsilon}_v$):

$$\epsilon_v = (F/2)\mathrm{Re}[\hat{\epsilon}_w] + j(F/3)\mathrm{Im}[\hat{\epsilon}_w]$$

[6]W.H. Peake and T.L. Oliver, *The Response of Terrestrial Surfaces at Microwave Frequencies,* Technical Report AFAL-TR-70-301, The Ohio State University, Electroscience Laboratory, AD-884 106.

where F is the fraction of water by weight in the vegetation; $\mathrm{Re}[\hat{\epsilon}_w]$ and $\mathrm{Im}[\hat{\epsilon}_w]$ are the real and imaginary parts of the relative complex dielectric constant of water ($\hat{\epsilon}_w$), which can be written as

$$\hat{\epsilon}_w = 5 + \frac{75}{1 + j(1.85/\lambda)}$$

where λ is the wavelength in centimeters. For particular values of λ and F, we can now compute $\hat{\epsilon}_v$. With a knowledge of $\hat{\epsilon}_v$, one can estimate the average relative complex dielectric constant ($\hat{\epsilon}_a$) by using the following

$$\hat{\epsilon}_a = (V_v \hat{\epsilon}_v + \epsilon_A V_A)/V_T$$

$$\hat{\epsilon}_a = \mathrm{Re}[\hat{\epsilon}_a] \qquad \sigma_a = -\omega\epsilon_0 \left(\frac{V_v}{V_T}\right) \mathrm{Im}(\hat{\epsilon}_v)$$

where V_V is the volume occupied by the vegetation; V_A is the volume occupied by air; V_T is the total volume equal to $V_V + V_A$; ϵ_A is the relative dielectric constant of air, assumed equal to 1. The variances η_1^2 and η_2^2 can be computed by using the following formulas:

$$\eta_1^2 = \frac{V_v(\epsilon_v' - \epsilon_a)^2 + V_A(\epsilon_A - \epsilon_a)^2}{V_T}$$

$$\eta_2^2 = \frac{V_v(\sigma_v - \sigma_a)^2 + V_A \sigma_a^2}{V_T}$$

where

$$\sigma_v = -\omega\epsilon_0 F\,\mathrm{Im}[\epsilon_w]/3 \qquad \text{and} \qquad \epsilon_v' = \mathrm{Re}[\hat{\epsilon}_v]$$

The symbol R_V shall be used to designate the volume ratio V_V / V_T.

The developed model for the radar backscatter coefficient is now complete and calculations can be made. In the next section, computed results will be shown, and the theory will be compared with some existing experimental data.

DISCUSSION OF RESULTS

In this section, some numerical calculations will be shown for the theory derived in the previous section, and a study will be presented of the influence of the various input parameters on the backscatter coefficient. Two computer programs were developed for solving equations (74) and (75). One program solves for equation (74) and the second solves for (75). The solutions to the half-space and plane layer problems are also generated for comparison. A listing of the computer program for solving equation (74) is given in appendix B. The 10 input parameters to the programs are

1. Fraction of water by weight in the vegetation (F)
2. Volume of vegetation divided by the total volume (R_V)
3. Correlation distance in the x direction (ℓ_x)
4. Correlation distance in the y direction (ℓ_y)
5. Correlation distance in the z direction (ℓ_z)
6. Mean thickness of the vegetation layer (L)
7. Relative dielectric constant of the soil below the vegetation (ϵ_g)
8. Conductivity of the soil below the vegetation (σ_3)
9. Frequency (f)
10. Ratio of the standard deviation of the rough surface fluctuations to the correlation distance of the fluctuations (m_s).

The output of the computer programs is the backscatter coefficient in decibels as a function of incidence angle. The backscatter coefficient in decibels is related to the backscatter coefficient as follows:

$$\sigma^\circ \text{ (in decibels)} = 10 \log_{10} \sigma^\circ$$

The backscatter coefficient on the right side of the above equation is computed by (74) or (75). The following discussion centers on figures 2 through 30, which show the results of computing equations (74) and (75). Figures 2 and 3 come from Ulaby and Bush and provide pertinent ground truth data associated with the experimental measurements. Figure 4 comes from Cihlar and Ulaby[7] and provides a relationship between soil moisture and relative complex dielectric constant. Figures 5 through 15 provide a comparison of the developed theory with experimental data taken from a cornfield by Ulaby and Bush.[8]

---

[7]F.T. Ulaby and T.F. Bush, *Corn Growth as Monitores by Radar*, The University of Kansas Center for Research, Inc. RSL Technical Report 117-57, November 1975.

[8]F.T. Ulaby and J. Cihlar, *Dielectric Properties of Soils as a Function of Moisture Content*, The University of Kansas Center for Research, Inc., RSL Technical Report 177-47, November 1974.

FIGURE 2. Corn Ground Truth, 1974.

	Soil Moisture (g/cm^3)			% Plant Moisture	Normalized Plant Water Content (g/m)	Plant Height (m)
Date	N	M	F			
May 20	.19	.19	.24	89.5	77	0.30
May 24	.28	.26	.26	86.5	167	0.40
May 30	.12	.10	.12	87.1	252	0.58
June 5	.10	.13	.10	88.5	262	0.88
June 13	.34	.34	.34	89.9	552	1.25
June 20	.30	.31	.32	89.9	442	1.90
June 26	.06	.09	.08	83.9	383	2.30
July 1	.05	.05	.07	82.4	425	2.60
July 8	.21	.27	.30	84.7	440	2.60
July 11	.17	.15	.15	81.5	490	2.60
July 16	.04	.07	.06	81.5	374	2.60
July 22	.04	.04	.04	73.4	482	2.60
August 5	.06	.07	.07	62.4	236	2.60
Autust 15	.26	.27	.26	52.9	99	2.70
September 5	.31	.30	.29	47.5	151	2.70
September 19	.12	.12	.10	16.5	58	0.23
July 30*	.26	.26	.26	74.8	413	2.60

* = irrigated corn field N = near range sample M = medium range sample F = far range sample

SOURCE : F.T. Ulaby and T.F. Bush, *Corn Growth as Monitored by Radar,* The University of Kansas Center for Research, Inc. RSL Technical Report 117–57, November 1975.

Figure 2. Corn Ground Truth, 1974.

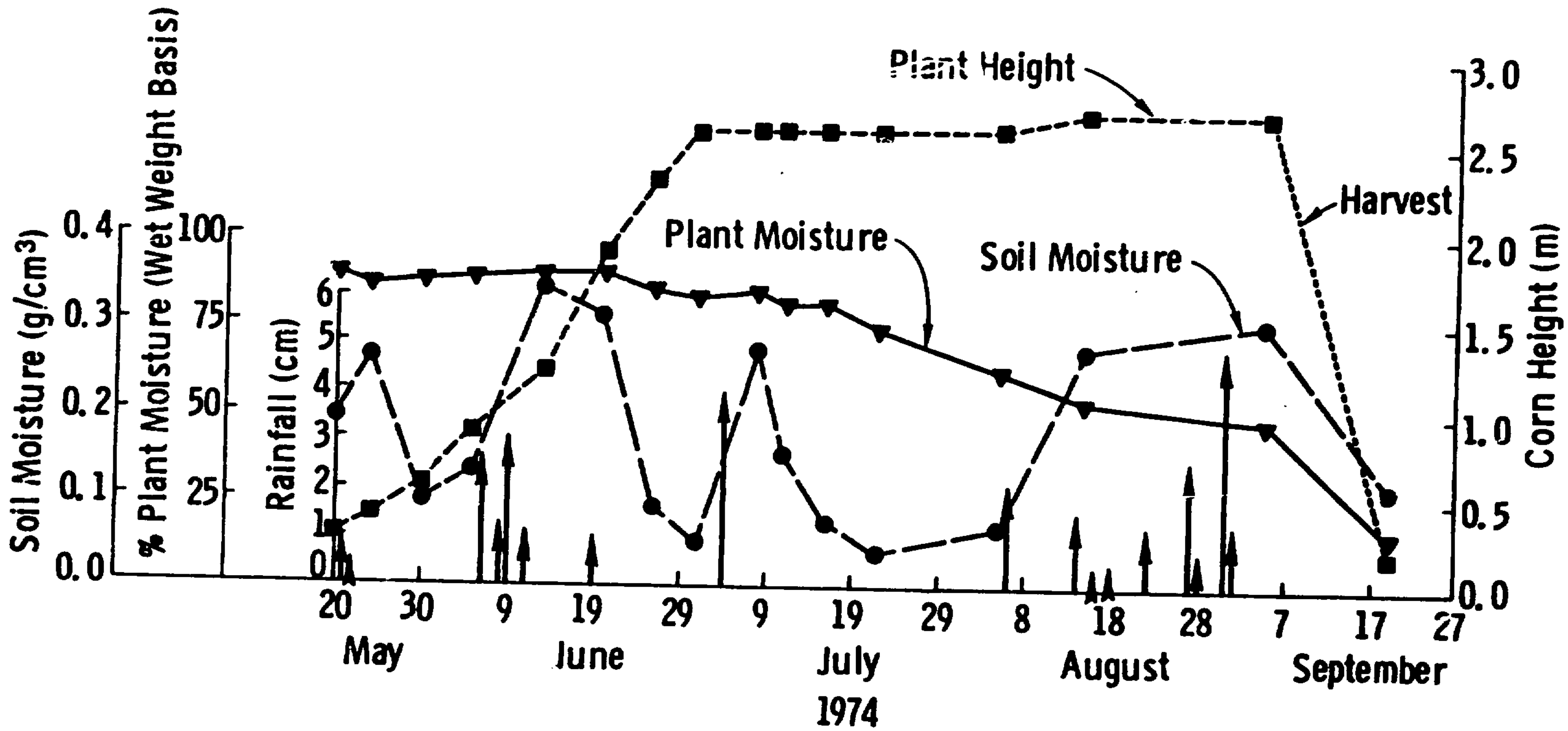

SOURCE : F.T. Ulaby and T.F. Bush, *Corn Growth as Monitored by Radar*, The University of Kansas Center for Research, Inc. RSL Technical Report 117–57, November 1975.

Figure 3. Data Record of Soil Moisture, Plant Moisture, Plant Height, and Precipitation as Measured During the Observation Period.

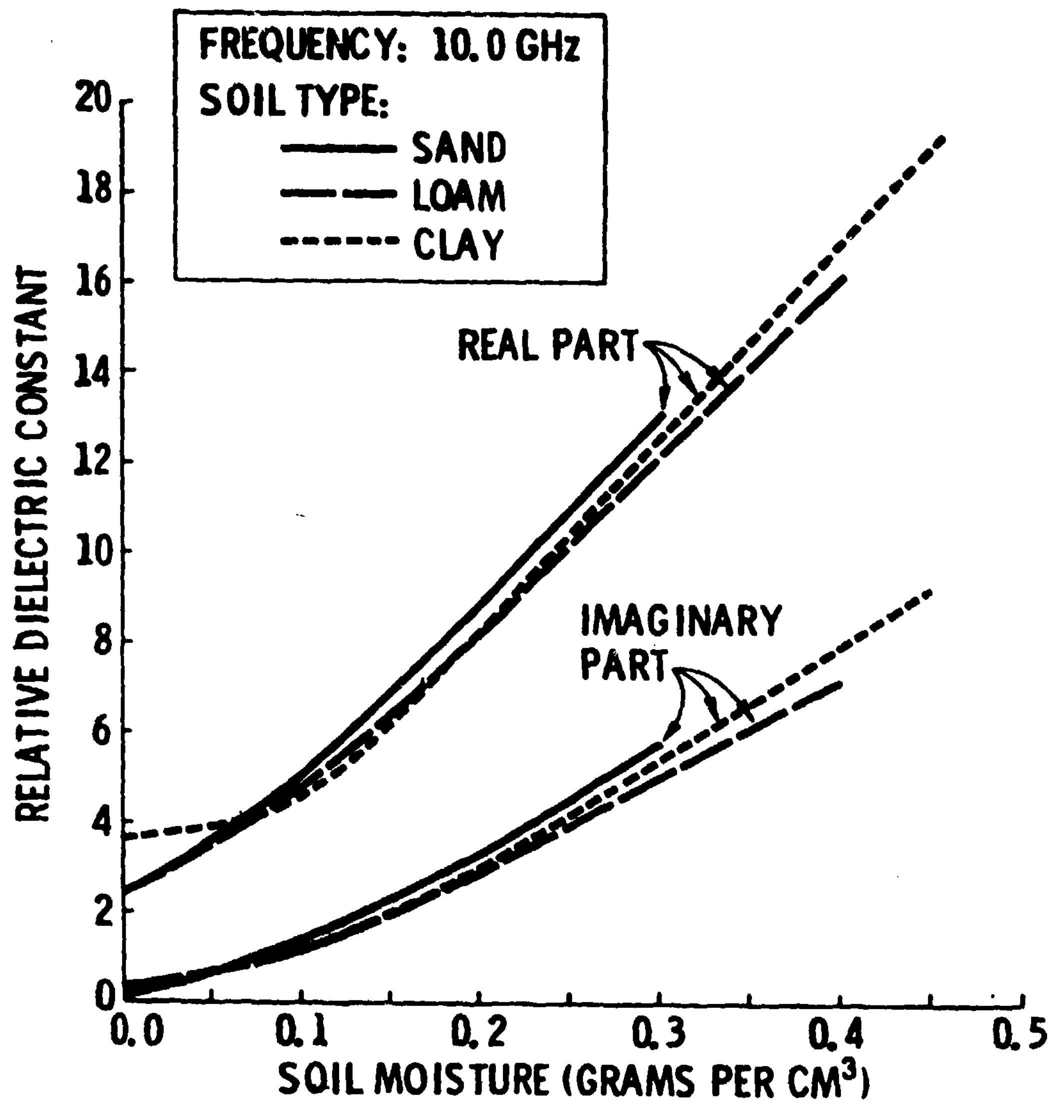

Source : F.T. Ulaby and J. Cihlar, *Dielectric Properties of Soils as a Function of Moisture Content*, The University of Kansas Center for Research, Inc., RSL Technical Report 177–47, November 1974.

Figure 4. Representative Dielectric Constant Values as a Function of Volumetric Water Content.

The soil moisture is obtained from figure 2 for a particular set of measurements performed on a given date. This soil moisture is used along with the curves of figure 4 to determine the relative dielectric constant and the conductivity of the soil. Throughout all comparisons of theory with experiment, it has been assumed that the soil type is a loam. In comparing theory with experiment, remember that certain input parameters to the theoretical model were not known and had to be estimated; whereas, other input parameters were known from the ground truth data collected during the experiment. The unknown input parameters are R_V, ℓ_x, ℓ_y, ℓ_z and m_s.

In figure 5, the theory is matched to the experimental data for corn that is at a height of 30 centimeters. The large rise that occurs in σ° as θ_i goes from 10° to 0° is indicative of a rough surface effect. In this case, the rough surface is quasi-specular since m_s is given such a small value. It can be seen that to match the theory with the experimental data, it was necessary to let ℓ_x be different from ℓ_y and to let ℓ_z be much smaller than ℓ_x or ℓ_y. The fact that ℓ_x is different from ℓ_y shows an anisotropic effect in the horizontal plane, which probably arises from the corn being planted in rows.

Figure 6 matches the theory to experimental data for corn that is 2.3 meters high. It can be seen that a good match is obtained for ℓ_x equal to ℓ_y, indicating that the anistropic effect in the horizontal plane has essentially disappeared for 8.6 GHz. The values of the parameters used for R_V, ℓ_x, ℓ_y, ℓ_z, and m_s in figure 6 are also used in figures 7 through 10 to determine whether the model could provide a correct prediction of σ° for different values of F, soil moisture, and vegetation height.

Figures [illegible] hrough 9 show an excellent agreement between theory and experiment. Figure 10 shows an excellent agreement between theory and experiment for angles of incidence equal to and greater than 30°. For angles of incidence less than 30°, the agreement is poor. A possible reason for this poor agreement may be due to the rainfall that came prior to the August 15th measurements. The rainfall could have disturbed the soil surface in both a physical and an electrical manner such that its scattering behavior is no longer predictable from prior values.

Figures 11 and 12 show an attempt to match the theory to the experimental data for frequencies of [illegible] GHz and 13 GHz. It can be seen that to obtain a good match, the [illegible] ℓ_y [illegible] ℓ_y must be altered from the values used at 8.6 GHz. This seems to indicate that as the frequency goes higher, the vegetation medium becomes more complicated and the anisotropic behavior becomes more pronounced.

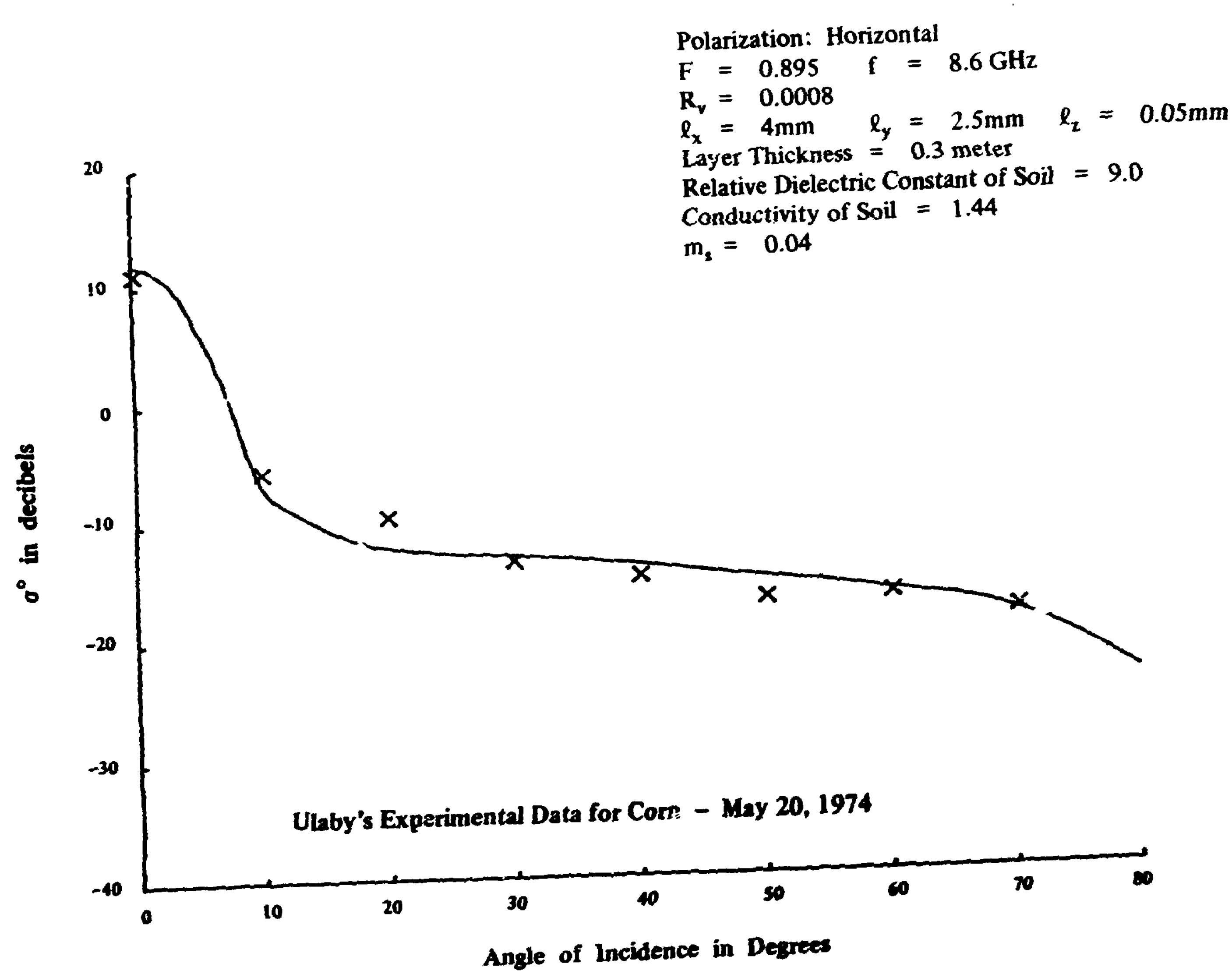

Figure 5. Comparison of Theory with Experimental Data.

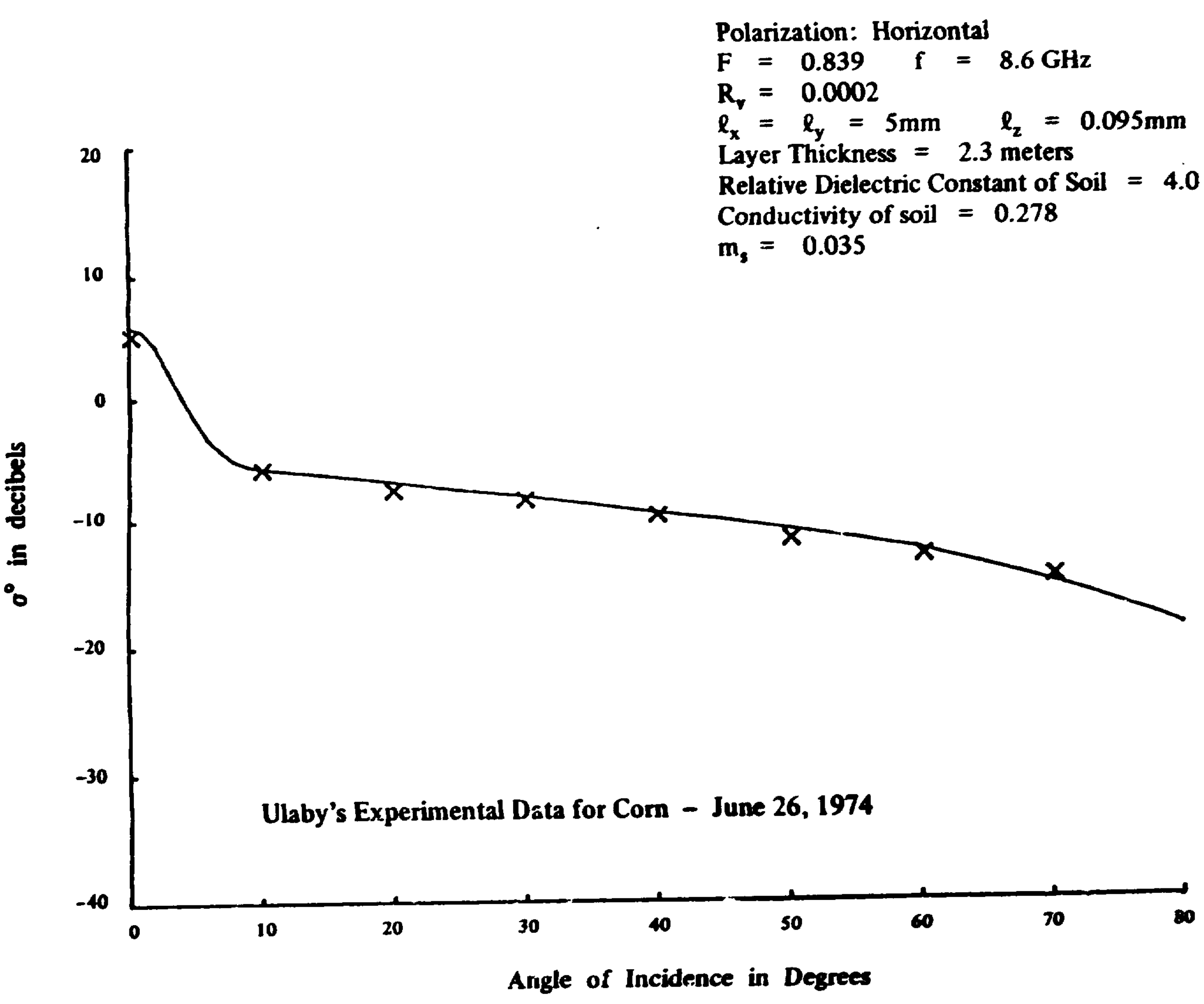

Figure 6. Comparison of Theory with Experimental Data.

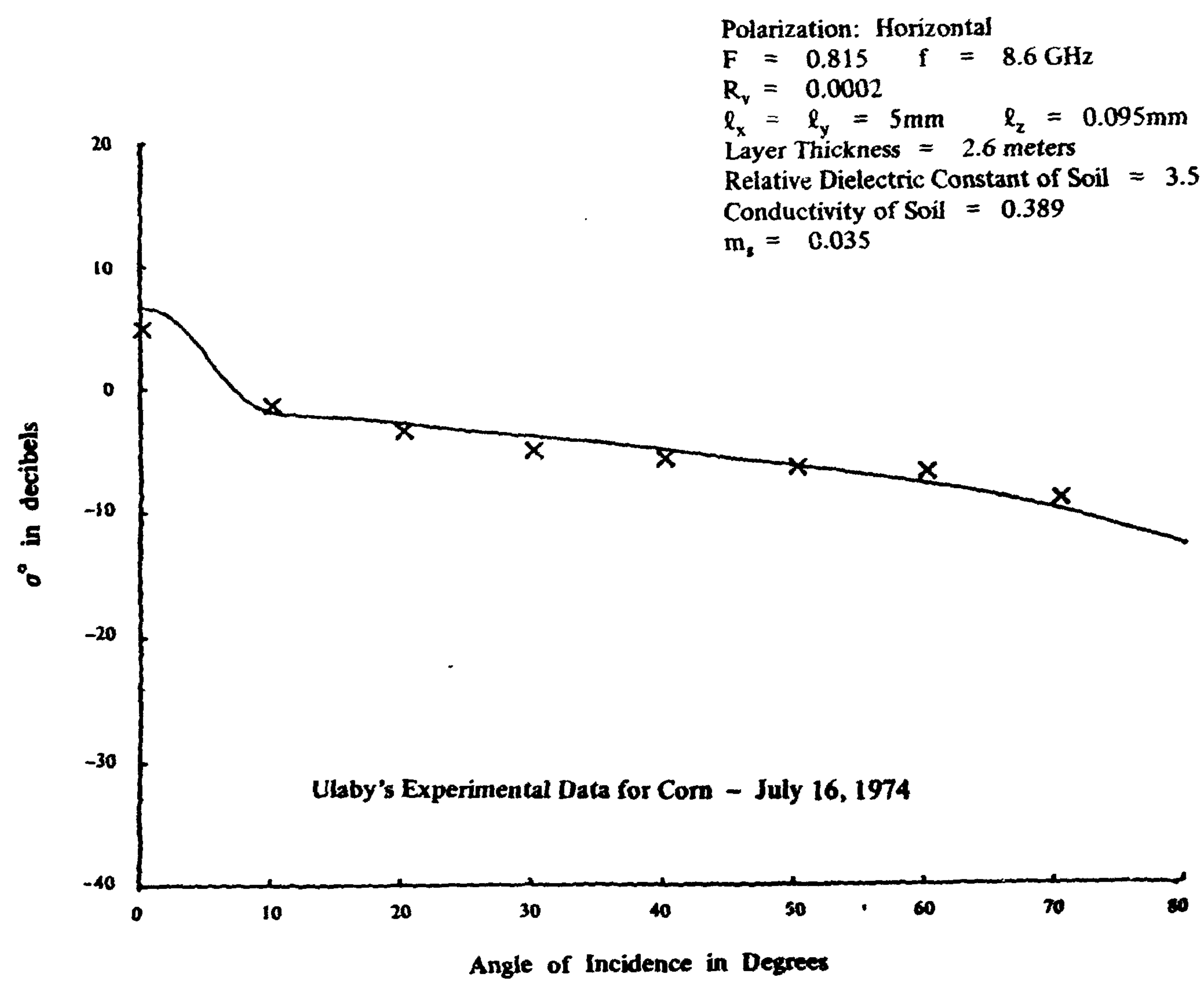

Figure 7. Comparison of Theory with Experimental Data.

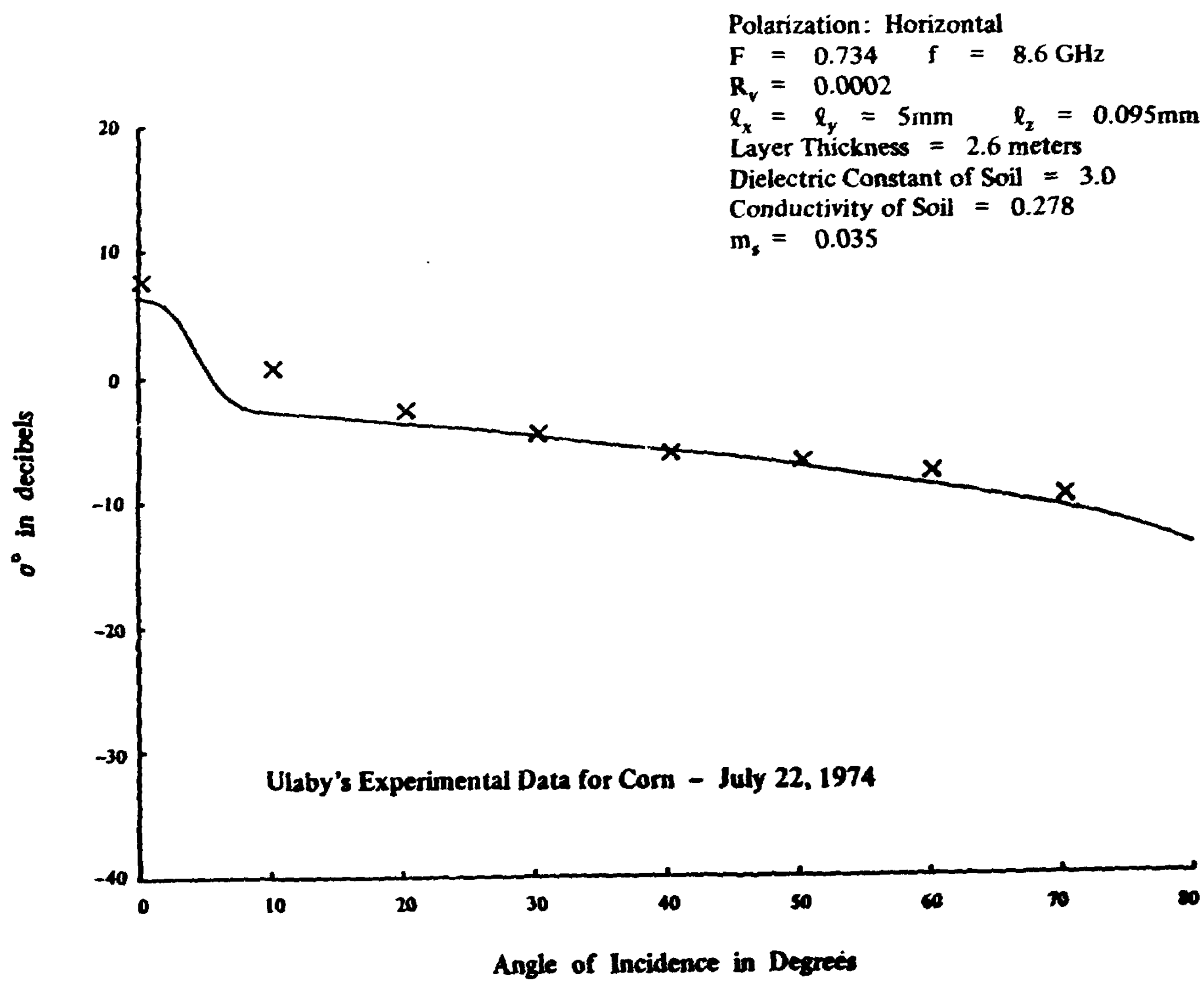

Figure 8. Comparison of Theory with Experimental Data.

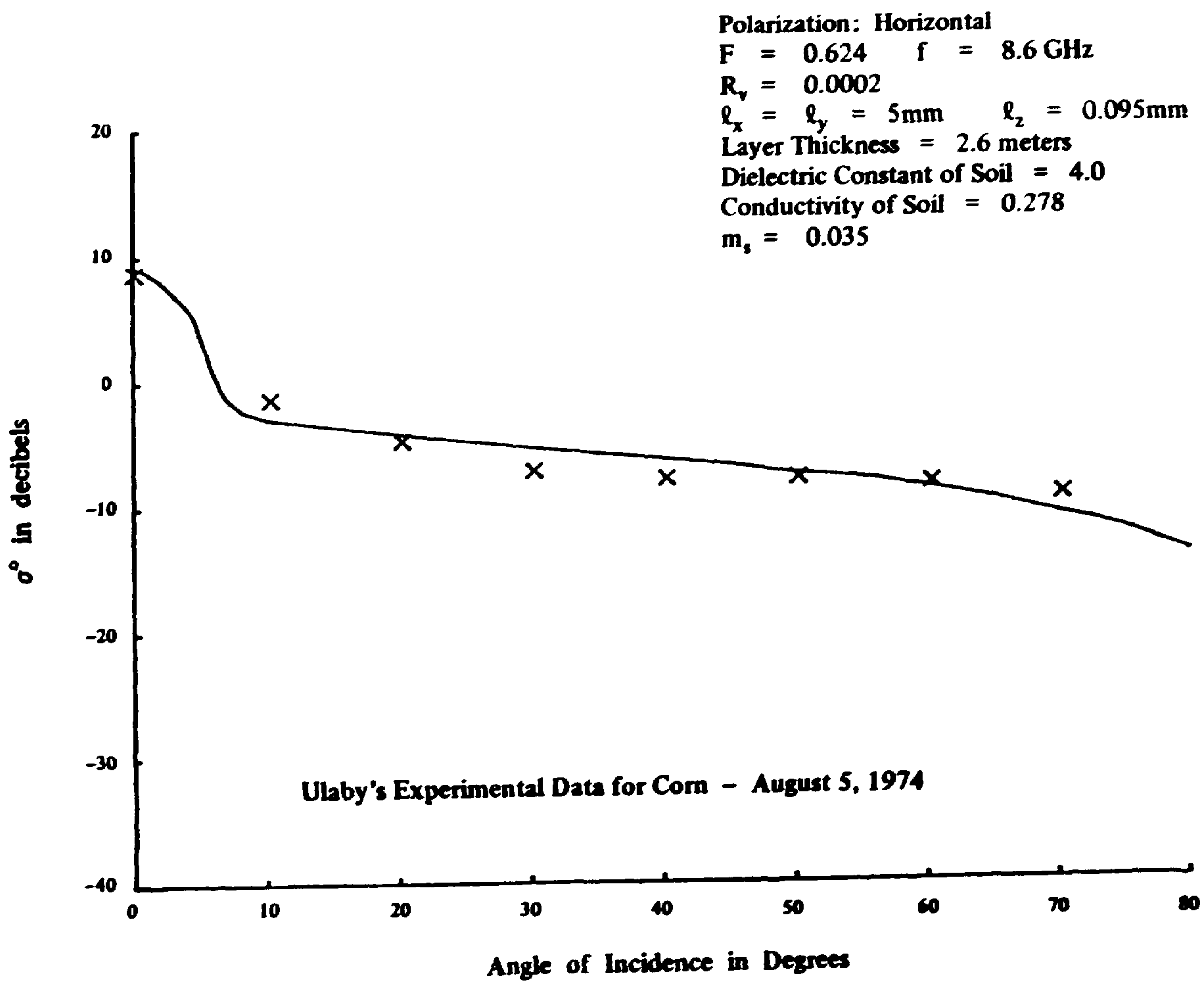

Figure 9. Comparison of Theory with Experimental Data.

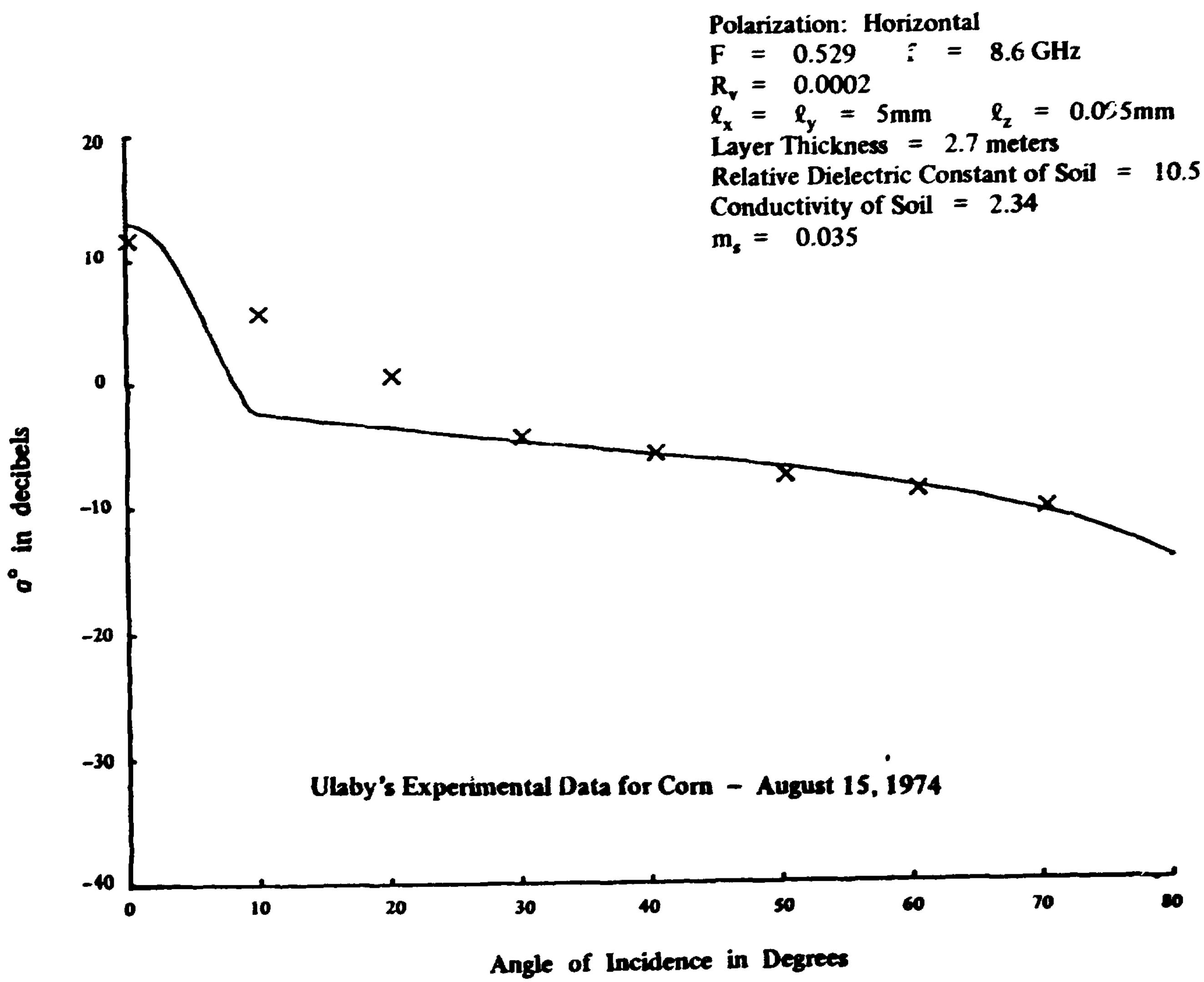

Figure 10. Comparison of Theory with Experimental Data.

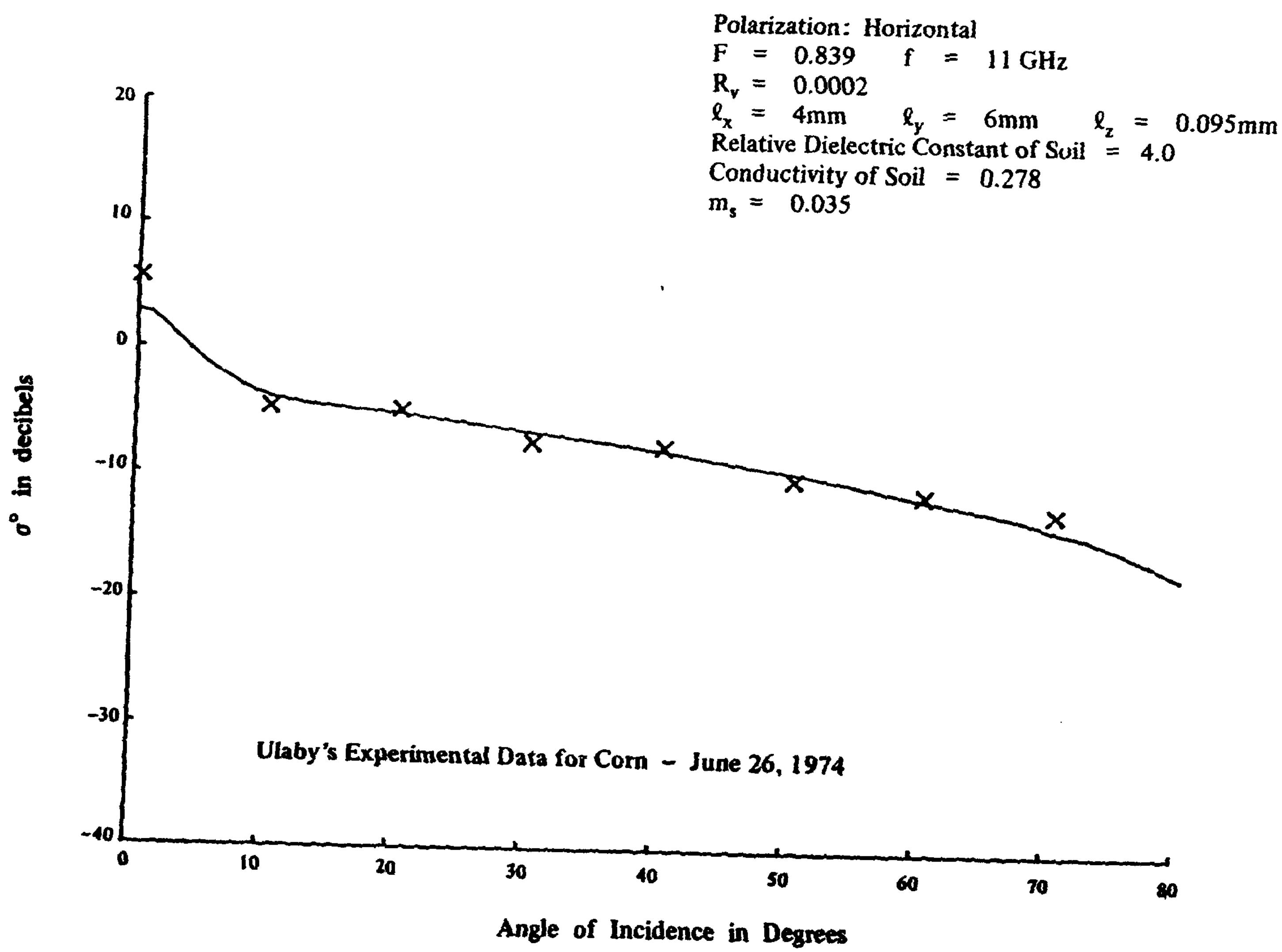

Figure 11. Comparison of Theory with Experimental Data.

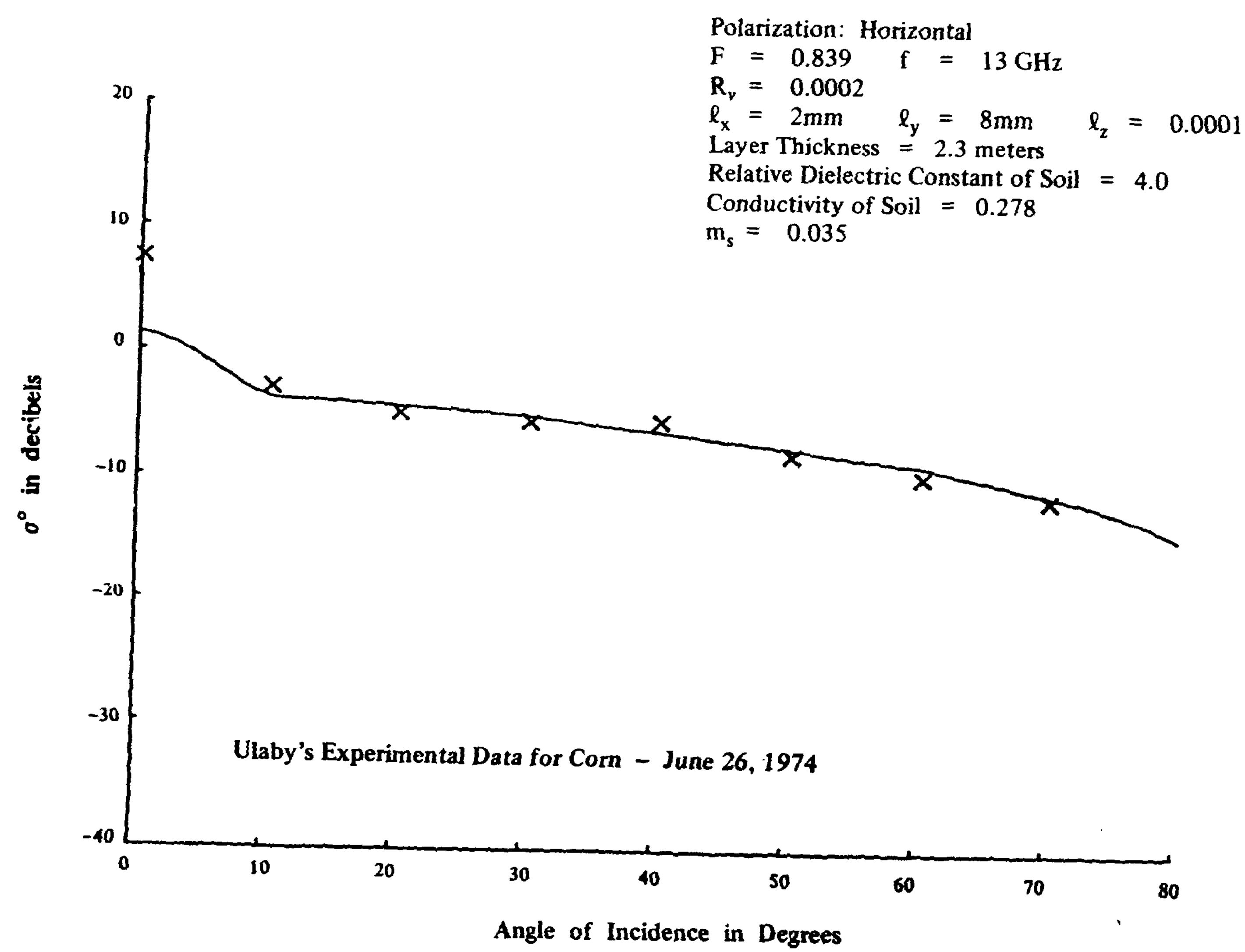

Figure 12. Comparison of Theory with Experimental Data.

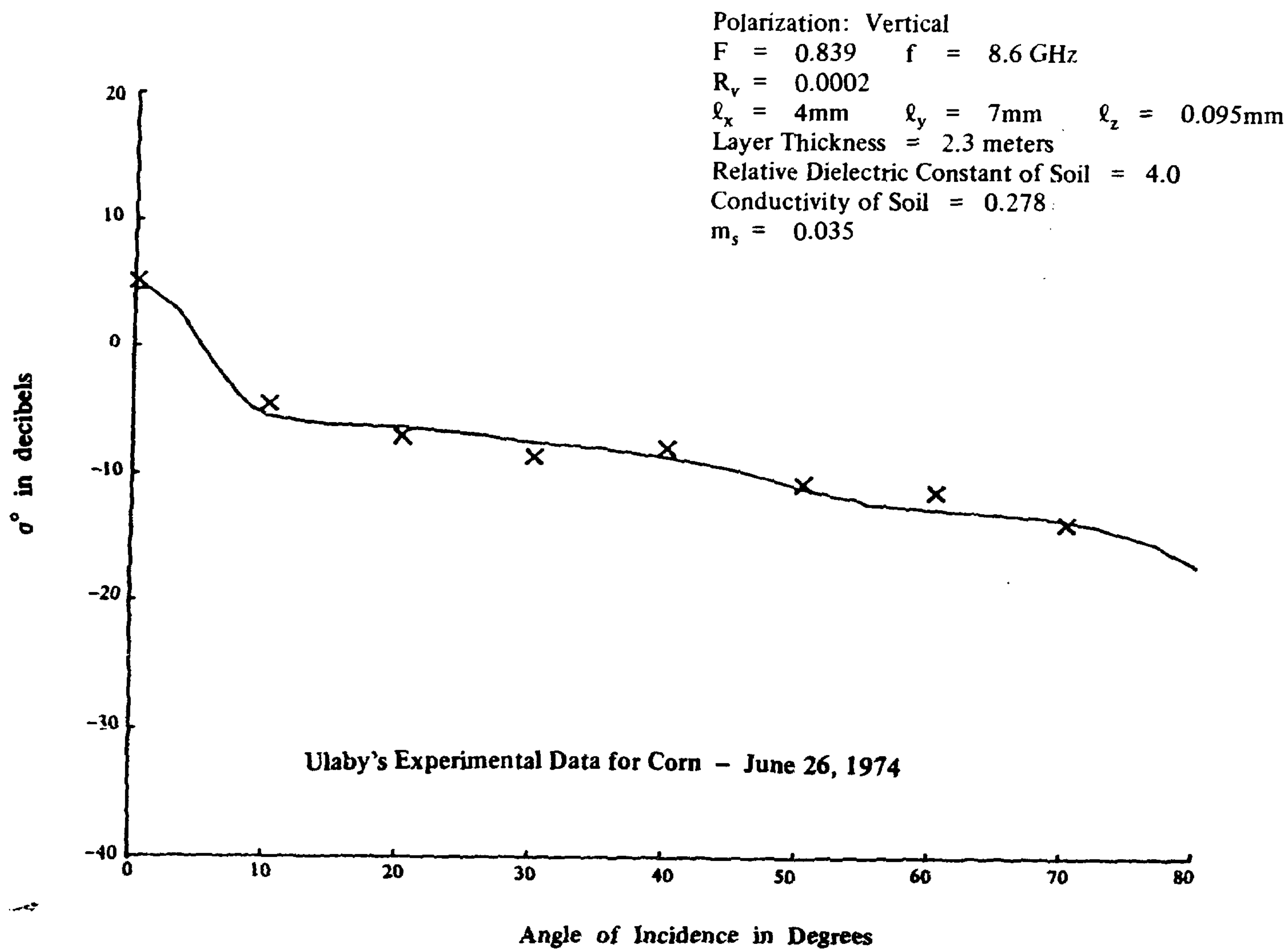

Figure 13. Comparison of Theory with Experimental Data.

In figures 13 through 15 a match is shown of the theory with experimental data for vertical polarization. For all three curves, ℓ_x must be made unequal to ℓ_y to obtain a good match. In figure 16, the variations are shown in the experimental measurements of σ°, which can occur throughout the spring and summer for alfalfa. Large variations in the backscatter coefficient occur prior to and after harvesting.

Figure 17 presents a study of sensor-look direction with respect to vegetation planted in rows. The two parameters $\sigma^{\circ}_{\perp}$ and $\sigma^{\circ}_{\parallel}$ represent the backscatter coefficient when the look direction is perpendicular and parallel to the rows, respectively. We see that when θ_i equals zero degrees, $\sigma^{\circ}_{\perp}$ and $\sigma^{\circ}_{\parallel}$ are equal. However, for θ_i greater than zero degrees, $\sigma^{\circ}_{\perp}$ is greater than $\sigma^{\circ}_{\parallel}$. The theoretical results agree only partically with the experimental results given in figure 18, which comes from Batlivala and Ulaby.[9]

Figure 19 provides a study of backscatter coefficient versus layer thickness for two angles of incidence. For the θ_i equal to zero curve, the solution for σ° with a rough layer differs from the half-space solution by approximately 16dB (decibels) for a layer thickness of 0.5 meters. As the layer thickness is increased, the solution for σ° at θ_i equal to zero, approaches the half-space solution. The θ_i equal to 20° curve also approaches the half-space solution when the layer thickness is increased. In this case, σ° differs from the half-space solution by only about 3.5dB when the layer thickness is 0.5 meters.

Figure 20 presents a study of the skin depth of the mean wave versus incidence angle for three different frequencics. For a horizontally polarized wave, the skin depth is taken to be the reciprocal of p_1, which was derived earlier as part of the solution to the Dyson's equation. It should be remembered that the mean wave decays for two reasons, absorption and scattering. For a frequency of 8.6 GHz, the skin depth goes from approximately 5 meters at θ_i equal to 0° down to 1 meter at θ_i equal to 80°. When the frequency is increased, the overall level of the curve is lowered considerably, but it does not drop off as fast with increasing incidence angle.

In figure 21, the solutions are compared for the half space, the plane layer, and the layer with a rough surface. For angles of incidence between 0° and 30°, the rough interface at the vegetation soil boundary can have a dramatic effect on σ°. In this case, it is clearly not sufficient to use a plane layer model.

---

[9] P.P. Batlivala and F.T. Ulaby, *The Effect of Look Direction on the Radar Return From a Row Crop,* National Aeronautics and Space Administration, Lyndon B. Johnson Space Center, Houston, Texas, RSL Technical Report 264–3, May 1975.

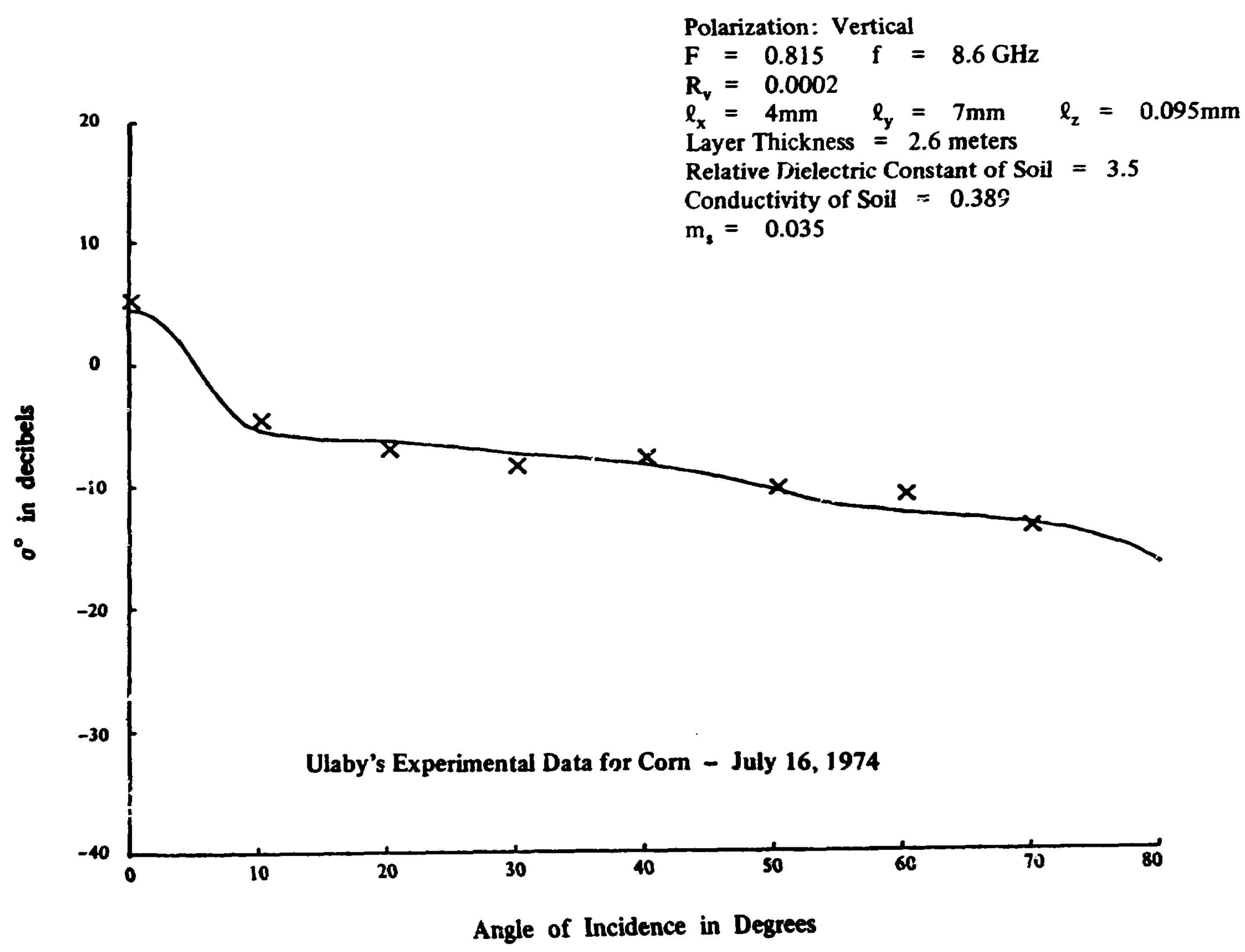

Figure 14. Comparison of Theory with Experimental Data.

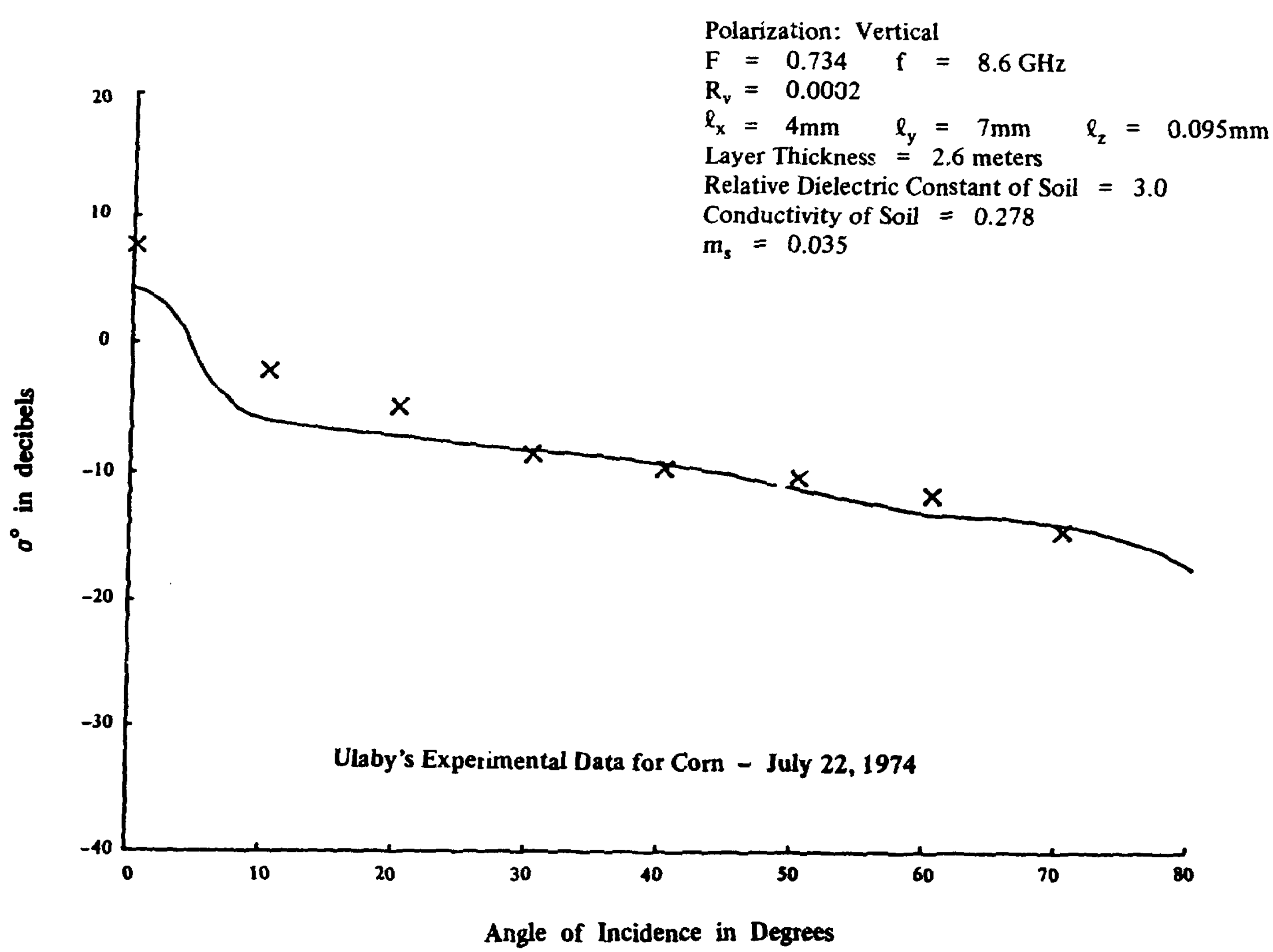

Figure 15. Comparison of Theory with Experimental Data.

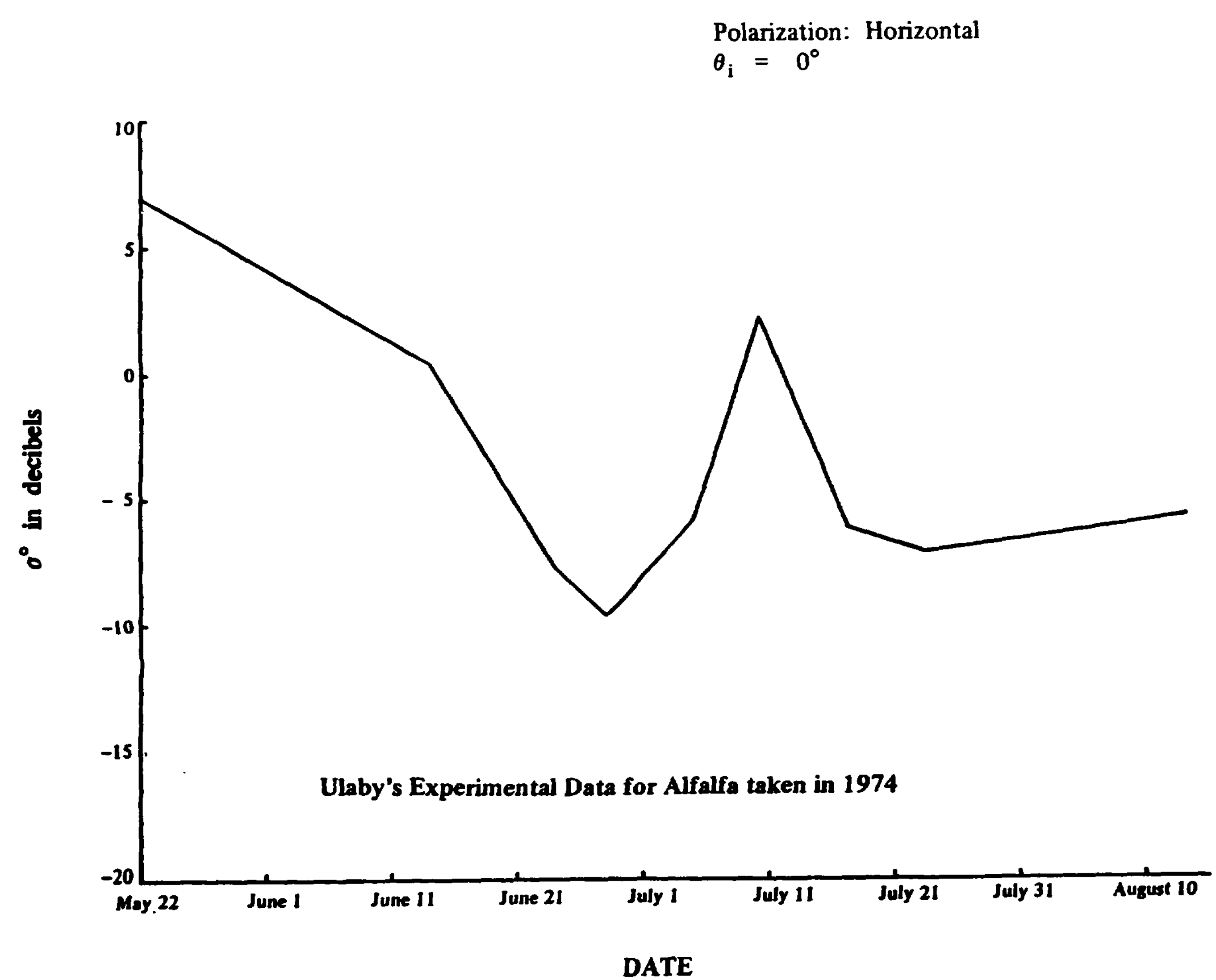

Figure 16. Study of the Experimental Variations of the σ° for Alfalfa.

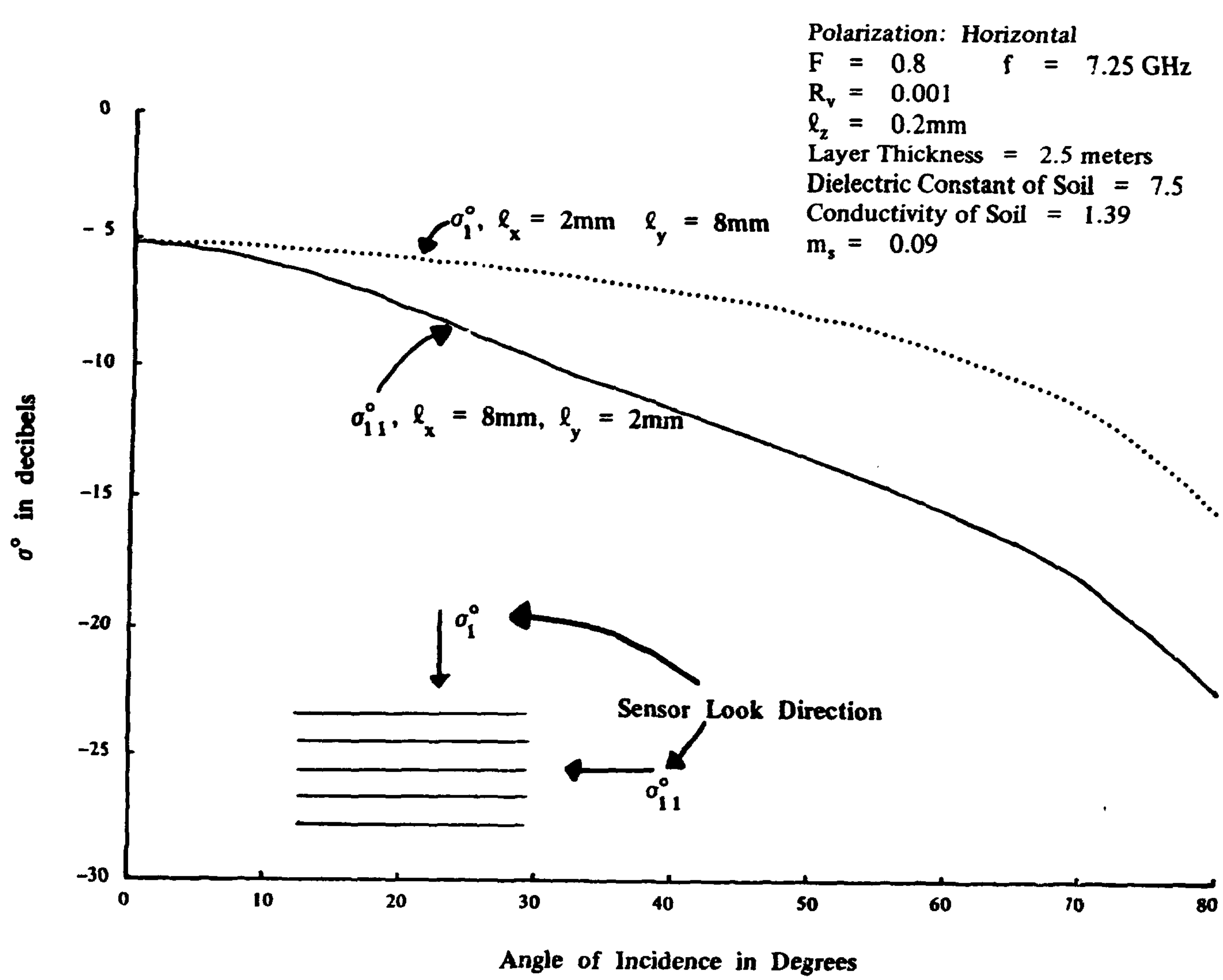

Figure 17. Study of the Sensor Look Direction.

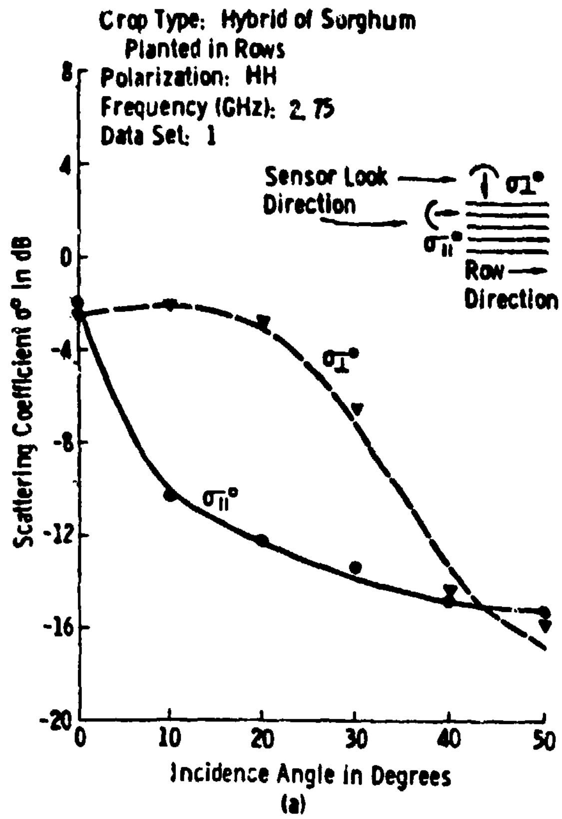

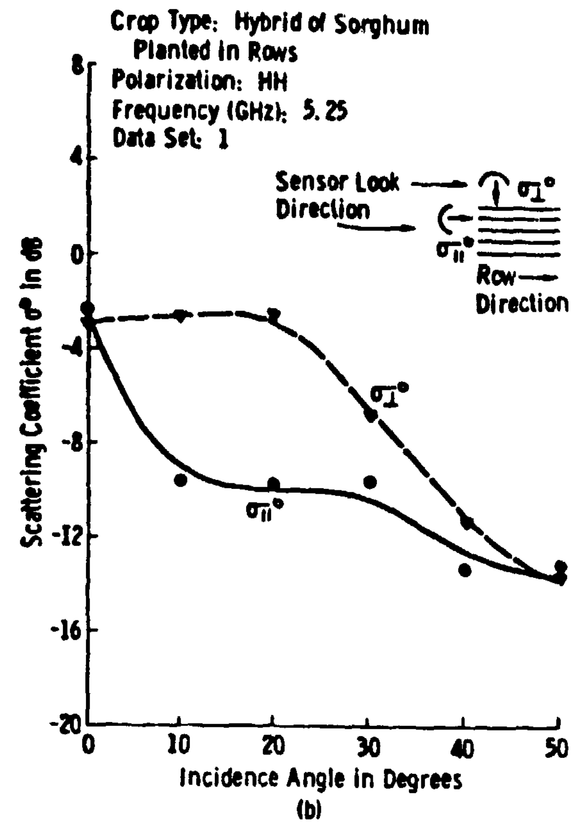

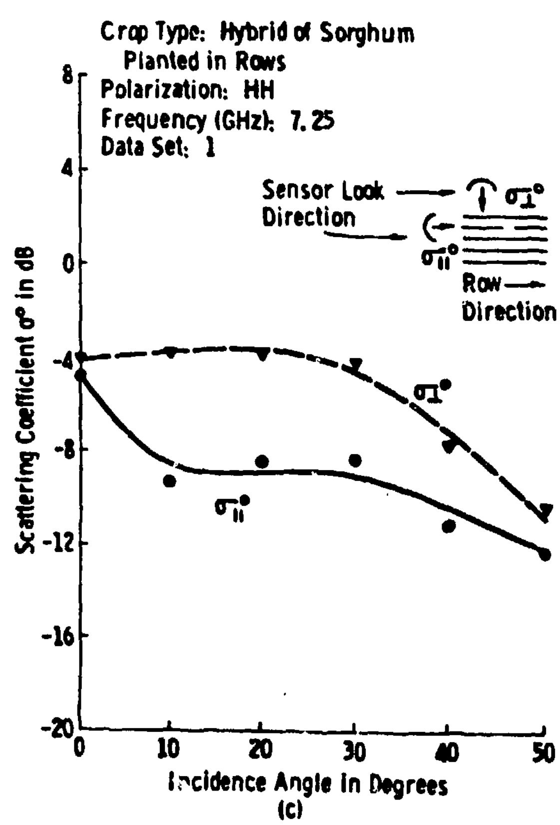

SOURCE: P.P. Batlivala and F.T. Ulaby, *The Effect of Look Direction on the Radar Return From a Row Crop*, National Aeronautics and Space Administration, Lyndon B. Johnson Space Center, Houston, Texas RSL Technical Report 264-3, May 1975.

Figure 18. Scattering Coefficient σ° as a Function of Incidence Angle at (a) 2.75GHz, (b) 5.25GHz, and (c) 7.25GHz. Data set ≠ 1, July 16, 1974.

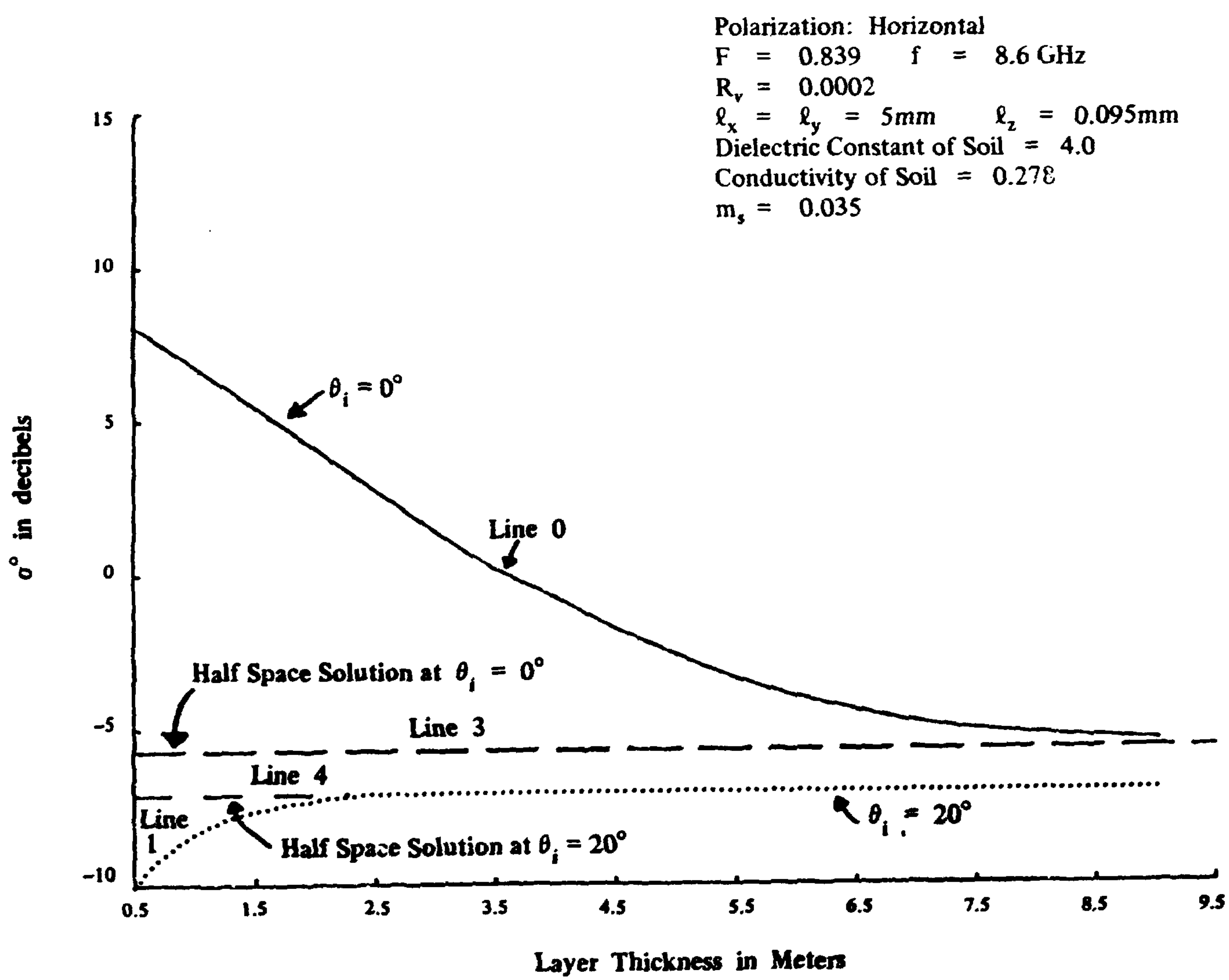

Figure 19. Study of the Variation of σ° with Layer Thickness.

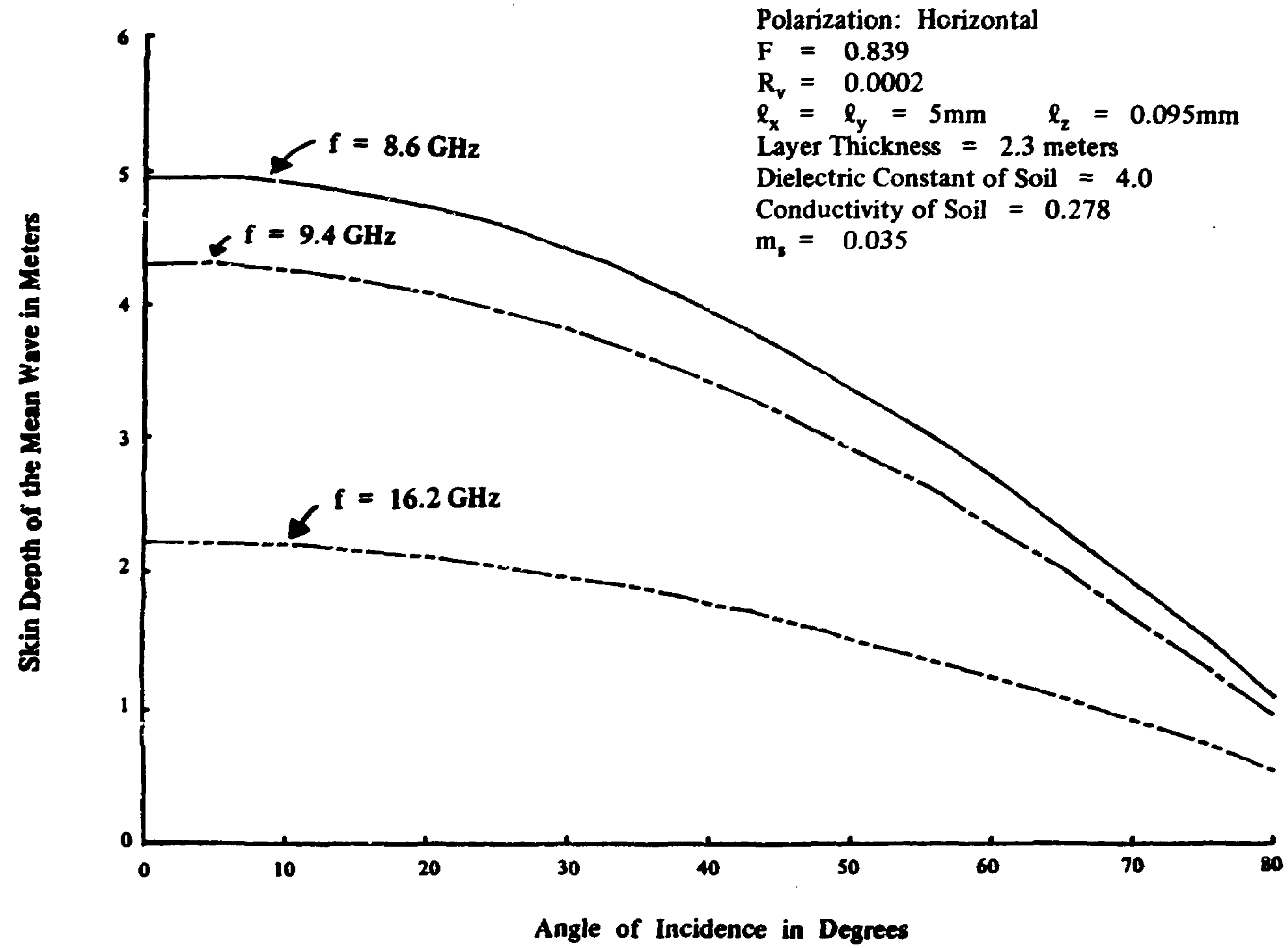

Figure 20. Study of the Skin Depth of the Mean Wave Versus Incidence Angle.

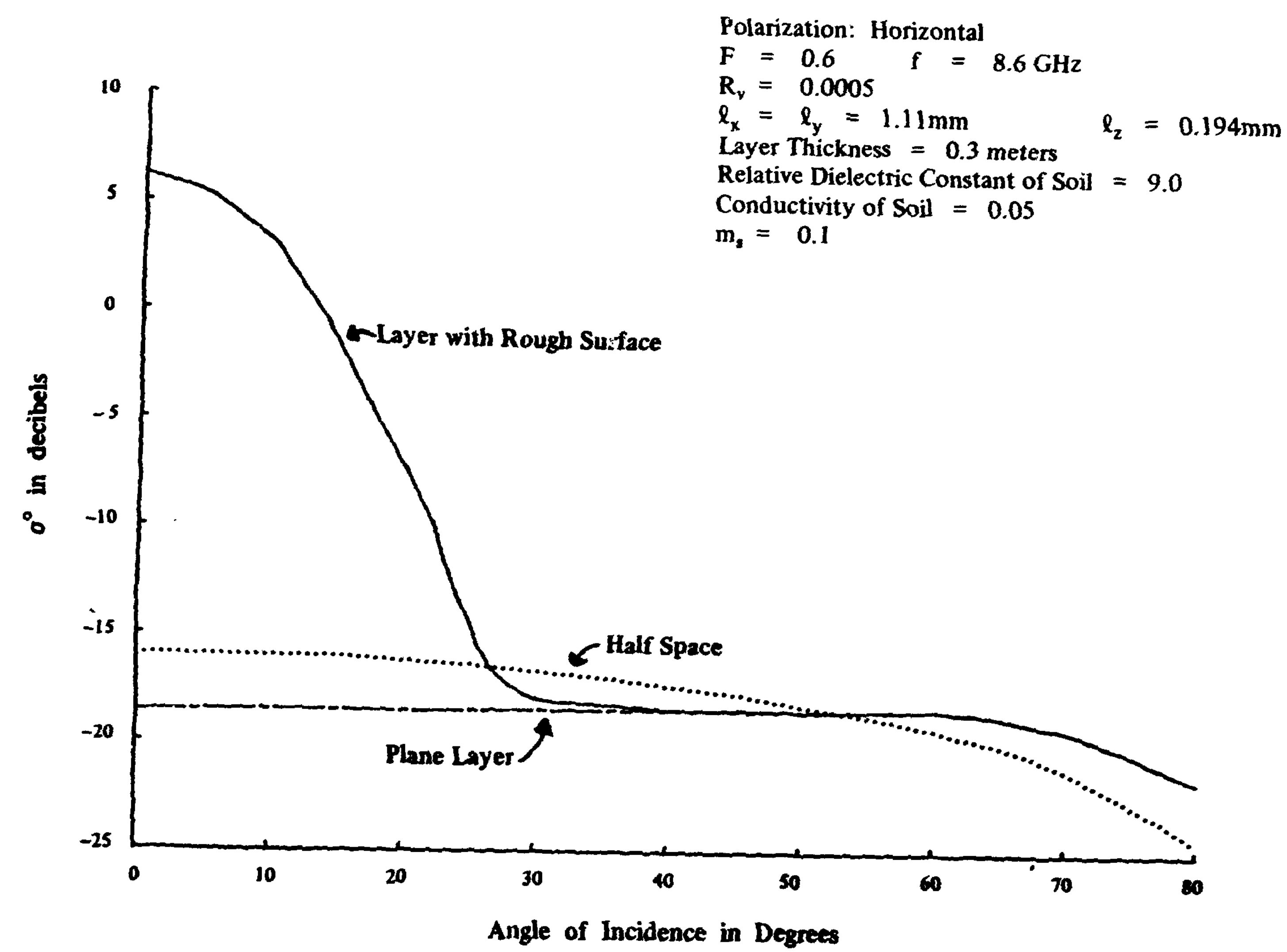

Figure 21. Comparison of Half Space, Plane Layer and Layer with Rough Surface Solutions.

In figures 22 through 30, a sensitivity-of-parameters study is presented. In this study, the input parameters are varied individually to determine the overall effect on the scattering coefficient. In figure 22, a study is provided of σ° variations with F (the vegetation moisture content). When θ_i is greater than 20°, the larger values of F produce higher levels of σ°. The shape of the σ° versus θ_i curve does not change much, but the overall level is significantly different. At approximately $\theta_i = 10°$, a crossover of the curves exists such that the curve with the highest moisture content now yields the lowest value of σ°. The reason for the crossover is that two entirely different mechanisms are responsible for scattering. For θ_i greater than 20°, the volume-scattering mechanism dominates so that higher moisture in the vegetation results in larger backscatter values. However, for angles of incidence θ_i less than 10° when the mechanism for scattering is dominated by the rough surface under the vegetation, the higher moisture values result in lower σ° values. This is because the higher moisture values provide more attenuation of the mean wave, which means that less is available for scattering from the rough surface.

Figure 23 presents a study of σ° variations with the parameter R_V. The smaller value of R_V yields a larger σ° value for small angles of incidence. This is again because rough surface scattering dominates for small angles, and smaller values of R_V mean that more energy gets down to the surface. A crossover occurs at approximately $\theta_i = 15°$ where the volume scattering result begins to dominate. Another crossover occurs between $\theta_i = 40°$ and $\theta_i = 50°$ such that for angles larger than 50°, σ° falls off faster for the larger value of R_V. The reason for this second crossover is possibly because that for the larger value of R_V, the lower interface between the vegetation and soil no longer provides a contribution for backscattering.

Figure 24 presents a study of σ° variations with L (the mean thickness of the vegetation layer). For small angles of incidence, the smaller value of L yields larger values of σ°. The rough surface below the vegetation is dominating the return and the smaller value of L provides a lower attenuation, thus making more energy available for scattering from the surface. A crossover point occurs around $\theta_i = 12°$, which indicates that volume scattering is now beginning to dominate and so the thicker layer will yield a larger value of σ°. Another crossover point occurs at approximately $\theta_i = 67°$. This crossover point possibly indicates that for L = 2 meters, the lower interface is having no influence, but for L = 0.5 meters, the lower interface still provides a contribution.

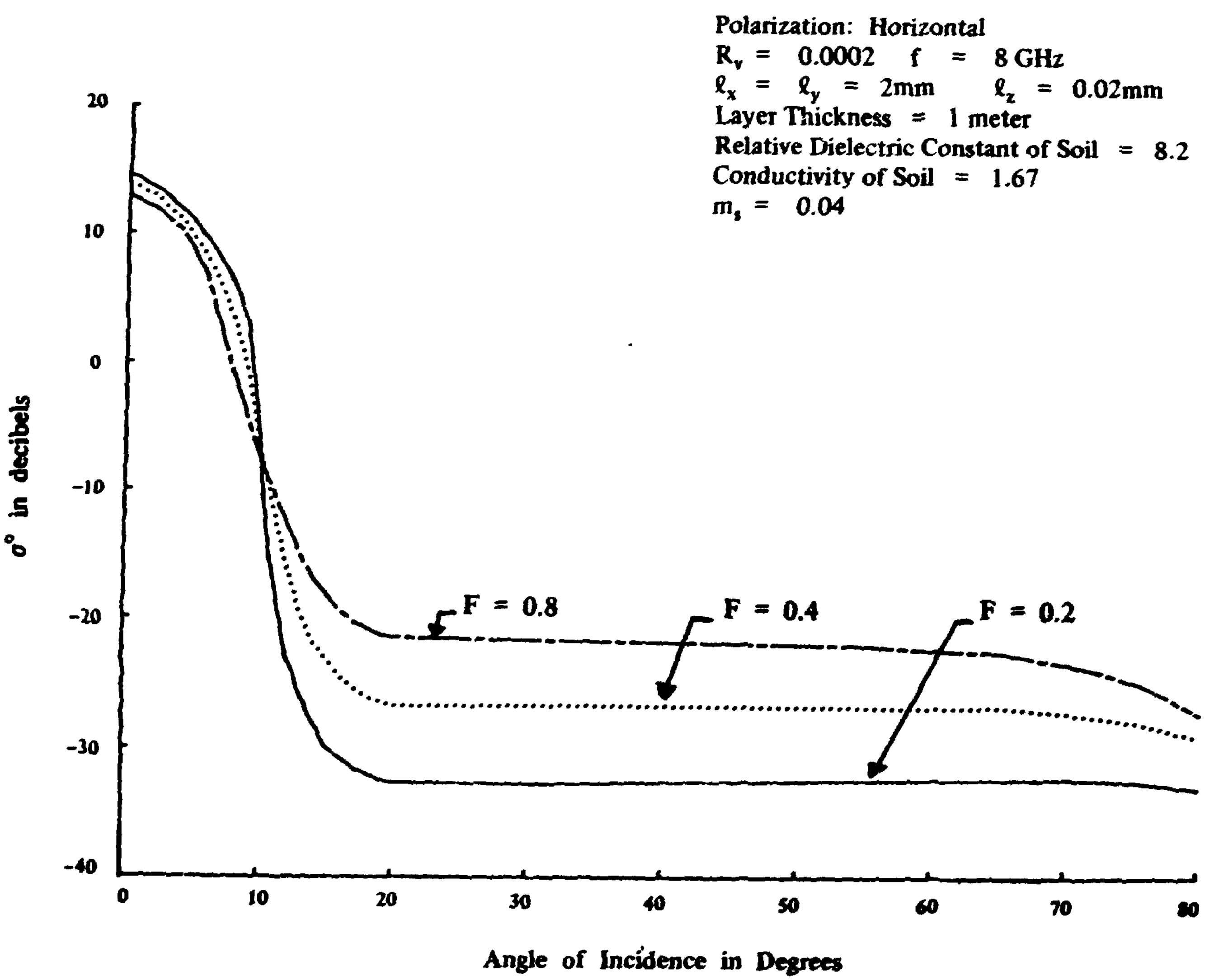

Figure 22. Study of σ° Variations with F.

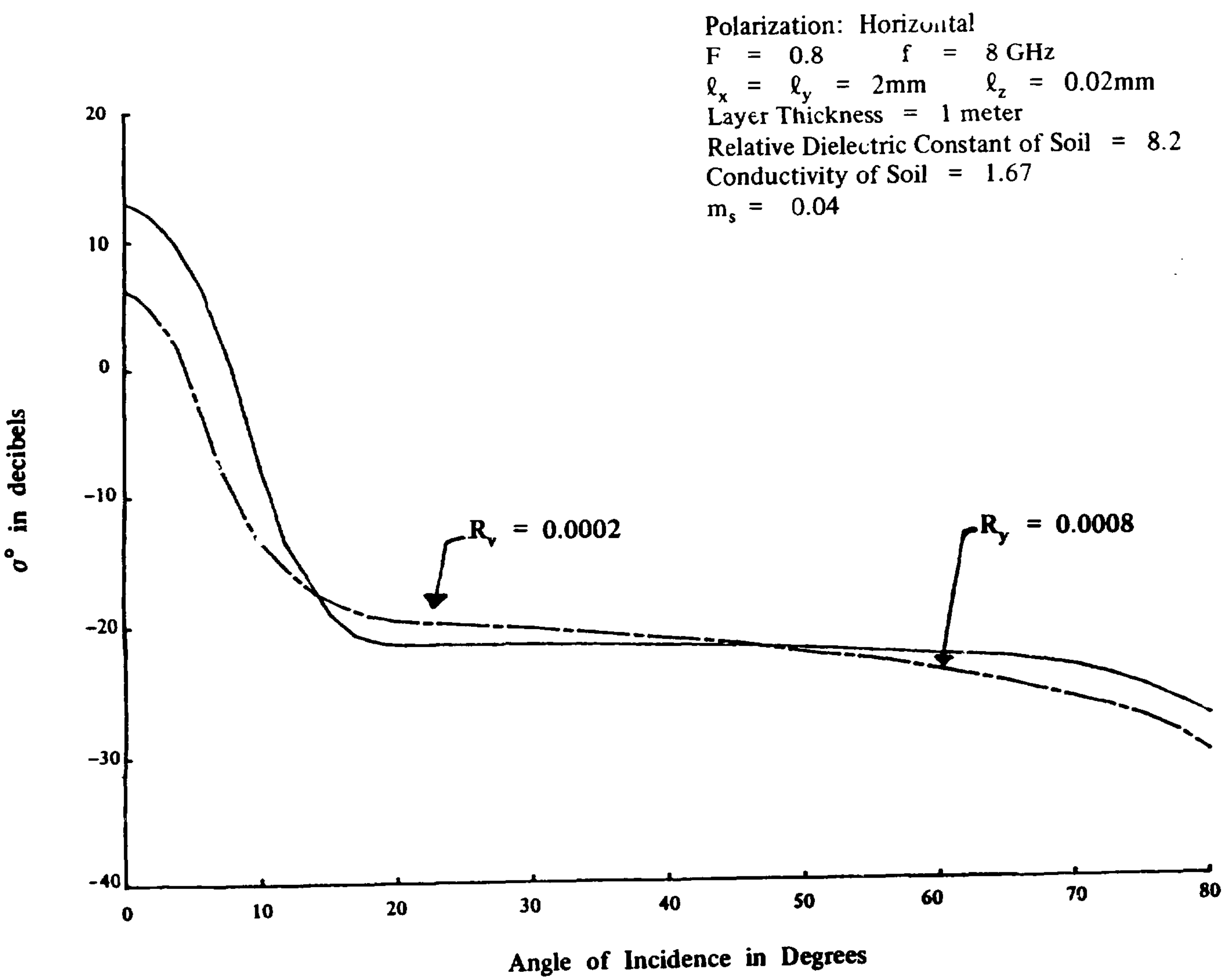

Figure 23. Study of σ° Variations with R_v.

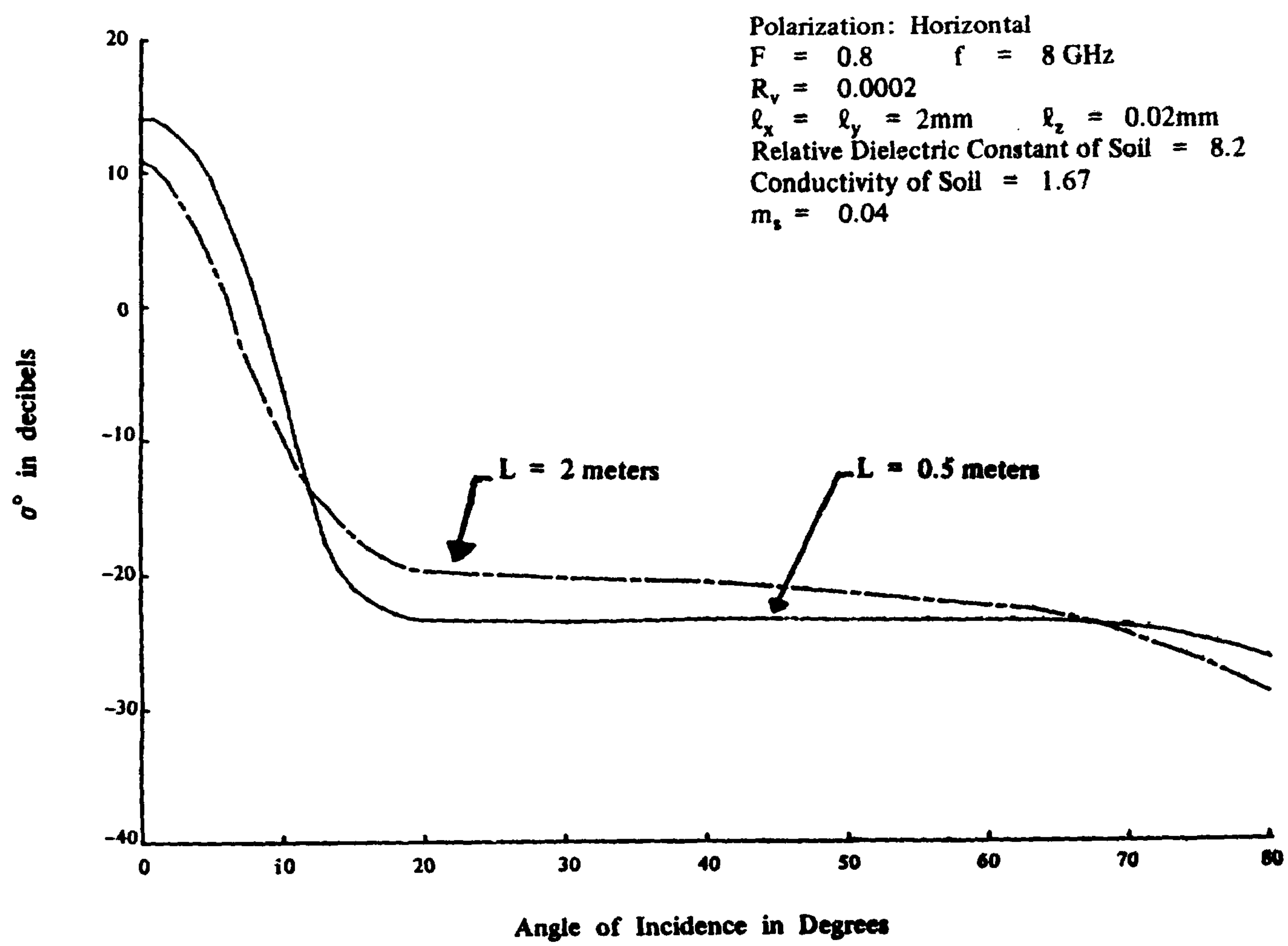

Figure 24. Study of σ° Variations with L.

Figure 25 shows a study of σ° variations with soil moisture. The soil moisture influences both the dielectric constant and the conductivity. The effect is shown of doubling the soil moisture underneath a 1-meter layer of vegetation. Thus, doubling the soil moisture content increases the level of σ° slightly over all angles of incidence.

In figure 26, a study is presented of σ° variations with frequency for two angles of incidence. We see only a slight frequency dependence at $\theta_i = 10^{\circ}$, because the rough surface scattering is independent of frequency except for the attenuation portion. At $\theta_i = 30^{\circ}$ where volume scattering is playing a more important role,we see a very significant frequency dependence.

In figure 27, σ° variations with the parameter m_s are shown. This parameter represents the ratio of the standard deviation of the rough surface undulations to the correlation distance. The most specular surface ($m_s = 0.04$) yields the highest value of σ° at $\theta_i = 0^{\circ}$. However, for this surface, σ° falls off very fast with increasing incidence angle so that at $\theta_i = 20^{\circ}$, the rough surface effect has disappeared. When m_s is allowed to increase, the value of σ° at $\theta_i = 0^{\circ}$ decreases. Also, as m_s increases, the rough surface influences σ° over a larger range of incidence angles.

In figure 28, σ° variations with ℓ_x are shown. Notice first that a change in ℓ_x yields virtually no influence upon σ° for angles of incidence less than 10°. For angles of incidence greater than 10°, the curve associated with the larger value of ℓ_x is higher until a crossover point is reached around $\theta_i = 48^{\circ}$. For angles of incidence greater than 48°, the curve associated with the larger value of ℓ_x falls off much faster than the curve associated with the smaller value of ℓ_x. Increasing the value of ℓ_x will then move the curve upward for angles of incidence less than about 50°, but will lower the curve for angles of incidence greater than about 50°.

In figure 29, σ° variations with ℓ_y are shown. Once again, notice that a change in ℓ_y has virtually no influence on σ° for angles less than 10°. For angles of incidence greater than or equal to 20°, an increase in ℓ_y results in an increase in σ°. Therefore, increasing ℓ_y simply increases the level of the curve for angles equal to and greater than 20°.

In figure 30, σ° variations with ℓ_z are shown. For angles of incidence less than 10°, changes in ℓ_z have no influence on σ° owing to the dominance of the rough surface. For angles of incidence greater than 20°, increasing the value of ℓ_z simply increases the overall level of the curve without changing the shape. It can be seen that the σ° curve is sensitive to slight changes in ℓ_z. A change in ℓ_z of only a fraction of a millimeter produces a significant change in σ°. This sensitivity may make any attempt to determine ℓ_z in a rigorous experimental manner very difficult.

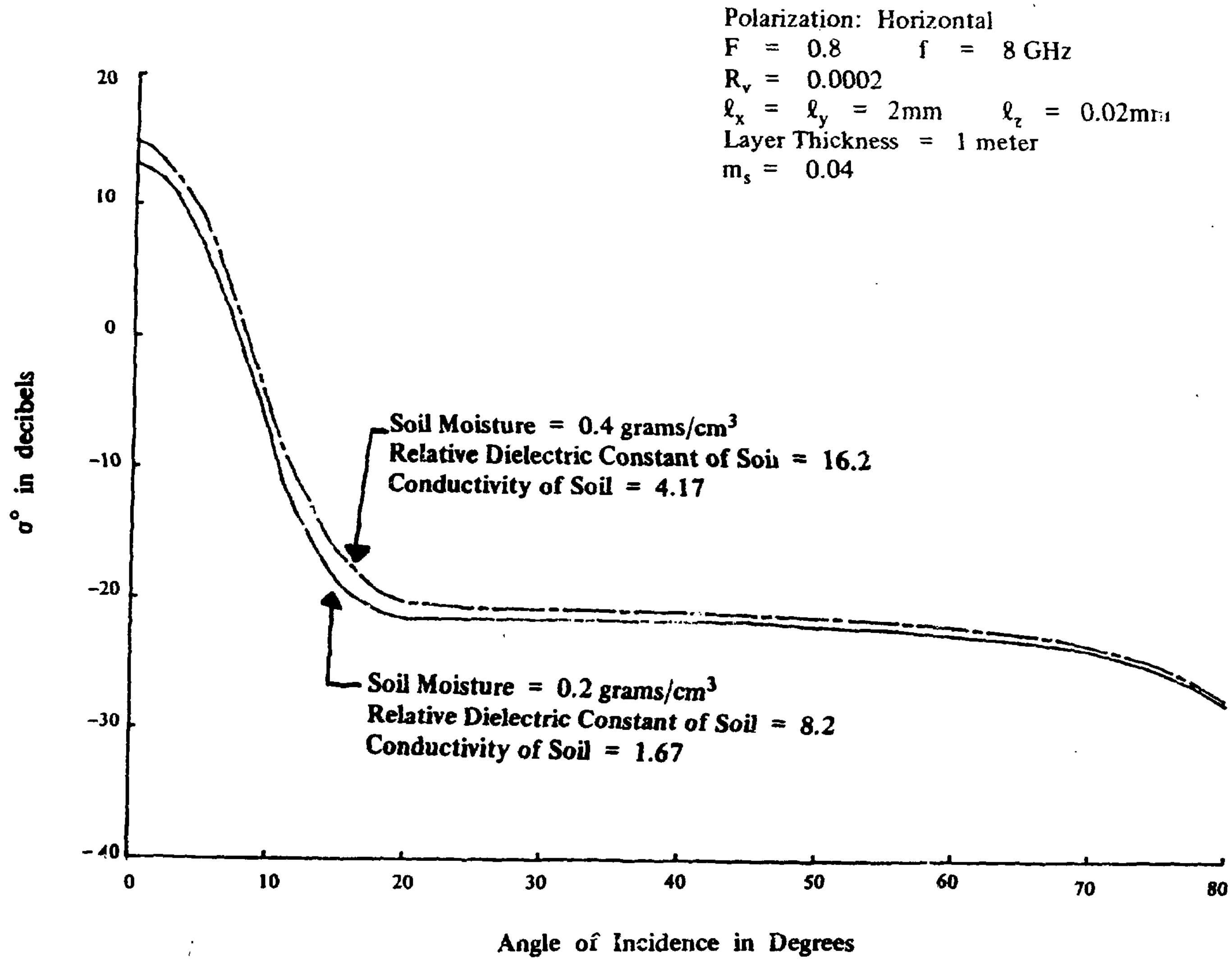

Figure 25. Study of σ° Variations with Soil Moisture.

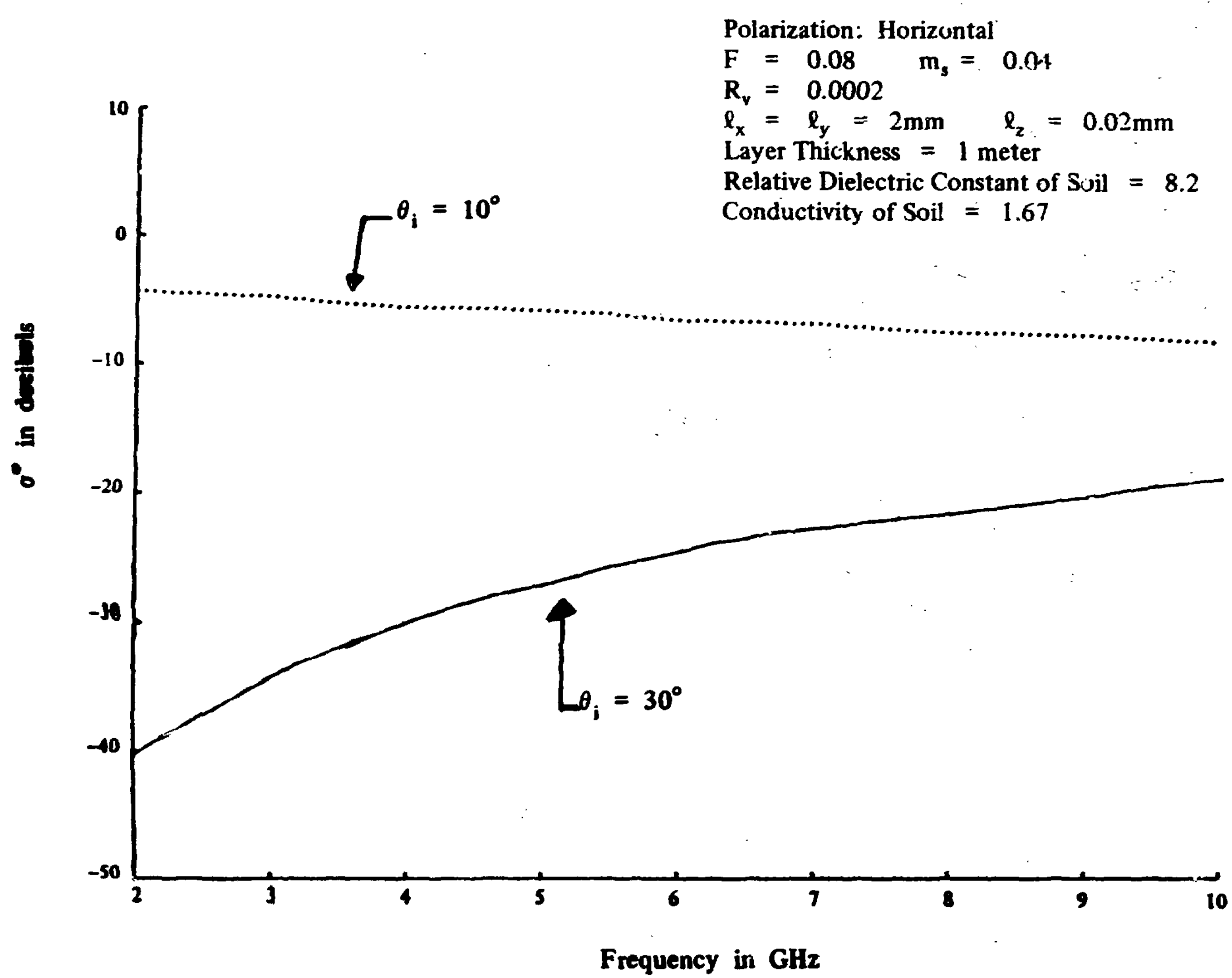

Figure 26. Study of σ° Variations with Frequency.

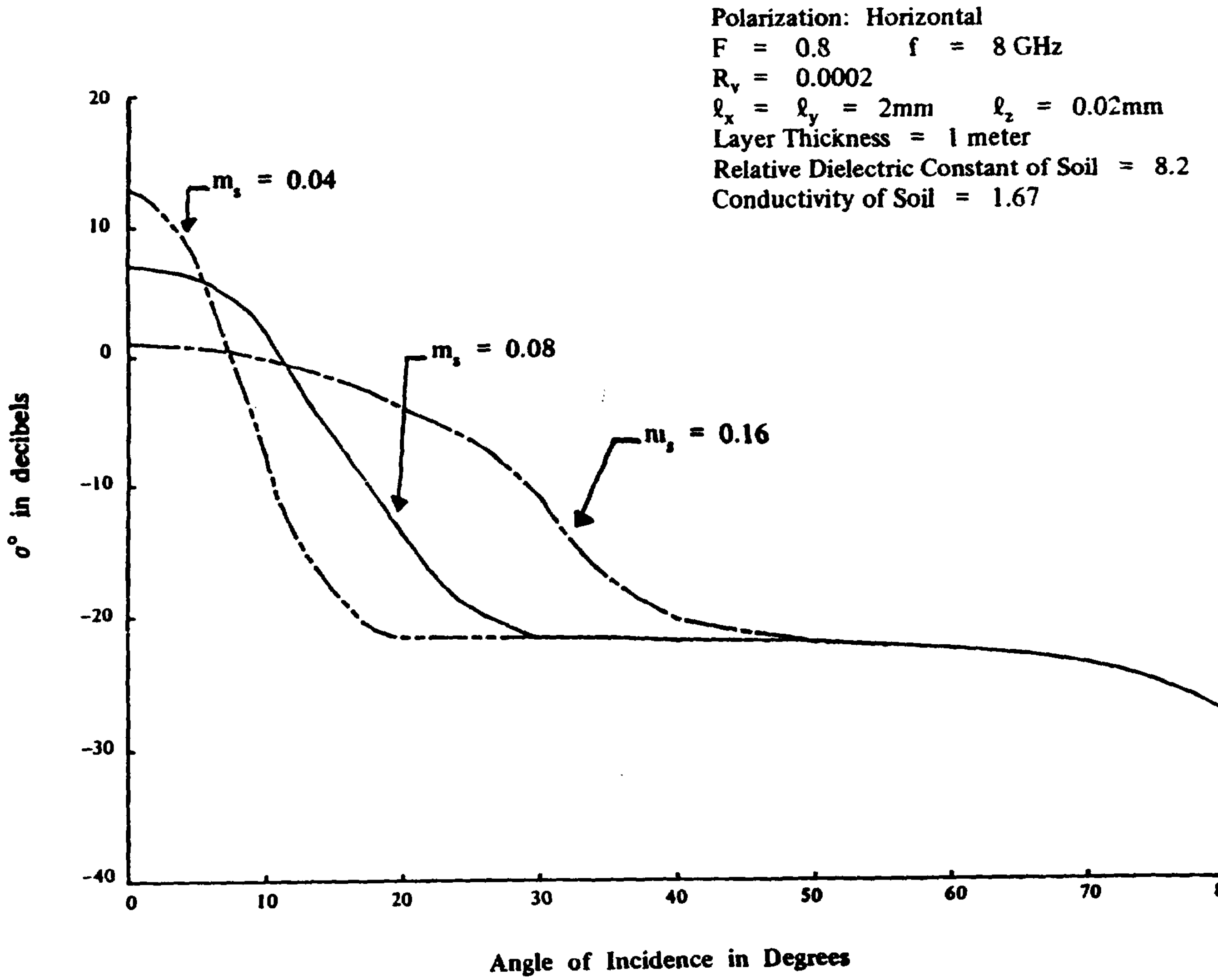

Figure 27. Study of σ° Variations with m_s.

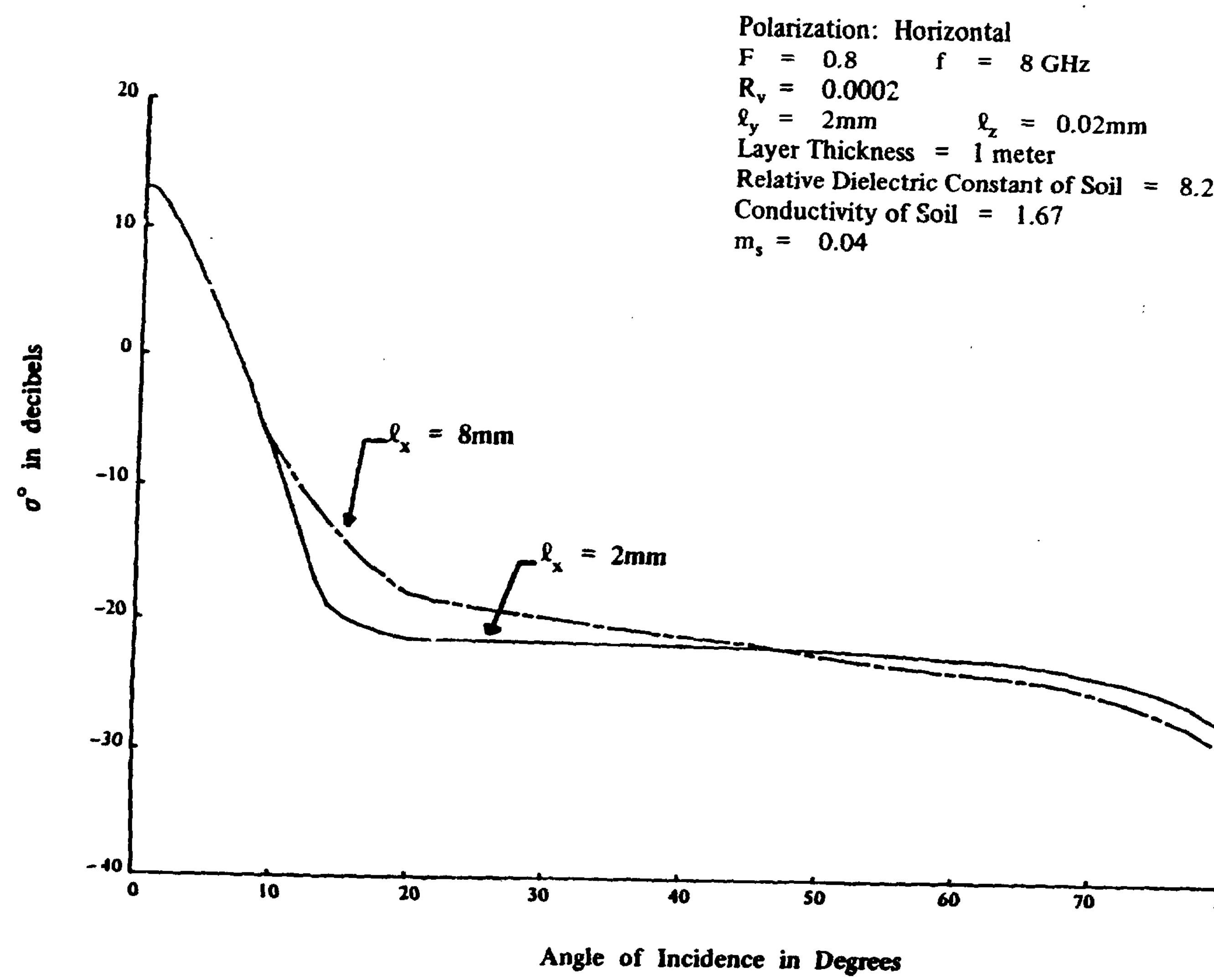

Figure 28. Study of σ° Variations with ℓ_x.

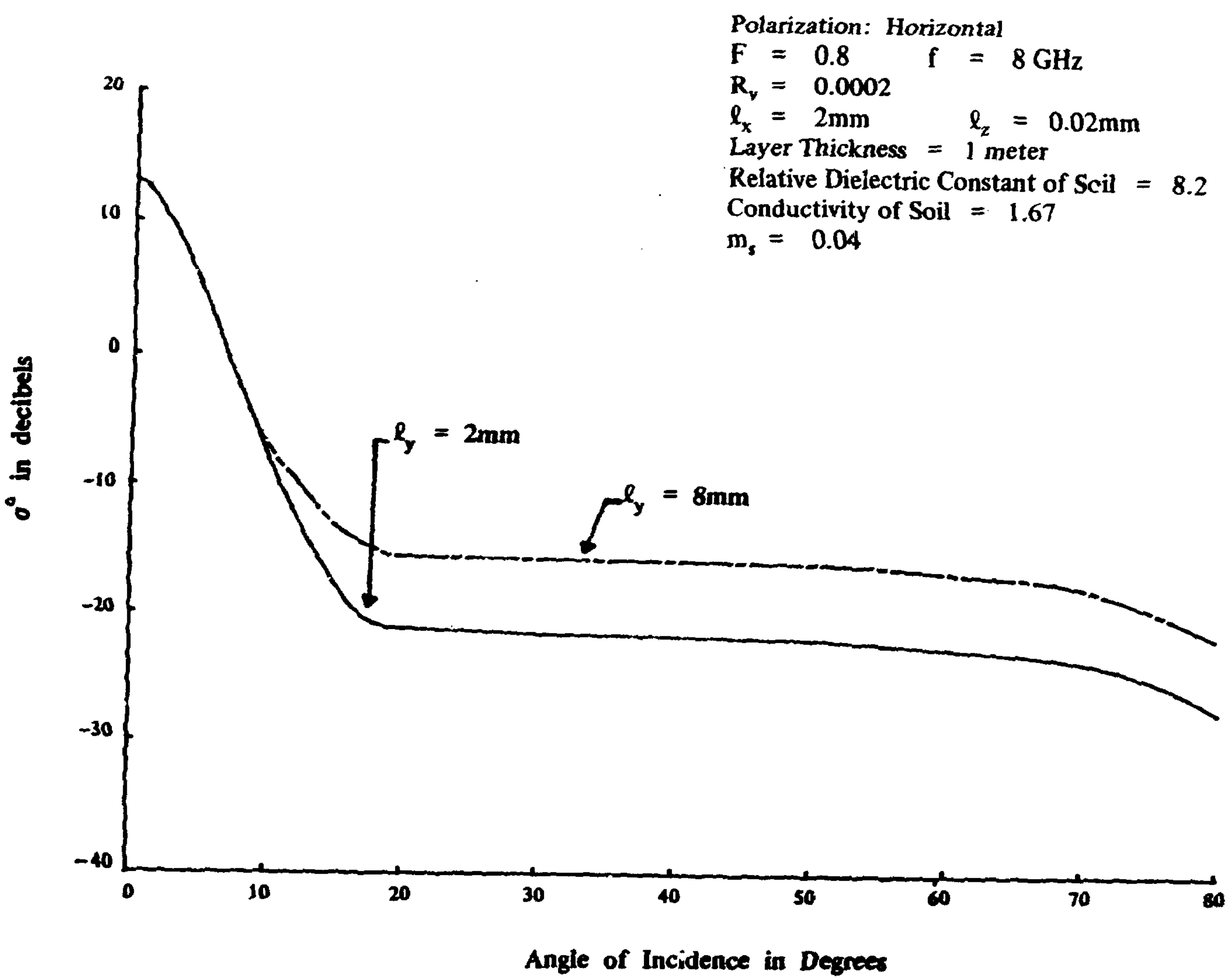

Figure 29. Study of σ° Variations with ℓ_y.

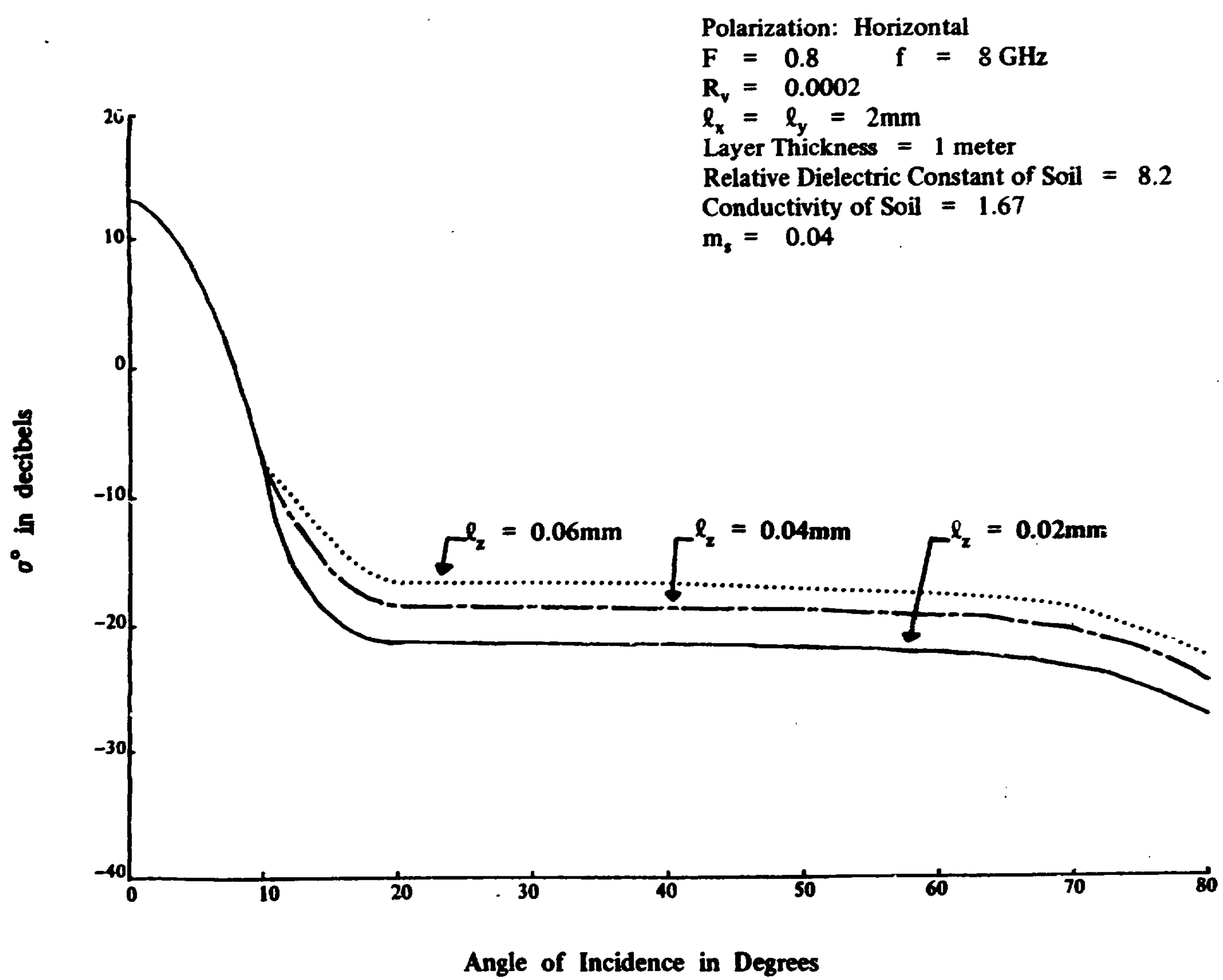

Figure 30. Study of σ° Variations with ℓ_z.

This section concludes with a brief discussion on the limitations and difficulties encountered in developing the theory presented in this report. It appears valid to simulate a region of vegetation with a continuous random medium, although it is not certain as to how well the first-order renormalization technique does in solving the problem. It is not clear how much multiple scattering is being considered, and it is not even clear as to how much multiple scattering must be considered. A free space dyadic Green's function was used in solving the Dyson's equation; however, what should have been used was a Green's function applicable to a layered problem. Such Green's functions are very complicated to develop and work with. Also, it is not clear how much the final result will change if a more complicated Green's function is used.

An equation for the radar backscatter coefficient σ° was developed by first obtaining plane wave solutions to the Dyson's equation. Expressions were found for the z component of the effective propagation constant for both horizontal and vertical polarizations. The mean wave was then used to calculate the scattered wave, which in turn was used to compute σ°. The final result for σ° indicated the necessity to develop a permittivity model that would relate some of the permittivity parameters in the scattering model to the physical parameters of the vegetation. This was accomplished with only limited success since a rather elementary permittivity model was used. The final result for σ° still contained five input parameters that were unknown. The five parameters are ℓ_x, ℓ_y, ℓ_z, R_V, and m_s.

Further work in this area should attempt to determine correlation functions and distances, as well as R_V and m_s to relate clearly theory and experiment. An anisotropic correlation function was used; however, this did not result in a depolarization term. The existance of depolarization is clearly evident from the experimental data. The reason for this depolarization is, as yet, unknown. A depolarization term could be obtained by computing the scattered field to a second-order approximation. It could also be obtained by initially allowing for an anisotropic random medium. At this time, it is unclear which approach is correct.

CONCLUSIONS

1. For certain types of vegetation, such as corn, the irregular vegetation soil boundary dominatos the backscattering results for angles of incidence between 0° and 20°. Any remote sensing of surface phenomena beneath vegetation should be done in this angular range.

2. The effect of the rough surface boundary between the vegetation and soil increases with decreases in frequency, vegetation moisture content, vegetation volume, and layer thickness.

3. Increasing the soil moisture content increases the level of the σ° curve slightly.

4. Using different correlation distances in x and y does not completely explain the effect of look direction on scattering from a row crop.

5. The σ° curve versus incidence angle curve is sensitive to very slight changes in the correlation distance in z.

6. The predictability of the σ° curve is dependent on meteorological phenomena, such as rain.

7. The correlation distances and the vegetation volume ratio do not stay constant throughout the entire growth cycle of the corn crop. However, once the crop matured, these parameters remained fairly constant.

8. Because different correlation distances were required to match the experimental data for horizontal and vertical polarizations, a more correct model for the vegetation may be an anisotropic random media model.

9. The predictability of the σ° versus incidence angle curve depends upon a very detailed knowledge of the dielectric fluctuations of the vegetation and the surface roughness properties of the soil below. However, such knowledge for particular vegetation features does not exist at the present time. This detailed understanding should be obtained if theoretical models are to have ultimate usefulness in predicting scattering from vegetation features.

APPENDIX A. Definition of Terms Involved in Computing

$<A_yA_y^*>,\quad <A_xA_x^*>,\quad <A_zA_z^*>,\quad <A_xA_z^*>,\quad <A_xA_y^*>$

Repeating equation (67) produces

$$<A_yA_y^*> = \frac{4\ell_x\ell_y\ell_z A_I(\omega^2\mu_o^2\eta_2^2 + k_o^4\eta_1^2)k_a^2k_a^{*2}M_oM_o^*}{(1 + 4k_o^2\ell_x^2\sin^2\theta_i)}$$

$$\cdot\sum_{n=1}^{16}\frac{A_n}{(c_n+d_n)}\left\{\frac{1-\ell_zd_n+\ell_z(c_n+d_n)e^{-L(c_n+1/\ell_z)}-(1+\ell_zc_n)e^{-L(c_n+d_n)}}{(1+\ell_zc_n)(1-\ell_zd_n)}\right.$$

$$\left.+\frac{1-\ell_zc_n+\ell_z(c_n+d_n)e^{-L(c_n+1/\ell_z)}-e^{-L(c_n+d_n)}(1+d_n\ell_z)}{(1+\ell_zd_n)(1-\ell_zc_n)}\right\}$$

The values for A_n, c_n, and d_n are defined below:

$A_1 = \tilde{a}_1\tilde{a}_1^*T_2T_2^*$ $\quad c_1 = D_1$ $\quad d_1 = D_1^*$

$A_2 = \tilde{a}_1T_2\tilde{a}_1^*V_2^*$ $\quad c_2 = D_1$ $\quad d_2 = D_2^*$

$A_3 = \tilde{a}_1T_2T_2^*$ $\quad c_3 = D_1$ $\quad d_3 = -D_2^*$

$A_4 = \tilde{a}_1T_2V_2^*$ $\quad c_4 = D_1$ $\quad d_4 = -D_1^*$

$A_5 = \tilde{a}_1V_2a_1^*T_2^*$ $\quad c_5 = D_2$ $\quad d_5 = D_1^*$

$A_6 = \tilde{a}_1\tilde{a}_1^*V_2V_2^*$ $\quad c_6 = D_2$ $\quad d_6 = D_2^*$

$A_7 = \tilde{a}_1V_2T_2^*$ $\quad c_7 = D_2$ $\quad d_7 = -D_2^*$

$A_8 = \hat{a}_1 V_2 V_2^*$	$c_8 = D_2$	$d_8 = -D_1^*$
$A_9 = \hat{a}_1^* T_2 T_2^*$	$c_9 = -D_2$	$d_9 = D_1^*$
$A_{10} = \hat{a}_1^* T_2 V_2^*$	$c_{10} = -D_2$	$d_{10} = D_2^*$
$A_{11} = T_2 T_2^*$	$c_{11} = -D_2$	$d_{11} = -D_2^*$
$A_{12} = T_2 V_2^*$	$c_{12} = -D_2$	$d_{12} = -D_1^*$
$A_{13} = V_2 \hat{a}_1^* T_2^*$	$c_{13} = -D_1$	$d_{13} = D_1^*$
$A_{14} = \hat{a}_1^* V_2 V_2^*$	$c_{14} = -D_1$	$d_{14} = D_2^*$
$A_{15} = V_2 T_2^*$	$c_{15} = -D_1$	$d_{15} = -D_2^*$
$A_{16} = V_2 V_2^*$	$c_{16} = -D_1$	$d_{16} = -D_1^*$

A basic expression for $< A_x A_x^* >$ can be written as follows:

$$< A_x A_x^* > = \frac{4 \ell_x \ell_y \ell_z A_1 (\omega^2 \mu_o^2 \eta_2^2 + k_o^4 \eta_1^2)}{(1 + 4 k_o^2 \ell_x^2 \sin^2 \theta_i)}$$

$$\cdot \sum_{n=1}^{16} \frac{\Lambda_n}{(\beta_n + \gamma_n)} \left\{ \frac{1 - \ell_z \gamma_n + \ell_z (\beta_n + \gamma_n) e^{-L(\beta_n + 1/\ell_z)} - (1 + \ell_z \beta_n) e^{-L(\beta_n + \gamma_n)}}{(1 + \ell_z \beta_n)(1 - \ell_z \gamma_n)} \right.$$

$$\left. + \frac{1 - \ell_z \beta_n + \ell_z (\beta_n + \gamma_n) e^{-L(\beta_n + \gamma_n)} (1 + \gamma_n \ell_z)}{(1 + \ell_z \gamma_n)(1 - \ell_z \beta_n)} \right\}$$

Before giving the values for Λ_n, β_n, and γ_n, the following parameters are defined:

$$D_1' = p_2 + jq_2 - jk_z'$$

$$D_2' = -(p_2 + jq_2 + jk_z')$$

$$h_1 = b_6\,[T_1(k_a^2 - k_o^2 \sin^2\theta_i) - T_3 k_o k_z' \sin\theta_i]$$

$$h_2 = b_6\,[V_1(k_a^2 - k_o^2 \sin^2\theta_i) - V_3 k_o k_z' \sin\theta_i]$$

$$h_3 = b_5\,[T_1(k_a^2 - k_o^2 \sin^2\theta_i) + T_3 k_o k_z' \sin\theta_i]$$

$$h_4 = b_5\,[V_1(k_a^2 - k_o^2 \sin^2\theta_i) + V_3 k_o k_z' \sin\theta_i]$$

The values of Λ_n, β_n, and γ_n will now be written in terms of the above parameters:

$$\Lambda_1 = h_1 h_1^* \qquad \beta_1 = D_1' \qquad \gamma_1 = D_1'^*$$

$$\Lambda_2 = h_1 h_2^* \qquad \beta_2 = D_1' \qquad \gamma_2 = D_2'^*$$

$$\Lambda_3 = h_1 h_3^* \qquad \beta_3 = D_1' \qquad \gamma_3 = D_2'^*$$

$$\Lambda_4 = h_1 h_4^* \qquad \beta_4 = D_1' \qquad \gamma_4 = D_1'^*$$

$$\Lambda_5 = h_2 h_1^* \qquad \beta_5 = D_2' \qquad \gamma_5 = D_1'^*$$

$$\Lambda_6 = h_2 h_2^* \qquad \beta_6 = D_2' \qquad \gamma_6 = D_2'^*$$

$$\Lambda_7 = h_2 h_3^* \qquad \beta_7 = D_2' \qquad \gamma_7 = -D_2'^*$$

Λ_8	=	$h_2h_4^*$	β_8	=	D_2'	γ_8	=	$-D_1'^*$
Λ_9	=	$h_3h_1^*$	β_9	=	$-D_2'$	γ_9	=	$D_1'^*$
Λ_{10}	=	$h_3h_2^*$	β_{10}	=	$-D_2'$	γ_{10}	=	$D_2'^*$
Λ_{11}	=	$h_3h_3^*$	β_{11}	=	$-D_2'$	γ_{11}	=	$-D_2'^*$
Λ_{12}	=	$h_3h_4^*$	β_{12}	=	$-D_2'$	γ_{12}	=	$-D_1'^*$
Λ_{13}	=	$h_4h_1^*$	β_{13}	=	$-D_1'$	γ_{13}	=	$D_1'^*$
Λ_{14}	=	$h_4h_2^*$	β_{14}	=	$-D_1'$	γ_{14}	=	$D_2'^*$
Λ_{15}	=	$h_4h_3^*$	β_{15}	=	$-D_1'$	γ_{15}	=	$-D_2'^*$
Λ_{16}	=	$h_4h_4^*$	β_{16}	=	$-D_1'$	γ_{16}	=	$-D_1'^*$

The basic equation for $<A_xA_y^*>$ can be written as

$$<A_xA_y^*> = \frac{-4\ell_x\ell_y\ell_zA_1(\omega^2\mu_o^2\eta_2^2 + k_o^4\eta_1^2)\,k_a^{*2}\,M_o^*}{(1 + 4k_o^2\ell_x^2\sin^2\theta_i)}$$

$$\cdot\sum_{n=1}^{16}\frac{P_n}{(\nu_n + \rho_n)}\left\{\frac{1 - \ell_z\rho_n + \ell_z(\nu_n + \rho_n)e^{-L(\nu_n + 1/\ell_z)} - (1 + \ell_z\nu_n)e^{-L(\nu_n + \rho_n)}}{(1 + \ell_z\nu_n)\;(1 - \ell_z\rho_n)}\right.$$

$$\left. + \frac{1 - \ell_z\nu_n + \quad + \rho_n)e^{-L(\rho_n + 1/\ell_z)} - e^{-L(\nu_n + \rho_n)}\;(1 + \rho_n\ell_z)}{(1 + \ell_z\rho_n)\;(1 - \ell_z\nu_n)}\right\}$$

The values of P_n, ρ_n, and ν_n can be defined in terms of previous parameters.

$P_1 = h_1\hat{a}_1^* T_2^*$	$\nu_1 = D_1'$	$\rho_1 = D_1^*$
$P_2 = h_1\hat{a}_1^* V_2^*$	$\nu_2 = D_1'$	$\rho_2 = D_2^*$
$P_3 = h_1 T_2^*$	$\nu_3 = D_1'$	$\rho_3 = -D_2^*$
$P_4 = h_1 V_2^*$	$\nu_4 = D_1'$	$\rho_4 = -D_1^*$
$P_5 = h_2\hat{a}_1^* T_2^*$	$\nu_5 = D_2'$	$\rho_5 = D_1^*$
$P_6 = h_2\hat{a}_1^* V_2^*$	$\nu_6 = D_2'$	$\rho_6 = D_2^*$
$P_7 = h_2 T_2^*$	$\nu_7 = D_2'$	$\rho_7 = -D_2^*$
$P_8 = h_2 V_2^*$	$\nu_8 = D_2'$	$\rho_8 = -D_1^*$
$P_9 = h_3\hat{a}_1^* T_2^*$	$\nu_9 = -D_2'$	$\rho_9 = D_1^*$
$P_{10} = h_3\hat{a}_1^* V_2^*$	$\nu_{10} = -D_2'$	$\rho_{10} = D_2^*$
$P_{11} = h_3 T_2^*$	$\nu_{11} = -D_2'$	$\rho_{11} = -D_2^*$
$P_{12} = h_3 V_2^*$	$\nu_{12} = -D_2'$	$\rho_{12} = -D_1^*$
$P_{13} = h_4\hat{a}_1^* T_2^*$	$\nu_{13} = -D_1'$	$\rho_{13} = D_1^*$
$P_{14} = h_4\hat{a}_1^* V_2^*$	$\nu_{14} = -D_1'$	$\rho_{14} = D_2^*$

$$P_{15} = h_4 T_2^* \qquad \nu_{15} = - D_1' \qquad \rho_{15} = - D_2^*$$

$$P_{16} = h_4 V_2^* \qquad \nu_{16} = - D_1' \qquad \rho_{16} = - D_1^*$$

Expressions for $< A_z A_z^* >$, and $< A_x A_z^* >$ can be obtained in terms of previous results.

$$< A_z A_z^* > = \frac{k_o^2 \sin^2 \theta_i}{k_{1z} k_{1z}^*} < A_x A_x^* >$$

$$< A_x A_z^* > = \frac{k_o \sin \theta_i}{k_{1z}^*} < A_x A_x^* >$$

APPENDIX B.

Computer Programs for Calculating the Backscattering Coefficients

```
      PROGRAM MODEL(INPUT,OUTPUT,TAPE5=INPUT,TAPE6=OUTPUT)
C     THIS PROGRAM CALCULATES THE RADAR BACKSCATTER COEFFICIENT
C     FROM A RANDOM MEDIA POSSESSING AN ANISOTROPIC CORRELATION
C     FUNCTION.  THE EFFECTIVE PROPAGATION CONSTANTS FOR THE
C     MEAN WAVE ARE CALCULATED FOR AN ARBITRARILY
C     POLARIZED INCIDENT PLANE WAVE
      COMPLEX QJ,QKA,QKK,QC,QF11(31),QMI11(31,31),QF12(31),QMI12(31,31),
     1QF13(31),QMI13(31,31),QF22(31),QMI22(31,31),QF23(31),QMI23(31,31),
     2QF33(31),QMI33(31,31),QI112(31),QI113(31),QI122(31),QI123(31),
     3QI132(31),QI133(31),QI222(31),QI223(31),QI232(31),QI233(31),
     4QI332(31),QI333(31),QI11(31),QI12(31),QI13(31),QI22(31),QI23(31),
     5QI33(31),QGI11,QGI12,QGI13,QGI22,QGI23,QGI33,QG112,QG122,QG132,
     6QG222,QG232,QG113,QG123,QG133,QG223,QG233,QG333,QG332,QES4,
     7QI11A(2),QI12A(2),QI13A(2),QM11,QM12,QM13,QM22,QSG,QES3,Q
     8M23,QM33,QEWN,QE11,QE12,QE13,QE22,QE23,QE33,QKV1,QKV2,QVN,QA3H,
     9QKV,QKH,QA1,QA3,QT21,QT22,QT2,QT131,QT132,QT133,QT134,QT13,QT3,
     1QT1,QAV1,QAX2,QAZ2,QKZP,Q11,Q22,Q,QAZ,QCX2,QCX1,QD(8),QKZPC,QSM,
     2QK(3),QAL(8),QC(4),QS(4),QERX,QERZ,QES1,QES2,QS11,QS12,QS13,QS,
     3QS14,QS8,QED,QK3C3,QK3,QA11,QA12,QA21,QA22,QT2N,QT2D,QV2N,QV2,
     4QAA1,QAL1,QB11,QB12,QB21A,QB21,QB22,QT1A,QT1N,QT1D,QV1N,QV1,
     5QT3A,QT3B,QT3C,QT3D,QV3,QK3Z,QA1HN,QA1HD,QA1H,QA2HA,QA2HB,QA2H,
     6QA3HA,QA3H,QA4H,QA5H,QA6H,QA7H,QB1,QB2,QB3,QB4,QM1,QM2,QM,QD1,
     7QD1C,QD2,QD2C,QA(16),QCC(16),QLC(16),QNYY1,QNYY2,QNYY,QAYY,QB5,
     8QB6,QD1P,QH11,QH12,QH1,QH21,QH22,QH2,QH3,QH4,QAXX,QAZZ,QAXZ,QD2P,
     9QAXY1,QAXY2,QAXY,QS01,QS02,QS03,QS04,QS05,QS51,QS06,QS1,QS2,QSA
      COMPLEX QI22A(2),QI23A(2),QI33A(2),QNJ1,QNJ2,QNJ3,QNJ4,
     1QNJ5,QNJ6,QNJ7,QJJ1,QJJ2
      COMMON DT,DK,A,B,C,D,XLZ,XLY,XLX,XKO,W,UO,EO,PI,SIGA,AER,BO,AO,SN,
     *XL
      MP=1
    7 CONTINUE
      READ(5,101)PM,RLV,ALX,ALY,XLZ
  101 FORMAT(5F10.8)
      READ(5,102)F
  102 FORMAT(F15.3)
      READ(5,109)XL,ES,SS
  109 FORMAT(3F10.8)
      READ(5,110)XMS
  110 FORMAT(F10.8)
      PI=3.1415926536
      EO=8.854*10.**(-12)
      U=4.*10.**(-7)
      UO=PI*U
      W=2.*PI*F
      QJ=(0.0,1.0)
      XLAMC=3.*10.**(10)/F
      QEWW=5.+75./(1.+QJ*1.85/XLAMC)
      ELP=0.5*PM*REAL(QEWW)
      ELPP=PM*AIMAG(QEWW)/3.
      SIGL=-W*EO*ELPP
      AER=ELP*RLV+(1.-RLV)
      SIGA=SIGL*RLV
      ETA11=RLV*(ELP-AER)**2+(1.-RLV)*(1.-AER)**2
      ETA1=SQRT(ETA11)
      ETA22=RLV*(SIGL-SIGA)**2+(1.-RLV)*SIGA**2
      ETA2=SQRT(ETA22)
      WRITE(6,106)PM
```

```
  10 FORMAT(1H ,45HFRACTION OF WATER BY WEIGHT IN THE VEGETATION=,
    1F6.3)
     WRITE(6,10)PLV
  10 FORMAT(1H ,45HVOLUME OF VEGETATION DIVIDED BY TOTAL VOLUME=,
    1F10.7)
     WRITE(6,11)F
  11 FORMAT(1H ,10HFREQUENCY=,E15.6)
     WRITE(6,12)YMS
  12 FORMAT(1H ,114HRATIO OF THE STANDARD DEVIATION OF THE ROUGH SURFAC
    1E FLUCTUATIONS TO THE CORRELATION DISTANCE OF THE FLUCTUATIONS=,
    2F10.3)
     WRITE(6,105)XLX,XLY,XLZ
 105 FORMAT(1H ,4HXLX=,F13.8,5X,4HXLY=,F13.8,5X,4HXLZ=,F13.8)
     WRITE(6,708)XL
 708 FORMAT(1H ,27HLAYER THICKNESS IN METERS =,F10.6)
     WRITE(6,709)EG
 709 FORMAT(1H ,33HDIELECTRIC CONSTANT OF THE SOIL =,F10.6)
     WRITE(6,710)SG
 710 FORMAT(1H ,27HCONDUCTIVITY OF THE SOIL =,F10.7)
     EA=AEP*EO
     XR1=SQRT(1.+(SIGA/(W*EA))**2)
     WRITE(6,711)AEP
 711 FORMAT(1H ,32HTHE AVERAGE DIELECTRIC CONSTANT=,F10.6)
     WRITE(6,712)ETA1
 712 FORMAT(1H ,37HSTD. DEV. OF DIELECTRIC FLUCTUATIONS=,F10.7)
     WRITE(6,713)ETA2
 713 FORMAT(1H ,39HSTD. DEV. OF CONDUCTIVITY FLUCTUATIONS=,F10.7)
     BO=W*SQRT(UO*EA*(XR1+1.)/2.)
     AO=W*SQRT(UO*EA*(XR1-1.)/2.)
     WRITE(6,714)AO
 714 FORMAT(1H ,3HAO=,E15.7)
     C=3.*10.**(8)
     YLAM=C/F
     XKO=W*SQRT(UO*EO)
     QKA=BO-IJ*AO
     THETA=0.0
 601 TH=PI*THETA/180.
     SN=SIN(TH)
     CS=COS(TH)
     ETA=UO*3.*10.**6
     CKK=IJ*PI*((ETA*ETA2)**2-(XKO*ETA1)**2)/(QKA*QKA)
     DC=4.*CKK*XLX*XLY*XLZ
     M=1
     A=0.0
     B=PI/2.
 406 C=0.0
     D=2.*PI
     NT=30
     NK=30
     FNK=NK
     FNT=NT
     DK=(B-A)/FNK
     DT=(D-C)/FNT
     NKK=NK+1
     NM=NT+1
     CALL SNOPT(NM,NKK,QMI11,QMI12,QMI13,QMI22,QMI23,QMI33)
     I=1
```

```
  202 QF11(I)=QMI11(I,1)+QMI11(I,NM)
      QF12(I)=QMI12(I,1)+QMI12(I,NM)
      QF13(I)=QMI13(I,1)+QMI13(I,NM)
      QF22(I)=QMI22(I,1)+QMI22(I,NM)
      QF23(I)=QMI23(I,1)+QMI23(I,NM)
      QF33(I)=QMI33(I,1)+QMI33(I,NM)
      QI112(I)=(0.0,0.0)
      QI113(I)=(0.0,0.0)
      QI122(I)=(0.0,0.0)
      QI123(I)=(0.0,0.0)
      QI132(I)=(0.0,0.0)
      QI133(I)=(0.0,0.0)
      QI222(I)=(0.0,0.0)
      QI223(I)=(0.0,0.0)
      QI232(I)=(0.0,0.0)
      QI233(I)=(0.0,0.0)
      QI332(I)=(0.0,0.0)
      QI333(I)=(0.0,0.0)
      DO 203 J=2,NT,2
      QI112(I)=QI112(I)+QMI11(I,J)
      QI122(I)=QI122(I)+QMI12(I,J)
      QI132(I)=QI132(I)+QMI13(I,J)
      QI222(I)=QI222(I)+QMI22(I,J)
      QI232(I)=QI232(I)+QMI23(I,J)
  203 QI332(I)=QI332(I)+QMI33(I,J)
      NTT=NT-1
      DO 204 J=3,NTT,2
      QI113(I)=QI113(I)+QMI11(I,J)
      QI123(I)=QI123(I)+QMI12(I,J)
      QI133(I)=QI133(I)+QMI13(I,J)
      QI223(I)=QI223(I)+QMI22(I,J)
      QI233(I)=QI233(I)+QMI23(I,J)
  204 QI333(I)=QI333(I)+QMI33(I,J)
      QI11(I)=(DT/3.)*(QF11(I)+4.*QI112(I)+2.*QI113(I))
      QI12(I)=(DT/3.)*(QF12(I)+4.*QI122(I)+2.*QI123(I))
      QI13(I)=(DT/3.)*(QF13(I)+4.*QI132(I)+2.*QI133(I))
      QI22(I)=(DT/3.)*(QF22(I)+4.*QI222(I)+2.*QI223(I))
      QI23(I)=(DT/3.)*(QF23(I)+4.*QI232(I)+2.*QI233(I))
      QI33(I)=(DT/3.)*(QF33(I)+4.*QI332(I)+2.*QI333(I))
      IF(I-NKK)205,206,206
  205 I=I+1
      GO TO 202
  206 QGI11=QI11(1)+QI11(NKK)
      QGI12=QI12(1)+QI12(NKK)
      QGI13=QI13(1)+QI13(NKK)
      QGI22=QI22(1)+QI22(NKK)
      QGI23=QI23(1)+QI23(NKK)
      QGI33=QI33(1)+QI33(NKK)
      QG112=(0.0,0.0)
      QG122=(0.0,0.0)
      QG132=(0.0,0.0)
      QG222=(0.0,0.0)
      QG232=(0.0,0.0)
      QG332=(0.0,0.0)
      QG113=(0.0,0.0)
      QG123=(0.0,0.0)
      QG133=(0.0,0.0)
```

```
      QG223=(0.0,0.0)
      QG233=(0.0,0.0)
      QG333=(0.0,0.0)
      DO 207 I=2,NK,2
      QG112=QG112+QI11(I)
      QG122=QG122+QI12(I)
      QG132=QG132+QI13(I)
      QG222=QG222+QI22(I)
      QG232=QG232+QI23(I)
  207 QG332=QG332+QI33(I)
      NM=NK-1
      DO 208 I=3,NM,2
      QG113=QG113+QI11(I)
      QG123=QG123+QI12(I)
      QG133=QG133+QI13(I)
      QG223=QG223+QI22(I)
      QG233=QG233+QI23(I)
  208 QG333=QG333+QI33(I)
      QI11A(M)=(DK/3.)*(QGI11+4.*QG112+2.*QG113)
      QI12A(M)=(DK/3.)*(QGI12+4.*QG122+2.*QG123)
      QI13A(M)=(DK/3.)*(QGI13+4.*QG132+2.*QG133)
      QI22A(M)=(DK/3.)*(QGI22+4.*QG222+2.*QG223)
      QI23A(M)=(DK/3.)*(QGI23+4.*QG232+2.*QG233)
      QI33A(M)=(DK/3.)*(QGI33+4.*QG332+2.*QG333)
      IF(M-1)306,306,307
  306 M=M+1
      ...D/2.
      ...
      GO TO 203
  307 QM11=QC*(QI11A(1)+QI11A(2))
      QM12=QC*(QI12A(1)+QI12A(2))
      QM13=QC*(QI13A(1)+QI13A(2))
      QM22=QC*(QI22A(1)+QI22A(2))
      QM23=QC*(QI23A(1)+QI23A(2))
      QM33=QC*(QI33A(1)+QI33A(2))
      QF11=(DK1/YK0)**2-QM11/((2.*PI)**3)
      QF12=-QM12/((2.*PI)**3)
      QF13=-QM13/((2.*PI)**3)
      QF22=(DK1/YK0)**2-QM22/((2.*PI)**3)
      QF23=-QM23/((2.*PI)**3)
      QF33=(DK1/YK0)**2-QM33/((2.*PI)**3)
C     CALCULATE THE EFFECTIVE PROPAGATION CONSTANTS FOR
C     HORIZONTALLY AND VERTICALLY POLARIZED WAVES
      X22=REAL(QM22)
      Y22=AIMAG(QM22)
      ...=X*U**SIGA/(KK0**2)+Y22/((2.*PI)**3)
      ...=...-X22/((2.*PI)**3)
      PH3=ATAN2(PH,PP)
      ...=SQRT(PH**2+PP**2)
      QKH=XK0*SQRT(P3)*CEXP(-QJ*PH3/2.)
      XH=REAL(QKH)
      YH=AIMAG(QKH)
      P1=YH
      Q1=XH
      QKV1=QE11*QF33*...-QE13**2
      QKV2=(...)**2-4.*E33*QKV1
      ...=REAL(QKV2)
```

```
      Y4=AIMAG(CKV2)
      [illegible]=SQRT(Y4**2+Y4**2)
      [illegible]=ATAN2(Y4,Y4)
      CV [illegible]*SN+SQRT(R4)*CEXP(QJ*PH4/2.)
      CKV=-KKO*(CVN/CE33)
      YV=REAL(CKV)
      Y4=AIMAG(CKV)
      R3=YV
      R2=-Y4
      Y[illegible]=REAL(CE11)
      [illegible]=AIMAG(CE11)
      [illegible]=REAL(CE12)
      [illegible]=AIMAG(CE12)
      [illegible]=REAL(CE13)
      [illegible]=AIMAG(CE13)
      [illegible]=REAL(CE22)
      [illegible]=AIMAG(CE22)
      [illegible]=REAL(CE23)
      [illegible]=AIMAG(CE23)
      [illegible]=REAL(CE33)
      [illegible]=AIMAG(CE33)
C     THE FOLLOWING CARDS CALCULATE THE RADAR
C     BACKSCATTER COEFFICIENT FOR A HALF SPACE BASED ON THE MEAN
C     WAVE [illegible] ABOVE
      [illegible]=(0.0,0.0)
      [illegible]=1.0
      [illegible]=(0.0,0.0)
      [illegible]=[illegible]*KKO*CS
      [illegible]=KKO*[illegible]
      QT2=QT21/QT22
      QT131=CKV*SN+KKO*CE13
      QT132=KKO*(SN*SN-CE33)
      QT13=QT131/QT132
      QT131=[illegible]*QA1*CS+QA3*SN
      QT132=QA1*[illegible]*SN/CS
      QT133=KKO*SN*QT13-CKV
      QT134=[illegible]
      [illegible]=KKO*(QT131+QT132)/(QT133+QT134)
      [illegible]=QT1*QT13
      [illegible]=0.0
      [illegible]=QT2
      [illegible]=0.0
      [illegible]
      [illegible]=0.0
      [illegible]
      [illegible]=KKO*SN
      [illegible]=KKO*CS
      [illegible]
      [illegible]-(KKO*SN)**2
      R2=SQRT(R11**2+R12**2)
      PH2=ATAN2(-11,R12)
      [illegible]=SQRT(R2)*CEXP(-QJ*PHZ/2.)
      [illegible]=CKZP*(QAZP+XKZ)
      [illegible]=XKX*[illegible]*(1.+[illegible]KZP/XKZ)
      [illegible]=-QJ*([illegible]11+[illegible]22)
      [illegible]=[illegible]+[illegible]Z72
      [illegible]=CKZP*[illegible]+[illegible]*XKC*SN
```

THIS PAGE IS BEST QUALITY PRACTICABLE FROM COPY FURNISHED TO DDC

```
      QUY2=QYZP*QAY2+QSZZ*XKO*SM
      QD(1)=P1+QJ*(Q1+QKZP)
      QKZPC=CONJG(QKZP)
      QK(1)=P1-QJ*(Q1+QKZPC)
      QD(2)=P1+QJ*(Q1+QKZP)
      QK(2)=P2-QJ*(Q2+QKZPC)
      QD(3)=P2+QJ*(Q2+QKZP)
      QK(3)=P1-QJ*(Q1+QKZPC)
      QD(4)=P2+QJ*(Q2+QKZP)
      QK(4)=P2-QJ*(Q2+QKZPC)
      QAL(1)=QCX1*CONJG(QCY1)
      QAL(2)=QCX1*CONJG(QCY2)
      QAL(3)=QCX2*CONJG(QCY1)
      QAL(4)=QCX2*CONJG(QCK2)
      QD(5)=P1+QJ*(Q1+QKZP)
      QK(5)=P1-QJ*(Q1+QKZPC)
      QD(6)=P1+QJ*(Q1+QKZP)
      QK(6)=P2-QJ*(Q2+QKZPC)
      QD(7)=P2+QJ*(Q2+QKZP)
      QK(7)=P1-QJ*(Q1+QKZPC)
      QD(8)=P2+QJ*(Q2+QKZP)
      QK(8)=P2-QJ*(Q2+QKZPC)
      QAL(5)=QCX1*CONJG(QAY1)
      QAL(6)=QCX1*AY2
      QAL(7)=QCX2*CONJG(QAY1)
      QAL(8)=QCX2*AY2
      QB(1)=QAY1*CONJG(QAY1)
      QB(2)=QAY1*AY2
      QB(3)=AY2*CONJG(QAY1)
      QB(4)=AY2*AY2
      QG(1)=QAY1*CONJG(QCX1)
      QG(2)=QAY1*CONJG(QCX2)
      QG(3)=AY2*CONJG(QCX1)
      QG(4)=AY2*CONJG(QCX2)
      QEPY=QA1
      EPY=A2
      QEPZ=QA3
      QES1=(0.0,0.0)
      QES2=(0.0,0.0)
      DO 510 I=1,4
      QS11=2.*XLZ*(QK(I)+QD(I))
      QS12=(1.+XLZ*QD(I))*(1.+XLZ*QK(I))
      QS13=QAL(I)/(QK(I)+QD(I))
      QS=QS13*QS11/QS12
      QES1=QES1+QS
      QS14=QB(I)/(QK(I)+QD(I))
      QS3=QS14*QS11/QS12
  510 QES2=QES2+QS3
      QES3=(0.0,0.0)
      QES4=(0.0,0.0)
      DO 511 I=5,8
      QS11=2.*XLZ*(QK(I)+QD(I))
      QS12=(1.+XLZ*QD(I))*(1.+XLZ*QK(I))
      QS13=QAL(I)/(QK(I)+QD(I))
      QS=QS13*QS11/QS12
      QES3=QES3+QS
      QS14=QG(I-4)/(QK(I)+QD(I))
```

```
      QS=QS1**QJ11/QS12
  311 QEL=QL2**QSO
      QS=QED*CONJG(QERY)
      QSB=Q*CONJG(Q)
      QJJ1=QS*QES1/QSB
      R1=REAL(QJJ1)
      QS=QLRY*ERY*QES3
      QED=QJ*Q*(XKZ+GKZPO)
      QJJ2=QS/QED
      R2=2.*REAL(QJJ2)
      QS=QERY*XKO*SN*QES1*CONJG(QERZ)
      QED=XKZ*QSL
      QJJ2=QS/QED
      R3=2.*REAL(QJJ2)
      QS=QRY*ERY*QES2
      QEL=(XKZ+GKZP)*(XKZ+GKZPO)
      QJJ2=QS/QED
      R4=REAL(QJJ2)
      QS=QJ*ERY*XKO*SN*QES4*CONJG(QERZ)
      QED=(KZ*(XKZ+GKZP)*CONJG(Q))
      QJJ2=QS/QED
      R5=2.*REAL(QJJ2)
      QS=QERZ*CONJG(QERZ)*QES1*(XKO*SN)**2
      QED=QSB*XKZ**2
      QJJ2=QS/QED
      R6=REAL(QJJ2)
      R=R1+R2+R3+R4+R5+R6
      ER1=XLY*XLY*XLZ*((W*UO*ETA2)**2+(XKO*XKO*ETA1)**2)
      ERD=PI*PI*(1.+(2.*XKO*XLX*SN)**2)
      EF=((XKO*CS)**2)*ER1*R/ERD
      SIG=4.*PI*EF
      DBSIG=10.*ALOG10(SIG)
C  THE FOLLOWING CARDS CALCULATE THE BACKSCATTER COEFFICIENT
C  FOR A PLANE LAYER
      PI=3.14159265
      EO=8.854*10.**(-12)
      U=4.*10.**(-7)
      UO=PI*U
      W=2.*PI*F
      E3=ES*EO
      EB=SQRT(1.+(SG/(W*E3))**2)
      B3=W*SQRT(E3*UO*(EB+1.)/2.)
      A3=W*SQRT(E3*UO*(E3-1.)/2.)
      PH1=B3**2-A3**2-(XKO*SN)**2
      PH2=2.*B3*A3
      R3=SQRT(PH1**2+PH2**2)
      PH3=ATAN2(PH2,PH1)
      QK3CS=SQRT(R3)*CEXP(-QJ*PH3/2.)
      QK3=B3-QJ*A3
      IF(THETA)300,311,312
  311 EH=(Q1**2-P1**2)/(W*W*UO)
      EV=(Q2**2-P2**2)/(W*W*UO)
  312 QA11=(QJ*QK3C3-P1-QJ*Q1)*CEXP(-XL*(P1+QJ*Q1))
      QA12=(QJ*QK3C3+P1+QJ*Q1)*CEXP(XL*(P1+QJ*Q1))
      QA21=QJ*XKO*CS+P1+QJ*Q1
      QA22=QJ*XKO*CS-P1-QJ*Q1
      QT2N=2.*QJ*XKO*QA12*A2*CS
```

```
      QT20=QA21*QA12-QA11*QA22
      QT2=QT2N/QT20
      QV2N=-2.*QJ*XKO*A2*QA11*CS
      QV2=QV2N/QT20
      CEA1=(QJ*(1.-E3/EV)*(XKO*SN)**2)/QK3C3
      QAL1=QJ*CK3C3+QA41
      QB11=(P2+QJ*Q2-QAL1)*CEXP(-XL*(P2+QJ*Q2))
      QB21=P2+QJ*Q2+QB21A
      QB12=-(P2+QJ*Q2+QAL1)*CEXP(XL*(P2+QJ*Q2))
      QB21A=QJ*XKO*(CS+SN*SN*(1.-EO/EV)/CS)
      QB22=-P2-QJ*Q2+QB21A
      QT1A=SN*(1.-EO/EV)*(QA3+QA1*SN/CS)
      QT1N=QJ*XKO*QB12*(2.*QA1*CS+QT1A)
      QT10=QB12*QB21-QB22*QB11
      QT1=QT1N/QT10
      QV1N=-QJ*XKO*QB11*(2.*QA1*CS+QT1A)
      QV1=QV1N/QT10
      QT3A=QT1*CEXP(-XL*(P2+QJ*Q2))+QV1*CEXP(XL*(P2+QJ*Q2))
      QT3N=EO*XKO*SN*QT3A/QK3C3
      QT3D=EO*(QA3-SN*(QT1+QV1-QA1)/CS)*CEXP(XL*(P2+QJ*Q2))
      QT3=(QT3N-QT3D)/QT30
      QV3=EO*(QA3-SN*(QT1+QV1-QA1)/CS)/EV-QT3
      XKX=XKO*SN
      XKY=0.0
      PH31=B3**2-A3**2-XKX**2-XKY**2
      PH32=2.*B3*A3
      PH3=SQRT(PH31**2+PH32**2)
      PHT=ATAN2(PH32,PH31)
      QK3Z=SQRT(PH3)*CEXP(-QJ*PH3/2.)
      XK1Z=SQRT(XKO**2-XKX**2-XKY**2)
      QA1HN=(QK3Z-XK1Z)*CEXP(-2.*QJ*QK3Z*XL)
      QA1HD=QK3Z+XK1Z
      QA1H=QA1HN/QA1HD
      QA2HA=(QK3Z**2+XKY**2)*XK1Z**2
      QA2HB=XK1Z*(QK3Z**2+XKX**2)*QK3Z
      QA2H=(QA2HA-QA2HB)*CEXP(-2.*QJ*QK3Z*XL)
      QA2H=QA2H/(QA2HB+QA2HA)
      QA3H=QK3Z*XKY*CEXP(-QJ*QK3Z*XL)
      QB3H=QA3H/(QA2HB+QA2HA)
      QC3H=XK1Z*(QK3Z**2+XKX**2)*QK3Z*(1.-QA2H)
      QA4H=XK1Z*(QK3Z**2+XKY**2)+QK3Z**2
      QB4H=XK1Z*(QK3Z**2+XKX**2)*QK3Z*QA3H
      QA5H=QA4H+QA3H*(QA2H+1.)
      QA1=QK3Z**2+QK3Z*XKX**2
      QB3=XK1Z*XKX*(QA2H+1.)*QA3H/QB3H
      QC3=QA3H*(QA2H+1.)/QB3H
      QC4=QA3H/(1.+QJ*QA3H*QK3Z*QK4*QK4)
      QH1=QK3Z*(1.-QA1H)
      QV2=XK1Z*(1.+QA1H)
      QV3=1./(QJ*QK4*QK4*(QA1+QH3))
      [illegible]
      [illegible]
      [illegible]
      [illegible]
```

UNCLASSIFIED

UNCLASSIFIED

```
      QNJ1=QA1H*QT2
      QA(1)=QNJ1*CONJG(QNJ1)
      QLC(1)=QD1
      QLD(1)=QD1C
      QNJ2=QA1H*QV2
      QA(2)=QNJ1*CONJG(QNJ2)
      QLC(2)=QD1
      QLD(2)=QD2C
      QA(3)=QT2*QA1H*CONJG(QT2)
      QLC(3)=QD1
      QLD(3)=-QD2C
      QA(4)=QA1H*QT2*CONJG(QV2)
      QLC(4)=QD1
      QLD(4)=-QD1C
      QA(5)=QA1H*QV2*CONJG(QNJ1)
      QLC(5)=QD2
      QLD(5)=QD1C
      QA(6)=QA1H*QV2*CONJG(QNJ2)
      QLC(6)=QD2
      QLD(6)=CONJG(QD2)
      QA(7)=QA1H*QV2*CONJG(QT2)
      QLC(7)=QD2
      QLD(7)=-QD2C
      QA(8)=QA1H*QV2*CONJG(QV2)
      QLC(8)=QD2
      QLD(8)=-QD1C
      QA(9)=QT2*CONJG(QNJ1)
      QLC(9)=-QD2
      QLD(9)=QD1C
      QA(10)=QT2*CONJG(QNJ2)
      QLC(10)=-QD2
      QLD(10)=QD2C
      QA(11)=QT2*CONJG(QT2)
      QLC(11)=-QD2
      QLD(11)=-QD2C
      QA(12)=QT2*CONJG(QV2)
      QLC(12)=-QD2
      QLD(12)=-QD1C
      QA(13)=QV2*CONJG(QNJ1)
      QLC(13)=-QD1
      QLD(13)=QD1C
      QA(14)=QV2*CONJG(QNJ2)
      QLC(14)=-QD1
      QLD(14)=QD2C
      QA(15)=QV2*CONJG(QT2)
      QLC(15)=-QD1
      QLD(15)=-QD2C
      QA(16)=QV2*CONJG(QV2)
      QLC(16)=-QD1
      QLD(16)=-QD1C
      IN=16
      CALL [illegible](IN,QA,QLC,QLD,QSM)
      AL11=([illegible]*MO*ETA2)**2+(XK0*XK0*ETA1)**2
      ALD=1.[illegible]*(WAO*XLK*SN)**2
      QNYY1=[illegible]*QM*CONJG(QM)
      QNYY2=4.*[illegible]*AL11*QNYY1
      QMYY=QNYY2*CONJG([illegible])*CONJG(QKA)
```

```
      QSIY=QHYY*QSH/SLU
      QU5=QD3*.5
      QD6=QD3-QD
      QD1F=QD2+QJ*Q2-QJ*QKZP
      QD2P=-(P2+CJ*Q2+QJ*QKZP)
      QH11=QT1*(XKA**2-(XKU*SN)**2)
      QH12=QT3*XKU*SN*QKZP
      QH1=QD6*(QH11-QH12)
      QH21=QV1*(CKA**2-(XKU*SN)**2)
      QH22=QV3*XKO*QKZP*SN
      QH2=QD6*(QH21-QH22)
      QH3=QD5*(QH11+QH12)
      QH4=QD5*(QH21+CH22)
      QA(1)=QH1*CONJG(QH1)
      QLC(1)=QD1P
      QLD(1)=CONJG(QD1P)
      QA(2)=QH1*CONJG(QH2)
      QLC(2)=QD1P
      QLD(2)=CONJG(QD2P)
      QA(3)=QH1*CONJG(QH3)
      QLC(3)=QD1P
      QLD(3)=-CONJG(QD2P)
      QA(4)=QH1*CONJG(QH4)
      QLC(4)=QD1P
      QLD(4)=-CONJG(QD1P)
      QA(5)=QH2*CONJG(QH1)
      QLC(5)=QD2P
      QLD(5)=CONJG(QD1P)
      QA(6)=QH2*CONJG(QH2)
      QLC(6)=QD2P
      QLD(6)=CONJG(QD2P)
      QA(7)=QH2*CONJG(QH3)
      QLC(7)=QD2P
      QLD(7)=-CONJG(QD2P)
      QA(8)=QH2*CONJG(QH4)
      QLC(8)=QD2P
      QLD(8)=-CONJG(QD1P)
      QA(9)=QH3*CONJG(QH1)
      QLC(9)=-QD2P
      QLD(9)=CONJG(QD1P)
      QA(10)=QH3*CONJG(QH2)
      QLC(10)=-QD2P
      QLD(10)=CONJG(QD2P)
      QA(11)=QH3*CONJG(QH3)
      QLC(11)=-QD2P
      QLD(11)=-CONJG(QD2P)
      QA(12)=QH3*CONJG(QH4)
      QLC(12)=-QD2P
      QLD(12)=-CONJG(QD1P)
      QA(13)=QH4*CONJG(QH1)
      QLC(13)=-QD1P
      QLD(13)=CONJG(QD1P)
      QA(14)=QH4*CONJG(QH2)
      QLC(14)=-QD1P
      QLD(14)=CONJG(QD2P)
      QA(15)=QH4*CONJG(QH3)
      QLC(15)=-QD1P
```

```
      QLD(15)=-CONJG(QD2P)
      QA(16)=QH4*CONJG(QH4)
      QLC(16)=-QD1P
      QLD(16)=-CONJG(QD1P)
      CALL SUM(IN,QA,QLC,QLD,QSM)
      AY1=4.*XLX*XLY*YLZ*AL11/ALD
      QAXX=AY1*QSM
      QAZZ=(QAXX*(XK0*SN)**2)/(XK1Z**2)
      QAYZ=XK0*SN*QAXX/XK1Z
      QNJ3=QA1H*QT2
      QA(1)=QH1*CONJG(QNJ3)
      QLC(1)=QD1P
      QLD(1)=CONJG(QD1)
      QNJ4=QA1H*QV2
      QA(2)=QH1*CONJG(QNJ4)
      QLC(2)=QD1P
      QLD(2)=CONJG(QD2)
      QA(3)=QH1*CONJG(QT2)
      QLC(3)=QD1P
      QLD(3)=-CONJG(QD2)
      QA(4)=QH1*CONJG(QV2)
      QLC(4)=QD1P
      QLD(4)=-CONJG(QD1)
      QA(5)=QH2*CONJG(QNJ3)
      QLC(5)=QD2P
      QLD(5)=CONJG(QD1)
      QA(6)=QH2*CONJG(QNJ4)
      QLC(6)=QD2P
      QLD(6)=CONJG(QD2)
      QA(7)=QH2*CONJG(QT2)
      QLC(7)=QD2P
      QLD(7)=-CONJG(QD2)
      QA(8)=QH2*CONJG(QV2)
      QLC(8)=QD2P
      QLD(8)=-CONJG(QD1)
      QA(9)=QH3*CONJG(QNJ3)
      QLC(9)=-QD2P
      QLD(9)=CONJG(QD1)
      QA(10)=QH3*CONJG(QNJ4)
      QLC(10)=-QD2P
      QLD(10)=CONJG(QD2)
      QA(11)=QH3*CONJG(QT2)
      QLC(11)=-QD2P
      QLD(11)=-CONJG(QD2)
      QA(12)=QH3*CONJG(QV2)
      QLC(12)=-QD2P
      QLD(12)=-CONJG(QD1)
      QA(13)=QH4*CONJG(QNJ3)
      QLC(13)=-QD1P
      QLD(13)=CONJG(QD1)
      QA(14)=QH4*CONJG(QNJ4)
      QLC(14)=-QD1P
      QLD(14)=CONJG(QD2)
      QA(15)=QH4*CONJG(QT2)
      QLC(15)=-QD1P
      QLD(15)=-CONJG(QD2)
      QA(16)=QH4*CONJG(QV2)
```

```
      QCC(16)=-QC1P
      QLD(16)=-CONJG(QC1)
      CALL SUM(IN,QA,QCC,QLD,QSM)
      QAXY1=CONJG(QKA)*CONJG(QKA)*CONJG(QM)
      QAXY2=-4.*XLX*XLY*XLZ*AL11*QAXY1/ALD
      QAXY=QAXY2*QSM
      QS01=QERX*CONJG(QERX)*QAAX
      QNJ5=QERX*ERY*QAXY
      QS02=2.*REAL(QNJ5)
      QNJ6=QERX*CAXZ*CONJG(QERZ)
      QS03=2.*REAL(QNJ6)
      QS04=ERY*ERY*QAYY
      QNJ7=ERY*QERZ*QAXY/XK1Z
      QS05=2.*XKO*SN*REAL(QNJ7)
      QSS1=QA1*CONJG(QA1)+A2**2+QA3*CONJG(QA3)
      QS06=QERZ*CONJG(QERZ)*QAZZ
      QS1=QS01+QS02+QS03
      QS2=QS04+QS05+QS06
      QSA=((XKO*CS)**2)*(QS1+QS2)/(PI*QSS1)
      SIGO=REAL(QSA)
      DESIGO=10.*ALOG10(SIGO)
C  THE FOLLOWING CARDS CALCULATE THE BACKSCATTER COEFFICIENT
C  FOR A VEGETATION LAYER WITH A ROUGH VEGETATION SOIL BOUNDARY
      Y1=2.*P1*Q1
      X1=Q1**2-P1**2+(XKO*SN)**2
      PHE=ATAN2(Y1,X1)
      RHOE=SQRT(Y1**2+X1**2)
      ALE=(SQRT(RHOE))*SIN(PHE/2.)
      BE=(SQRT(RHOE))*COS(PHE/2.)
      A=XKO*BE/(BE**2+ALE**2)
      B=XKO*ALE/(BE**2+ALE**2)
      G1=2.*A*B*SN**2
      G2=1.-(A**2-B**2)*SN**2
      GAM=0.5*ATAN2(G1,G2)
      RHO=(G1**2+G2**2)**0.25
      D1=RHO*(BE*COS(GAM)-ALE*SIN(GAM))
      D2=SQRT((XKO*SN)**2+D1**2)
      SECS=D2/D1
      SINS=XKO*SN/D2
      COSS=D1/D2
      TANS=SINS/COSS
      R1=SQRT(R3**2-(BE*SINS)**2)
      R2=BE*COSS
      R0=(R2-R1)/(R2+R1)
      R3=(R0/(2.*XMS))**2
      ZZ1=(TANS/(2.*XMS))**2
      ZZ2=4.*ALE*XL*SECS
      GT0=1.-2.*EE*COSS/P1
      GT1=(1.+GT0**2)*SINS*SINS
      GT2=2.*(1.-GT0*COSS*COSS)
      GT=1.-SINS*SINS*(GT2-GT1)
      R4=R3*GT/COSS**4
      IF(ZZ1-500.)801,802,802
  802 R5=0.0
      GO TO 803
  801 R5=R4*EXP(-ZZ1)*EXP(-ZZ2)
  803 AYY=REAL(QAYY)
```

```
      SIGHH=R5*(AYY*(XKO*CS)**2)/PI
      DBHH=10.*ALOG10(SIGHH)
      WRITE(6,601)THETA
  601 FORMAT(1H ,6HTHETA=,F5.2)
      DD1=1./P1
      WRITE(6,715)P1,DD1
  715 FORMAT(1H ,3HP1=,E15.7,10X,3HD1=,E15.7)
      WRITE(6,602)DBSIG
  602 FORMAT(1H ,10X,22HHALF SPACE SIGMA ZERO=,F15.8)
      WRITE(6,603) DBSIGO
  603 FORMAT(1H ,10X,17HLAYER SIGMA ZERO=,F15.8)
      WRITE(6,604)DBHH
  604 FORMAT(1H ,10X,39HLAYER WITH ROUGH SURFACE SIGMA ZERO HH=,F15.8//)
      IF(THETA-FC.130C,304,304
  303 THETA=THETA+1.
      GO TO 401
  304 IF(MO-4)605,606,606
  605 MO=MO+1
      GO TO 7
  606 STOP
      END
```

SYMBOLIC REFERENCE MAP (R=1)

ENTRY POINTS
4135 MODEL

VARIABLES		SN	TYPE	RELOCATION				
2	A		REAL	/ /	17	AER	REAL	/ /
12213	ALD		REAL		12242	ALE	REAL	
12212	ALAT		REAL		21	AO	REAL	/ /
12151	AX1		REAL		12245	AYY	REAL	
12153	AY2		REAL		12152	AZ1	REAL	
12150	A2		REAL		12177	A3	REAL	
7	B		REAL	/ /	12175	GB	REAL	
12223	BE		REAL		40	BO	REAL	/ /
12176	B3		REAL		4	C	REAL	/ /
12071	CC		REAL		12234	COSS	REAL	
12075	CS		REAL		5	D	REAL	/ /
12247	DBHH		REAL		12173	DBSIG	REAL	
12215	DBSIGO		REAL		12251	DD1	REAL	
1	DK		REAL	/ /	0	DT	REAL	/ /
12230	D1		REAL		12231	D2	REAL	
12067	EA		REAL		12053	EC	REAL	
12202	EH		REAL		12069	ELP	REAL	
12661	ELPP		REAL		14	EO	REAL	/ /
12171	ER		REAL		12173	ERO	REAL	
12162	EXY		REAL		12167	ER1	REAL	
12076	ETA		REAL		12064	ETA1	REAL	
12063	ETA11		REAL		12366	ETA2	REAL	
12066	ETA22		REAL		12203	EV	REAL	
12174	E3		REAL		12052	F	REAL	
12197	FNK		REAL		12103	FNT	REAL	

```
VARIABLES      SN  TYPE         RELOCATION
12226  SAM         REAL                         12244  GT      REAL
12241  GTO         REAL                         12242  GT1     REAL
12243  GT2         REAL                         12224  G1      REAL
12225  G2          REAL                         12106  I       INTEGER
12211  IN          INTEGER                      12107  J       INTEGER
12077  M           INTEGER                      12047  MQ      INTEGER
12101  NK          INTEGER                      12104  NKK     INTEGER
12105  NM          INTEGER                      12111  NN      INTEGER
12100  NT          INTEGER                      12110  NTT     INTEGER
12115  PD          REAL                         12220  PHE     REAL
12161  PH2         REAL                         12116  PH3     REAL
12127  PH4         REAL                            15  PI      REAL
12056  PM          REAL                         12114  PN      REAL
12122  P1          REAL                         12132  P2      REAL
11515  Q           COMPLEX                      43721  QA      COMPLEX  ARRAY
11603  QAA1        COMPLEX                      43661  QAL     COMPLEX  ARRAY
11605  QAL1        COMPLEX                      11763  QAXX    COMPLEX
11777  QAXY        COMPLEX                      11773  QAXY1   COMPLEX
11775  QAXY2       COMPLEX                      11767  QAXZ    COMPLEX
11507  QAY2        COMPLEX                      11733  QAYY    COMPLEX
11501  QAY1        COMPLEX                      11517  QAZ     COMPLEX
11765  QAZZ        COMPLEX                      11505  QAZ2    COMPLEX
11451  QA1         COMPLEX                      11653  QA1H    COMPLEX
11651  QA1HD       COMPLEX                      11647  QA1HN   COMPLEX
11563  QA11        COMPLEX                      11565  QA12    COMPLEX
11561  QA2H        COMPLEX                      11655  QA2HA   COMPLEX
11657  QA24H       COMPLEX                      11567  QA21    COMPLEX
11571  QA22        COMPLEX                      11453  QA3     COMPLEX
11665  QA3H        COMPLEX                      11663  QA3HA   COMPLEX
11667  QA4H        COMPLEX                      11671  QA5H    COMPLEX
11673  QA6H        COMPLEX                      11675  QA7H    COMPLEX
11447  QA9H        COMPLEX                      43701  QB      COMPLEX  ARRAY
11677  QB1         COMPLEX                      11667  QB11    COMPLEX
11611  QB12        COMPLEX                      11701  QB2     COMPLEX
11615  QB21        COMPLEX                      11613  QB21A   COMPLEX
11617  QB22        COMPLEX                      11703  QB3     COMPLEX
11725  QB4         COMPLEX                      11735  QB5     COMPLEX
11737  QB6         COMPLEX                      11327  QC      COMPLEX
43751  QCC         COMPLEX  ARRAY               11523  QCX1    COMPLEX
11521  QCX2        COMPLEX                      43571  QD      COMPLEX  ARRAY
11725  QD1         COMPLEX                      11717  QD1C    COMPLEX
11741  QD1P        COMPLEX                      11721  QD2     COMPLEX
11727  QD2C        COMPLEX                      11771  QD2P    COMPLEX
11555  QE          COMPLEX                      11531  QERX    COMPLEX
11543  QESZ        COMPLEX                      11535  QES1    COMPLEX
11537  QES2        COMPLEX                      11491  QES3    COMPLEX
11775  QES4        COMPLEX                      11417  QEHH    COMPLEX
11424  QE11        COMPLEX                      11423  QE12    COMPLEX
11425  QE13        COMPLEX                      11427  QE22    COMPLEX
11431  QE23        COMPLEX                      11433  QE33    COMPLEX
12751  QF11        COMPLEX  ARRAY               15151  QF12    COMPLEX  ARRAY
27051  QF13        COMPLEX  ARRAY               25751  QF22    COMPLEX  ARRAY
31051  QF23        COMPLEX  ARRAY               35551  QF33    COMPLEX  ARRAY
43711  QG          COMPLEX  ARRAY               11331  QGI11   COMPLEX
11337  QGI12       COMPLEX                      11335  QGI17   COMPLEX
11757  QGI22       COMPLEX                      11341  QGI23   COMPLEX
11343  QGI32       COMPLEX                      11345  QGI12   COMPLEX
```

VARIABLES	SN	TYPE	RELOCATION				
11357	QG113	COMPLEX		11347	QG122	COMPLEX	
11361	QG123	COMPLEX		11351	QG132	COMPLEX	
11363	QG133	COMPLEX		11353	QG222	COMPLEX	
11365	QG223	COMPLEX		11355	QG232	COMPLEX	
11367	QG233	COMPLEX		11373	QG332	COMPLEX	
11371	QG333	COMPLEX		11747	QH1	COMPLEX	
11743	QH11	COMPLEX		11745	QH12	COMPLEX	
11755	QH2	COMPLEX		11751	QH21	COMPLEX	
11757	QH22	COMPLEX		11757	QH3	COMPLEX	
11761	QH4	COMPLEX		43021	QI11	COMPLEX	ARRAY
43005	QI11A	COMPLEX	ARRAY	41451	QI112	COMPLEX	ARRAY
41547	QI113	COMPLEX	ARRAY	43117	QI12	COMPLEX	ARRAY
43011	QI12A	COMPLEX	ARRAY	41645	QI122	COMPLEX	ARRAY
41743	QI123	COMPLEX	ARRAY	43215	QI13	COMPLEX	ARRAY
43015	QI13A	COMPLEX	ARRAY	42041	QI132	COMPLEX	ARRAY
42137	QI133	COMPLEX	ARRAY	43313	QI22	COMPLEX	ARRAY
44661	QI22A	COMPLEX	ARRAY	42235	QI222	COMPLEX	ARRAY
42333	QI223	COMPLEX	ARRAY	43411	QI23	COMPLEX	ARRAY
44455	QI23A	COMPLEX	ARRAY	42431	QI232	COMPLEX	ARRAY
42527	QI233	COMPLEX	ARRAY	43507	QI33	COMPLEX	ARRAY
44071	QI33A	COMPLEX	ARRAY	42625	QI332	COMPLEX	ARRAY
42723	QI333	COMPLEX	ARRAY	11521	QJ	COMPLEX	
12043	QJJ1	COMPLEX		12045	QJJ2	COMPLEX	
43641	QK	COMPLEX	ARRAY	11323	QKA	COMPLEX	
11447	QKH	COMPLEX		11325	QKK	COMPLEX	
11445	QKV	COMPLEX		11435	QKV1	COMPLEX	
11477	QKV2	COMPLEX		11507	QKZP	COMPLEX	
11525	QKZPC	COMPLEX		11561	QK3	COMPLEX	
11557	QKZC3	COMPLEX		11645	QK3Z	COMPLEX	
44021	QLD	COMPLEX	ARRAY	11713	QM	COMPLEX	
12347	QMI11	COMPLEX	ARRAY	16247	QMI12	COMPLEX	ARRAY
22147	QMI13	COMPLEX	ARRAY	26047	QMI22	COMPLEX	ARRAY
31747	QMI23	COMPLEX	ARRAY	35647	QMI33	COMPLEX	ARRAY
11707	QM1	COMPLEX		11377	QM11	COMPLEX	
11401	QM12	COMPLEX		11403	QM13	COMPLEX	
11711	QM2	COMPLEX		11405	QM22	COMPLEX	
11413	QM23	COMPLEX		11415	QM33	COMPLEX	
12025	QNJ1	COMPLEX		12027	QNJ2	COMPLEX	
12031	QNJ3	COMPLEX		12033	QNJ4	COMPLEX	
12035	QNJ5	COMPLEX		12037	QNJ6	COMPLEX	
12041	QNJ7	COMPLEX		11731	QNYY	COMPLEX	
11725	QNYY1	COMPLEX		11727	QNYY2	COMPLEX	
11547	QS	COMPLEX		12023	QSA	COMPLEX	
11557	QSH	COMPLEX		11407	QSG	COMPLEX	
11527	QSM	COMPLEX		12001	QS01	COMPLEX	
12003	QS02	COMPLEX		12005	QS03	COMPLEX	
12007	QS04	COMPLEX		12011	QS05	COMPLEX	
12015	QS06	COMPLEX		12013	QSS1	COMPLEX	
12017	QS1	COMPLEX		11541	QS11	COMPLEX	
11543	QS12	COMPLEX		11545	QS13	COMPLEX	
11551	QS14	COMPLEX		12021	QS2	COMPLEX	
11477	QT1	COMPLEX		11621	QT1A	COMPLEX	
11625	QT1D	COMPLEX		11623	QT1N	COMPLEX	
11473	QT13	COMPLEX		11463	QT131	COMPLEX	
11465	QT132	COMPLEX		11467	QT133	COMPLEX	
11471	QT134	COMPLEX		11461	QT2	COMPLEX	
11575	QT2D	COMPLEX		11573	QT2N	COMPLEX	

```
VARIABLES    SN  TYPE        RELOCATION
11455  QT21   COMPLEX                     11457  QT22    COMPLEX
11475  QT3    COMPLEX                     11633  QT3A    COMPLEX
11635  QT[illegible]  COMPLEX             11637  QT3C    COMPLEX
11641  QT[illegible]  COMPLEX             11441  QVN     COMPLEX
11631  QV1    COMPLEX                     11627  QV1N    COMPLEX
11621  QV2    COMPLEX                     11577  QV2N    COMPLEX
11647  QV[illegible]  COMPLEX             12123  Q1      REAL
11571  QX[illegible]  COMPLEX             12133  Q2      REAL
11571  [illegible]  COMPLEX               12165  R       REAL
12227  [illegible]  REAL                  12271  RHOF    REAL
12225  [illegible]  REAL                  12261  RH2     REAL
12[illegible]  [illegible]  REAL          12205  RH31    REAL
12[illegible]  [illegible]  REAL          12051  RLV     REAL
12[illegible]  [illegible]  REAL          12167  R1      REAL
12176  R11    REAL                        12157  R12     REAL
12150  R2     REAL                        12117  R3      REAL
12126  R4     REAL                        12164  R5      REAL
12155  RF     REAL                        12232  SECS    REAL
12054  SG     REAL                        12172  SIG     REAL
   44  SIGS   REAL        //              12265  SIGHH   REAL
12064  SIGL   REAL                        12214  SIGO    REAL
12237  SIGT   REAL                           22  SN      REAL        //
12235  THRS   REAL                        12074  TH      REAL
12073  THETA  REAL                        12056  U       REAL
   13  UF     REAL        //                 12  V       REAL        //
12370  Y24    REAL                        12134  XE11    REAL
12136  YE12   REAL                        12140  YE13    REAL
12142  YE22   REAL                        12144  YE23    REAL
12145  YE33   REAL                        12120  XH      REAL
   11  XKC    REAL        //              12154  XKX     REAL
12204  XKY    REAL                        12155  XKZ     REAL
12210  XK1Z   REAL                           23  XL      REAL        //
12072  XLAM   REAL                        12057  XLAMC   REAL
   10  XLX    REAL        //                  7  XLY     REAL        //
    6  XLZ    REAL        //              12055  XMS     REAL
12130  XV     REAL                        12217  X1      REAL
12112  X2?    REAL                        12124  X4      REAL
12135  YE11   REAL                        12137  YE12    REAL
12141  YE13   REAL                        12143  YE22    REAL
12145  YE23   REAL                        12147  YE33    REAL
12121  YH     REAL                        12131  YV      REAL
12215  Y1     REAL                        12113  Y22     REAL
12125  Y4     REAL                        12237  ZZ1     REAL
12246  ZZ2    REAL

FILE NAMES    MODE
    0  INPUT          2054  OUTPUT          0  TAPE5     FMT     2054  TAPE6     FMT

EXTERNALS        TYPE     ARGS
    ALOG10       REAL      1 LIBRARY          ATAN2    REAL    2 LIBRARY
    CEXP         COMPLEX   1 LIBRARY          COS      REAL    1 LIBRARY
    EXP          REAL      1 LIBRARY          SIN      REAL    1 LIBRARY
    SNORT                  8                  SQRT     REAL    1 LIBRARY
    SUM                    5
```

```
INLINE FUNCTIONS    TYPE    ARGS
       AIMAG        REAL      1  INTRIN                        CONJG      COMPLEX    1  INTRIN
       REAL         REAL      1  INTRIN

STATEMENT LABELS
  4149   7
 11066  13       FMT                       11043  10     FMT                           11056  11     FMT
 11142  105      FMT                       10777  101    FMT                           11002  102    FMT
 11022  110      FMT                       11036  106    FMT                           11013  109    FMT
     0  294                                 4367  202                                      0  203
     0  207                                    0  285         INACTIVE                  4627  236
 10723  704                                    0  298                                      0  303         INACTIVE
  4352  388                                    0  305         INACTIVE                  5336  307
  4312  401                                    0  311         INACTIVE                  6270  312
 11226  601      FMT                           0  510                                      0  511
 11270  604      FMT                       11244  602    FMT                           11257  603     FMT
 11164  708      FMT                           0  605         INACTIVE                 10727  606
 11160  711      FMT                       11135  709    FMT                           11147  710     FMT
 11247  714      FMT                       11174  712    FMT                           11234  713     FMT
     0  802            INACTIVE            11236  715    FMT                           10066  801
                                           10674  803

LOOPS   LABEL    INDEX     FROM-TO    LENGTH    PROPERTIES
 4436   203      J         133 139     274         OPT
 4511   204      J         141 147     279         OPT
 4710   207      I         175 181     276         OPT
 4735   208      I         183 189     273         OPT
 5620   510      I         325 330     623         OPT
 5710   511      I         336 344     623         OPT

COMMON BLOCKS    LENGTH
      //            2E

STATISTICS
  PROGRAM LENGTH                 77453    16357
  BUFFER LENGTH                  41303     4176
  CM BLANK COMMON LENGTH           24,      20
          564C0B CM USED
```

THIS PAGE IS BEST QUALITY PRACTICABLE
FROM COPY FURNISHED TO DDC

```
      SUBROUTINE SNOFT(NPH,NKK,QMI11,QMI12,QMI13,QMI22,QMI23,QMI33)
      COMPLEX QW,QWOO,OKA,QKEZ,COQ1,QG,QWQ2,QH,QM1,QM12,QQO,
     1QMI12(31,31),QM13,QMI13(31,31),QM22,QMI22(31,31),QM23,QMI23(31,31)
     2,QM33,QMI33(31,31),QMI11(31,31)
      COMMON DT,DK,A,H,C,D,XLZ,XLY,XLK,KKO,N,UO,EO,PI,SIGA,AER,BO,AU,SN,
     1YL
      DO 231 J=1,NPH
      DO 231 I=1,NKK
      AI=I-1
      AJ=J-1
      XK=A+AI*DK
      ETC=H+AJ*DT
      P11=N*UO*SIGA
      P12=XKO*XKO*AER-XK*XK
      P1=SQRT(P11**2+P12**2)
      IF(P12)501,502,503
  501 PH1=PI-ASIN(P11/P1)
      GO TO 504
  502 PH1=PI/2.
      GO TO 504
  503 PH1=ASIN(P11/P1)
  504 QJ=(0.0,1.0)
      QWO=SQRT(-1)*CEXP(-QJ*PH1/2.)
      QKA=SQ-QJ*AO
      P22=XKO*XKO*BO-(XKO*SN)**2
      P2=SQRT(P11**2+P22**2)
      PH2=ATAN2(P11,P22)
      QKEZ=-SQRT(P2)*CEXP(-QJ*PH2/2.)
      COQ1=QJ*XLZ*(QKEZ+QWOO)
      QG=-1./(1.+COQ1)
      QWQ2=QJ*XLY*(QKEZ-QWQO)
      QH=1./(QWQ2-1.)
      SNT=SIN(ET)
      CNT=COS(ET)
      QM1=(QG+QH)*(QKA**2-(XK*CNT)**2)
      QM11=1.+XLX*XLY*(XKO*SN*XK[illegible]**2
      QM12=1.+(XLY*XK*SNT)**2
      [illegible]=XK/QOO
      QMI11(I,J)=[illegible]/(QM11*QM22)
      QM12=-XK*XK*SNT*SNT*(QG+QH)
      QMI12(I,J)=[illegible]*QM12/(QM11*QM12)
      [illegible]*(QH-QG)
      QMI13(I,J)=[illegible]13/(QM11*QM22)
      QM22=(QK[illegible]*(XK*[illegible])**2)*(QH+QG)
      [illegible]/(QM11*QM22)
      [illegible](QH-QG)
      QMI23(I,J)=[illegible]23/(QM11*QM22)
      [illegible](QG+[illegible])
      QMI33(I,J)[illegible]/(QM11*QM22)
  231 CONTINUE
```

```
SYMBOLIC REFERENCE MAP (R=1)

ENTRY POINTS
    3  SHORT

VARIABLES       SN  TYPE          RELOCATION
    7  A            REAL                //          17  AER        REAL              //
   21  AO           REAL                //           ?  B          REAL              //
   20  BO           REAL                //           4  C          REAL              //
  40?  CNN          REAL                             5  D          REAL              //
    1  DK           REAL                //           0  DT         REAL              //
   14  EO           REAL                //         363  I          INTEGER
    ?  NMM          INTEGER           F.P.           ?  NKK        INTEGER          F.P.
  37?  PH2          REAL                           373  PH1        REAL
  350  QDD          COMPLEX                         15  PI         REAL              //
  34?  QH           COMPLEX                        375  QG         COMPLEX
  33?  QKA          COMPLEX                        324  QJ         COMPLEX
  401  QMD1         REAL                           ?3?  QKEZ       COMPLEX
    0  QMI11        COMPLEX  ARRAY    F.P.         402  QMD2       REAL
    ?  QMI13        COMPLEX  ARRAY    F.P.           0  QMI12      COMPLEX  ARRAY   F.P.
    ?  QMI23        COMPLEX  ARRAY    F.P.           0  QMI22      COMPLEX  ARRAY   F.P.
  346  QM1          COMPLEX                          0  QMI33      COMPLEX  ARRAY   F.P.
  352  QM13         COMPLEX                        34?  QM12       COMPLEX
  356  QM23         COMPLEX                        354  QM22       COMPLEX
  37?  QM?3         COMPLEX                        36?  QM33       COMPLEX
  34?  QM?2         COMPLEX                        334  QQD1       COMPLEX
  37?  R11          REAL                           372  R1         REAL
  37?  R2           REAL                           371  R12        REAL
   1?  SIGA         REAL                //         ?74  R22        REAL
  377  SNN          REAL                            2?  SN         REAL              //
   13  UD           REAL                //         ?67  TT         REAL
  364  WT           REAL                            12  W          REAL              //
  ?06  XK           REAL                           365  WJ         REAL
   23  XL           REAL                //          11  XKO        REAL              //
    7  XLY          REAL                //          1?  XLX        REAL              //
                                                     6  XLZ        REAL              //

EXTERNALS         TYPE      ARGS
       ASIN       REAL       1 LIBRARY              ATAN2      REAL       2 LIBRARY
       CEXP       COMPLEX    1 LIBRARY              COS        REAL       1 LIBRARY
       SIN        REAL       1 LIBRARY              SQRT       REAL       1 LIBRARY

STATEMENT LABELS
    C  201                                  0  501       INACTIVE              45  502
   5?  503                                 53  33?

LOOPS  LABEL   INDEX    FROM-TO   LENGTH     PROPERTIES
   16  201     * J       7 5?      267B           EXT REFS  NOT INNER
   ?7  ?01     * I       ? 5?      264?           EXT REFS

COMMON BLOCKS   LENGTH
    / /            20

STATISTICS
  PROGRAM LENGTH                4233     275
  CM BLANK COMMON LENGTH         24?      20
```

STATISTICS
PROGRAM LENGTH

```
      SUBROUTINE SUM(IM,QA,QLC,QLD,QSM)
      COMPLEX QA(15),QLC(16),QLD(16),QSM,Q1,Q2,Q3,Q4,Q5,QCHK,QCHKK,
     1Q6,Q1N,Q1D,Q7,Q8,Q9,Q10,Q11,Q12N,Q12D,Q12,QS
      COMMON CT,DK,A,E,C,J,XLZ,XLY,XLX,XKO,W,UO,EO,PI,SIGA,AER,BO,AO,SN,
     1XL
      QSM=(0.0,0.0)
      DO 520 II=1,IM
      Q1=QA(II)/(QLC(II)+QLD(II))
      Q2=1.-XLZ*QLD(II)
      Q3=XLZ*(QLC(II)+QLD(II))
      QCHK=XL*(QLC(II)+1./XLZ)
      ACHK=REAL(QCHK)
      IF(ACHK-600.)522,522,521
  521 Q4=(0.0,0.0)
      GO TO 523
  522 Q4=Q3*CEXP(-QCHK)
  523 Q5=1.+XLZ*QLC(II)
      Q6=Q5*CEXP(-XL*(QLC(II)+QLD(II)))
      Q1N=Q2+Q4-Q6
      Q1D=Q5*Q2
      Q7=Q1N/Q1D
      Q8=1.-XLZ*QLC(II)
      QCHKK=XL*(1./XLZ+QLD(II))
      ACHKK=REAL(QCHKK)
      IF(ACHKK-600.)525,525,524
  524 Q9=(0.0,0.0)
      GO TO 526
  525 Q9=Q3*CEXP(-QCHKK)
  526 Q10=1.+QLD(II)*XLZ
      Q11=Q10*CEXP(-XL*(QLC(II)+QLD(II)))
      Q12N=Q8+Q9-Q11
      Q12D=Q10*Q8
      Q12=Q12N/Q12D
      QS=Q1*(Q7+Q12)
      QSM=QSM+QS
  520 CONTINUE
      RETURN
      END
```

SYMBOLIC REFERENCE MAP (R=1)

ENTRY POINTS
3 SUM

VARIABLES	SN	TYPE	RELOCATION					
2	A	REAL	/ /	254	QCHK	REAL		
265	ACHKK	REAL		17	AER	REAL	/ /	
21	AO	REAL	/ /	3	C	REAL	/ /	
22	BO	REAL	/ /	4	E	REAL	/ /	
5	C	REAL	/ /	1	DK	REAL	/ /	
0	CT	REAL	/ /	16	EO	REAL	/ /	
407	II	INTEGER		0	IM	INTEGER	F.P.	
15	PI	REAL	/ /	2	QA	COMPLEX	ARRAY	F.P.

THIS PAGE IS BEST QUALITY PRACTICABLE FROM COPY FURNISHED TO DDC

```
VARIABLES      SN  TYPE              RELOCATION
   2  DLC          COMPLEX    ARRAY     F.P.        227  DLHK       COMPLEX
 231  DMHKK        COMPLEX                            7  Q.D        COMPLEX    ARRAY    F.P.
 261  DP           COMPLEX                            3  QSM        COMPLEX             F.P.
 215  Q1           COMPLEX                          237  Q1D        COMPLEX
 235  Q1M          COMPLEX                          247  Q10        COMPLEX
 251  Q11          COMPLEX                          257  Q12        COMPLEX
 2?5  Q12?         COMPLEX                          253  Q12N       COMPLEX
 217  Q2           COMPLEX                          221  Q3         COMPLEX
 273  Q4           COMPLEX                          225  Q5         COMPLEX
 263  Q6           COMPLEX                          241  Q7         COMPLEX
 243  Q8           COMPLEX                          245  Q9         COMPLEX
  15  SIGA         REAL               / /            22  SN         REAL               / /
  13  W0           REAL               / /            12  4          REAL               / /
  21  4K0          REAL               / /            23  XL         REAL               / /
  17  XLY          REAL               / /             7  ALY        REAL               / /
   6  XLZ          REAL               / /

EXTERNALS          TYPE      ARGS
     CEXP          COMPLEX     1 LIBRARY

INLINE FUNCTIONS   TYPE      ARGS
     REAL          REAL        1  INTRIN

STATEMENT LABELS
     0  520                                   0  521        INACTIVE            52  522
    61  523                                   0  52?        INACTIVE           132  525
   141  526

LOOPS  LABEL    INDEX     FROM-TO     LENGTH     PROPERTIES
   26  520      * 4?        7  75       1713              EXT REFS

COMMON BLOCKS   LENGTH
     / /            2?

STATISTICS
   PROGRAM LENGTH                     3063      139
   CM BLANK COMMON LENGTH              2??       2?
          [illegible]
FRACTION OF WATER BY WEIGHT IN THE VEGETATION=  .400
VOLUME OF VEGETATION DIVIDED BY TOTAL VOLUME=  .0016050
FREQUENCY=    .72??????+10
RATIO OF THE STANDARD DEVIATION OF THE ROUGH SURFACE FLUCTUATIONS TO THE CORRELATION DISTANCE OF THE FLUCTUATIONS=    .10000
ALX=    .[illegible]      ALY=    .[illegible]      KLZ=    .[illegible]
LAYER THICKNESS IN METER =  ?.50????
DIELECTRIC CONSTANT OF THE SOIL =  ?.?2????
CONDUCTIVITY OF THE SOIL = 1.?3?????
THE AVERAGE DIELECTRIC CONSTANT=  ?.??5??2
STD. DEV. OF DIELECTRIC FLUCTUATIONS=  .5219577
STD. DEV. OF CONDUCTIVITY FLUCTUATIONS=  .[illegible]
S0=    .[illegible]
THETA= [illegible]
P1=   .?0?1??????+01          Q1=   .130????E+?0
        HALF SPACE [illegible]  =    -1.56341??3
        LOWER [illegible]  =    -?.?????1?
        LAYER WITH ROUGH SURFACE SIGMA ZERO HHS    -1.?5????1?

THETA=10.??
P1=   .7??????+01          Q1=   .1?7?????+0?
        HALF [illegible]  =    -1.7?????1??
```

```
      LAYER SIGMA ZERO=     -1.65635636
      LAYER WITH ROUGH SURFACE SIGMA ZERO HH=     -1.65635606

THETA=20.00
P1=   .82953/9E+01           D1=    .1205493E+00
      HALF SPACE SIGMA ZERO=     -2.14150169
      LAYER SIGMA ZERO=     -2.16972929
      LAYER WITH ROUGH SURFACE SIGMA ZERO HH=     -2.15372925

THETA=30.00
P1=   .9153439E+01           D1=    .1391286E+00
      HALF SPACE SIGMA ZERO=     -2.60139690
      LAYER SIGMA ZERO=     -2.64657649
      LAYER WITH ROUGH SURFACE SIGMA ZERO HH=     -2.64657649

THETA=40.00
P1=   .1055435E+02           D1=    .9475032E-01
      HALF SPACE SIGMA ZERO=     -3.14455143
      LAYER SIGMA ZERO=     -3.11359811
      LAYER WITH ROUGH SURFACE SIGMA ZERO HH=     -3.11359811

THETA=50.00
P1=   .1276579E+02           D1=    .7831595E-01
      HALF SPACE SIGMA ZERO=     -3.53355751
      LAYER SIGMA ZERO=     -3.54758324
      LAYER WITH ROUGH SURFACE SIGMA ZERO HH=     -3.54758324

THETA=60.00
P1=   .1655454E+02           D1=    .6046637E-01
      HALF SPACE SIGMA ZERO=     -3.94924145
      LAYER SIGMA ZERO=     -3.94716745
      LAYER WITH ROUGH SURFACE SIGMA ZERO HH=     -3.94716745

THETA=70.00
P1=   .2371631E+02           D1=    .4216551E-01
      HALF SPACE SIGMA ZERO=     -5.04035386
      LAYER SIGMA ZERO=     -5.03837894
      LAYER WITH ROUGH SURFACE SIGMA ZERO HH=     -5.03837894

THETA=80.00
P1=   .3470571E+02           D1=    .2881370E-01
      HALF SPACE SIGMA ZERO=     -9.53713292
      LAYER SIGMA ZERO=     -9.53709514
      LAYER WITH ROUGH SURFACE SIGMA ZERO HH=     -9.53709514

FRACTION OF WATER BY WEIGHT IN THE VEGETATION=  .900
VOLUME OF VEGETATION DIVIDED BY TOTAL VOLUME=  .0010000
FREQUENCY=    .725000E+10
RATIO OF THE STANDARD DEVIATION OF THE ROUGH SURFACE FLUCTUATIONS TO THE CORRELATION DISTANCE OF THE FLUCTUATIONS=    .03000
XLX=    .01000000      XLY=    .00400000      XLZ=    .00800000
LAYER THICKNESS IN METERS =  2.500000
DIELECTRIC CONSTANT OF THE SOIL =  7.500000
CONDUCTIVITY OF THE SOIL = 1.3900000
THE AVERAGE DIELECTRIC CONSTANT=  1.026002
STD. DEV. OF DIELECTRIC FLUCTUATIONS=  .8218577
STD. DEV. OF CONDUCTIVITY FLUCTUATIONS=  .0349991
A0=   .5589396E+00
THETA= 0.00
```

```
P1=   .67978720E+01          Q1=   .1471049E+00
          HALF SPACE SIGMA ZERO=    -1.09287153
          LAYER SIGMA ZERO=    -1.07253785
          LAYER WITH ROUGH SURFACE SIGMA ZERO HH=     -1.07253785

THETA=10.00
P1=   .69794?3E+01           Q1=   .1453115E+00
          HALF SPACE SIGMA ZERO=    -2.15424333
          LAYER SIGMA ZERO=    -2.06511277
          LAYER WITH ROUGH SURFACE SIGMA ZERO HH=     -2.06511277

THETA=20.00
P1=   .7531446E+01           Q1=   .1363087E+00
          HALF SPACE SIGMA ZERO=    -4.14902047
          LAYER SIGMA ZERO=    -4.17178520
          LAYER WITH ROUGH SURFACE SIGMA ZERO HH=     -4.17178520

THETA=30.00
P1=   .8032544E+01           Q1=   .1244936E+00
          HALF SPACE SIGMA ZERO=    -5.98710841
          LAYER SIGMA ZERO=    -5.97414737
          LAYER WITH ROUGH SURFACE SIGMA ZERO HH=     -5.97414737

THETA=40.00
P1=   .9114428E+01           Q1=   .1097543E+00
          HALF SPACE SIGMA ZERO=    -7.34962664
          LAYER SIGMA ZERO=    -7.32183067
          LAYER WITH ROUGH SURFACE SIGMA ZERO HH=     -7.32183067

THETA=50.00
P1=   .1077268E+02           Q1=   .9282571E-01
          HALF SPACE SIGMA ZERO=    -8.27761762
          LAYER SIGMA ZERO=    -8.28943467
          LAYER WITH ROUGH SURFACE SIGMA ZERO HH=     -8.28943467

THETA=60.00
P1=   .1357143E+02           Q1=   .7368202E-01
          HALF SPACE SIGMA ZERO=    -8.99010703
          LAYER SIGMA ZERO=    -8.98650962
          LAYER WITH ROUGH SURFACE SIGMA ZERO HH=     -8.98650962

THETA=70.00
P1=   .1692412E+02           Q1=   .5284261E-01
          HALF SPACE SIGMA ZERO=    -10.13759989
          LAYER SIGMA ZERO=    -10.13592344
          LAYER WITH ROUGH SURFACE SIGMA ZERO HH=    -10.13592344

THETA=80.00
P1=   .2820540E+02           Q1=   .3545672E-01
          HALF SPACE SIGMA ZERO=    -14.30669351
          LAYER SIGMA ZERO=    -14.30665782
          LAYER WITH ROUGH SURFACE SIGMA ZERO HH=    -14.30665782

FRACTION OF WATER BY WEIGHT IN THE VEGETATION=  .900
VOLUME OF VEGETATION DIVIDED BY TOTAL VOLUME=  .0010000
FREQUENCY=    .5290003E+10
RATIO OF THE STANDARD DEVIATION OF THE ROUGH SURFACE FLUCTUATIONS TO THE CORRELATION DISTANCE OF THE FLUCTUATIONS=    .10000
```

```
XLX=     .00400000       XLY=     .01000000       XLZ=     .00800000
LAYER THICKNESS IN METERS =  2.500000
DIELECTRIC CONSTANT OF THE SOIL =  7.500000
CONDUCTIVITY OF THE SOIL = 4.790000
THE AVERAGE DIELECTRIC CONSTANT=  1.048154
STD. DEV. OF DIELECTRIC FLUCTUATIONS=  .0398569
STD. DEV. OF CONDUCTIVITY FLUCTUATIONS=  .0541019
AO=    .3179828E+00
THETA= 0.00
P1=    .3682050E+01
                              Q1=    .2715674E+00
          HALF SPACE SIGMA ZERO=       -1.35917420
          LAYER SIGMA ZERO=       -1.00289420
          LAYER WITH ROUGH SURFACE SIGMA ZERO HH=       -1.00289420

THETA=10.00
P1=    .3752208E+01
                              Q1=    .2605097E+00
          HALF SPACE SIGMA ZERO=       -1.44297546
          LAYER SIGMA ZERO=       -1.25050475
          LAYER WITH ROUGH SURFACE SIGMA ZERO HH=       -1.25050475

THETA=20.00
P1=    .3972387E+01
                              Q1=    .4517378E+00
          HALF SPACE SIGMA ZERO=       -1.67452567
          LAYER SIGMA ZERO=       -1.46087852
          LAYER WITH ROUGH SURFACE SIGMA ZERO HH=       -1.46087852

THETA=30.00
P1=    .4375752E+01
                              Q1=    .2295531E+00
          HALF SPACE SIGMA ZERO=       -1.93958543
          LAYER SIGMA ZERO=       -1.94811031
          LAYER WITH ROUGH SURFACE SIGMA ZERO HH=       -1.94811031

THETA=40.00
P1=    .5031195E+01
                              Q1=    .1967598E+00
          HALF SPACE SIGMA ZERO=       -2.3605875
          LAYER SIGMA ZERO=       -2.2236987
          LAYER WITH ROUGH SURFACE SIGMA ZERO HH=       -2.2236987

THETA=50.00
P1=    .6037564E+01
                              Q1=    .1542693E+00
          HALF SPACE SIGMA ZERO=       -2.73990125
          LAYER SIGMA ZERO=       -2.91635312
          LAYER WITH ROUGH SURFACE SIGMA ZERO HH=       -2.91635312

THETA=60.00
P1=    .7634465E+01
                              Q1=    .1259317E+00
          HALF SPACE SIGMA ZERO=       -3.4[illegible]698
          LAYER SIGMA ZERO=       -3.44713[illegible]1
          LAYER WITH ROUGH SURFACE SIGMA ZERO HH=       -3.44713[illegible]1

THETA=70.00
P1=    .1127[illegible]E+02
                              Q1=    .[illegible]E-01
          HALF SPACE SIGMA ZERO=       -4.[illegible]
          LAYER SIGMA ZERO=       -4.[illegible]
          LAYER WITH ROUGH SURFACE SIGMA ZERO HH=       -4.7[illegible]

THETA=[illegible]
P1=    .[illegible]
                              Q1=    .[illegible]
```

THIS PAGE IS BEST QUALITY PRACTICABLE
FROM COPY FURNISHED TO DDC

```
     HALF SPACE SIGMA ZERO=     -8.97023184
     LAYER SIGMA ZERO=      -8.98272473
     LAYER WITH ROUGH SURFACE SIGMA ZERO HH=      -8.98272473


FRACTION OF WATER BY WEIGHT IN THE VEGETATION=  .900
VOLUME OF VEGETATION DIVIDED BY TOTAL VOLUME=  .0010000
FREQUENCY=     .52500E+02
RATIO OF THE STANDARD DEVIATION OF THE ROUGH SURFACE FLUCTUATIONS TO THE CORRELATION DISTANCE OF THE FLUCTUATIONS=     .03000
XLX=     .3100000     XLY=     .0300000     XLZ=     .0000000
LAYER THICKNESS IN METERS =  2.500000
DIELECTRIC CONSTANT OF THE SOIL =  4.500000
CONDUCTIVITY OF THE SOIL = 1.0900000
THE AVERAGE DIELECTRIC CONSTANT=  1.029154
STD. DEV. OF DIELECTRIC FLUCTUATIONS=  .8694589
STD. DEV. OF CONDUCTIVITY FLUCTUATIONS=  .05410218
AO=   .31796285E+00
THETA= 0.00
P1=    .33477862E+01              Q1=    .23874065E+00
        HALF SPACE SIGMA ZERO=        -.5921 [illegible]325
        LAYER SIGMA ZERO=       -.6 [illegible] 3693
        LAYER WITH ROUGH SURFACE SIGMA ZERO HH=       -.56883693


THETA=10.00
P1=    .3 [illegible] E+01              Q1=    .29400227E+00
        HALF SPACE SIGMA ZERO=      -1.5176610 [illegible]
        LAYER SIGMA ZERO=      -1.5491125 [illegible]
        LAYER WITH ROUGH SURFACE SIGMA ZERO HH=      -1.54911258


THETA=20.00
P1=    .3 [illegible] E+01              Q1=    . [illegible] E+00
        HALF SPACE SIGMA ZERO=      -2.8255320 [illegible]
        LAYER SIGMA ZERO=      -2.61360 [illegible] 3
        LAYER WITH ROUGH SURFACE SIGMA ZERO HH=      -2.51 [illegible]


THETA=30.00
P1=    .3 [illegible] E+01              Q1=    .25862555E+00
        HALF SPACE SIGMA ZERO=      -4.17250386
        LAYER SIGMA ZERO=      -4.12 [illegible]
        LAYER WITH ROUGH SURFACE SIGMA ZERO HH=      -4.12 [illegible]


THETA=40.00
P1=    [illegible]              Q1=    .2 [illegible] E+00
        HALF SPACE SIGMA ZERO=      -5.7 [illegible] 23194
        LAYER SIGMA ZERO=      -5.2245 [illegible]
        LAYER WITH ROUGH SURFACE SIGMA ZERO HH=      -5.22455 [illegible]


THETA=50.00
P1=    [illegible]              Q1=    .19 [illegible] E+00
        HALF SPACE SIGMA ZERO=      [illegible] 7137
        LAYER SIGMA ZERO=      [illegible]
        LAYER WITH ROUGH SURFACE SIGMA ZERO HH=      [illegible]


THETA=60.00
P1=    [illegible]              Q1=    [illegible]
        HALF SPACE SIGMA ZERO=      [illegible]
        LAYER SIGMA ZERO=      [illegible]
        LAYER WITH ROUGH SURFACE SIGMA ZERO HH=      -7.5113 [illegible]
```

```
THETA=[illegible]
P1=    [illegible]             D1=    [illegible] 1349-[illegible]
           HALF SPACE SIGMA ZERO=     -[illegible]
           LAYER SIGMA ZERO=     -8.75987527
           LAYER WITH ROUGH SURFACE SIGMA ZERO HH=     -[illegible]

THETA=[illegible]
P1=    .13[illegible]             D1=    .7227+195-01
           HALF SPACE SIGMA ZERO=    -12.[illegible]
           LAYER SIGMA ZERO=    -12.[illegible]
           LAYER WITH ROUGH SURFACE SIGMA ZERO HH=    -12.[illegible]
```

UNCLASSIFIED UNCLASSIFIED UNCLASSIFIED

```
 [illegible]   [illegible] 1.2     [illegible] 09/08/80
09.21.[illegible]  FROM
09.21.[illegible]  [illegible] WORDS - FILE INPUT  , DC 04
09.21.[illegible]    UNCLASSIFIED
09.21.[illegible]TASK([illegible]767[illegible]
09.21.[illegible]
09.22.[illegible]  [illegible] OF SECONDS COMPILATION TIME
09.22.[illegible]
09.22.[illegible]  [illegible] = 615154, LOADER USED  753008
09.29.[illegible]   [illegible]
09.29.[illegible]  1.2.777 OF SECONDS EXECUTION TIME
09.29.[illegible]ITS(ITEM)
09.29.[illegible]
09.29.[illegible]UNCLASSIFIED
09.29.[illegible] CLIST COMPLETE.
09.29.[illegible]EXIT(S)
09.29.[illegible]  [illegible] WORDS - FILE OUTPUT , DC 40
09.29.[illegible]MS   1.75[illegible] WORDS (  [illegible] MAX USED)
09.29.[illegible]    101.725 SEC.          [illegible]  $ CP
09.29.[illegible]      4.120 SEC.          .352  $ IO
09.29.[illegible]    [illegible]7.171 KWS.          [illegible].097  $ CM
09.29.[illegible] MAINFRAME CHARGES      1[illegible] TOT.
09.29.[illegible]        * * * * NOTE * * * *
09.29.[illegible]CHARGES FOR CARDS READ/PUNCHED AND
09.29.[illegible]LINES PRINTED NOT INCLUDED. ADD $1.00 FOR
09.29.[illegible]EACH TAPE/DISK MOUNTED.
09.29.[illegible]      1[illegible] SEC.      DATE 09/08/80
09.29.[illegible]
09.29.[illegible]I CERTIFY THAT I HAVE REVIEWED THE
09.29.[illegible]CONTENTS OF THIS ADP INFORMATION AND
09.29.[illegible]THAT, TO THE BEST OF MY KNOWLEDGE, IT
09.29.[illegible]CONTAINS NO SCA/COLLATERAL DATA.
09.29.[illegible]
09.29.[illegible]
09.29.[illegible]                 --------------------
09.29.[illegible]                 SIGNATURE/DATE
09.29.[illegible]
09.29.[illegible]  END OF JOB, **
```

LIST OF SYMBOLS

$\underline{r}$	Position vector
$\epsilon(\underline{r})$	Permittivity of the random medium
$\sigma(\underline{r})$	Conductivity of the random medium
ϵ_a	Average relative dielectric constant of the random medium
σ_a	Average conductivity of the random medium
η_1	Standard deviation of the dielectric fluctuations
η_2	Standard deviation of the conductivity fluctuations
L	Mean thickness of the vegetation layer
k_3	Complex propagation constant in the soil
θ_i	Angle of incidence
k_o	Free space propagation constant
$\underline{\underline{\Gamma}}(\underline{r},\underline{r}')$	Infinite space dyadic Green's function
$<\underline{E}(\underline{r})>$	Mean wave in the random medium
$G_o(\underline{r},\underline{r}')$	Infinite space scalar Green's function
$\underline{E}_s(\underline{r})$	Scattered electric field in the random medium
$\delta(\underline{r}-\underline{r}')$	Three-dimensional Dirac delta function equal to $\delta(x-x')\,\delta(y-y')\,\delta(z-z')$
$\underline{\underline{I}}$	Unit dyadic
$\underline{a}_x, \underline{a}_y, \underline{a}_z$	Unit vectors in x, y, and z

k_x, k_y	Fourier transform variables
i	$\sqrt{-1}$
δ_{ij}	Kronecker Delta
k_{ex}, k_{ey}, k_{ez}	Components of the effective propagation constant
k_h	Value of k_{ez} for horizontal polarization
k_v	Value of k_{ez} for vertical polarization
$\underline{G}_s(\underline{k}_t, z)$	Two-dimensional Fourier transform of the scattered electric field in the random medium
$A_x(k_x, k_y)$, $A_y(k_x, k_y)$, $A_z(k_x, k_y)$	Fourier transform of the amplitudes of the scattered electric field in air
A_I	Illuminated surface area
ℓ_x, ℓ_y, ℓ_z	Correlation distances in x, y, and z, repectively
σ°_{HHv}	Backscatter coefficient for volume scattering and for the case of horizontal polarization transmit, horizontal polarization receive
σ°_{VVv}	Backscatter coefficient for volume scattering and for the case of vertical polarization transmit, vertical polarization receive
σ°_{HHs}	Backscatter coefficient for a randomly rough surface for the case of horizontal polarization transmit, horizontal polarization receive
σ°_{HH}	Final backscatter coefficient result that includes both volume scattering and rough surface scattering for the case of horizontal polarization transmit, horizontal polarization receive

σ°_{VV}	Final backscatter coefficient result that includes both volume scattering and rough surface scattering for the case of vertical polarization transmit, vertical polarization receive
F	Fraction of water by weight in the vegetation
R_V	Volume of vegetation divided by the total volume
m_s	Standard deviation of the rough surface fluctuations divided by the correlation distance
f	Frequency